GEORGIA INSTITUTE OF TECHNOLOGY — OFFICE OF CONTRACT ADMINISTRATION

PROJECT ADMINISTRATION DATA SHEET

[x] ORIGINAL [ ] REVISION NO. _____

Project No. A-3384 GTRI/~~GIT~~ DATE 11/3/82

Project Director: Atlon G. Dunn, III ~~School~~/Lab STL

Sponsor: Scientific Atlanta, Inc.
Atlanta, GA

Type Agreement: Research Project Agreement dated 10/13/82, P.O. #A461502

Award Period: From 10/13/82 To ~~2/12/83~~ 4/30/83 (Performance) _____ (Reports)

Sponsor Amount: Total Estimated: $ _____ Funded: $ 20,000*

Cost Sharing Amount: $ _____ Cost Sharing No: _____

Title: KU-Band Feed for 2.8 Meter Diameter Satellite Communications Antenna

ADMINISTRATIVE DATA

OCA Contact John W. Burdette

1) Sponsor Technical Contact:

Mr. Robert M. Fitzgerald
(404) 449-2000
Scientific Atlanta, Inc.
Video Communications Division
Box 105027
Atlanta, GA 30348

2) Sponsor Admin/Contractual Matters:

Same

Defense Priority Rating: NA

Military Security Classification: NA
(or) Company/Industrial Proprietary: NA

RESTRICTIONS

See Attached NA Supplemental Information Sheet for Additional Requirements.

Travel: Foreign travel must have prior approval – Contact OCA in each case. Domestic travel requires sponsor approval where total will exceed greater of $500 or 125% of approved proposal budget category.

Equipment: Title vests with None proposed

COMMENTS:

*Includes $1,000 for Patent & Data Rights Fee

COPIES TO:

Research Administrative Network
Research Property Management
Accounting
Procurement/EES Supply Services
~~Research Security Services~~
Reports Coordinator (OCA)
GTRI
Library
Research Communications (2)
Project File
Other _____
Other _____

GEORGIA INSTITUTE OF TECHNOLOGY · OFFICE OF CONTRACT ADMINISTRATION

SPONSORED PROJECT TERMINATION/CLOSEOUT SHEET

Date May 22, 1984

Project No. A-3384 School/Lab STL

Includes Subproject No.(s) G-37-601

Project Director(s) Alton G. Dunn GTRI / ~~GIT~~

Sponsor Scientific Atlanta

Title Ku-Band Feed for 2.8 Meter Diameter Satellite Communications Antenna

Effective Completion Date: 5/31/83 (Performance) _____ (Reports)

Grant/Contract Closeout Actions Remaining:

- [ ] None
- [X] Final Invoice or Final Fiscal Report
- [ ] Closing Documents
- [ ] Final Report of Inventions
- [ ] Govt. Property Inventory & Related Certificate
- [ ] Classified Material Certificate
- [ ] Other _____

Continues Project No. _____ Continued by Project No. _____

COPIES TO:

Project Director
Research Administrative Network
Research Property Management
Accounting
Procurement/EES Supply Services
Research Security Services
Reports Coordinator (OCA)
Legal Services
Library
GTRI
Research Communications (2)
Project File
Other _____

Form OCA 60:1028

FINAL REPORT
(EES/GIT PROJECT A-3384)

KU-BAND FEED FOR A 2.8 METER
DIAMETER SATELLITE COMMUNICATIONS ANTENNA

Submitted to

Scientific Atlanta, Inc.
Antenna Communications Division
Box 105027, Atlanta, Georgia 30348
ATTENTION: Mr. Robert M. Fitzgerald

Submitted by

Georgia Institute of Technology
Engineering Experiment Station
Systems and Techniques Laboratory
Microwave Systems Division
Atlanta, Georgia 30332

Contracting through

Georgia Tech Research Institute
Atlanta, Georgia 30332

P.O. No. A461502

21 June 1983

TABLE OF CONTENTS

LIST OF TABLES

LIST OF FIGURES

1.0 BACKGROUND

1.1 SCOPE

The purpose of this project is to design a Ku-band feed system which can be implemented in a given paraboloidal reflector to achieve desired secondary pattern and gain performance. A prototype feed will be constructed and tested based on the initial design analysis. The feed will then be tested and evaluated in the given reflector.

The given reflector is a 2.8 meter diameter receive-only earth station antenna designed to operate at a frequency near 4 GHz. The purpose of this project includes an assessment of the adequacy of this reflector for operation at Ku-band frequencies with a properly designed feed system.

1.2 INTRODUCTION

High efficiency and low sidelobes are primary performance characteristics for a satellite communications earth station antenna. Low sidelobes are important for minimizing interference. The interference may be from random noise or off-axis signal sources, such as adjacent satellites or terrestrial microwave links. High gain is important for maximizing the signal strength with the minimum required aperture size. The two parameters of gain and sidelobes are combined in one figure of merit which is the ratio of antenna gain to noise temperature (G/T).

Many design approaches which optimize reflector antenna gain also produce high sidelobes. Therefore, gain and sidelobe levels are interdependent and must be controlled together. The design goal for a reflector antenna feed to meet both gain and sidelobe requirements is a feed which illuminates the reflector efficiently, yet exhibits steep skirts to reduce the spillover energy. In addition, a circularly symmetric feed pattern is desirable for low cross-polarization and for dual-polarized feed applications. Table 1-1 lists the desired antenna performance characteristics.

Table 1-1. Antenna Performance Requirements

Item	Specification
Diameter	2.8 meters
Focal Length	45.25 inches
Surface Tolerance	.025 inches RMS max.
Frequency	11.7 - 12.2 GHz
VSWR	1.3:1 Max.
Gain	48.5 dBi Min. at 11.95 GHz
Sidelobes (dBi)*	
Region 1 (1st Sidelobe to 7°)	29-25 Log θ
Region 2 (7° to 9.2°)	8
Region 3 (9.2° to 48°)	32-25 Log θ
Region 4 (48°) to 180°)	-10
Polarization	Dual Linear
Isolation (Port-to-Port)	30 dB Min.
Axial Ratio (On-Axis)	35 dB Min.
G/T (Midband at 20° Elevation Angle)	22 dB/° K
Feed Interface	WR-75

*A sidelobe shall be defined as a region of the antenna radiation pattern, exclusive of the main beam, which is higher than the adjacent power levels on each side by at least 3dB. Theta (θ) shall be defined as the angle in degrees measured from the main beam axis. No sidelobe in region 1 shall exceed the specified envelope by more than 3 dB. No more than 10% of the sidelobes in the combined regions 2 through 4 shall exceed the specified envelope.

1.3 Design Analysis

1.3.1 Feed Design

The following feed design candidates are considered:

a) Cutler or "Splash-Plate"

b) Square Corrugated

c) Circular Corrugated

d) Multimode

The Cutler feed is an open-ended waveguide terminated with a reflective disc or cap to direct the feed energy back towards the reflector. [1] The advantages of a Cutler feed are reduced aperture blockage (since the feed is small and is supported from the center of the reflector), simplicity of construction, light weight, and convenience of locating feed electronics behind the reflector as in a Cassegrain antenna. The disadvantages of a Cutler feed are unequal beamwidths in the principal planes (and likewise inability to shape the illumination), lack of a definite focus, and poor impedance match. Realistically, the Cutler feed is limited to a single polarization and to applications which do not require precise illumination control and can tolerate a high VSWR.

Corrugated feeds are highly efficient horns with low spillover and low cross-polarization. [2] By propagating a hybrid HE mode the feed pattern is circularly symmetric and therefore well suited for dual-polarized applications. The corrugated horn can be implemented in a square or circular geometry. The disadvantages of the corrugated horn are complexity of construction, difficulty of impedance matching (although tuning can be accomplished), and weight since the side walls must be thick enough to accommodate the grooves. Even if the grooves are made by attaching thin walls or slabs to the inside of the feed, additional material is used for the slabs and the overall size of the feed is increased compared with a smooth-walled feed.

A multimode feed generates higher order waveguide modes in addition to the dominant mode which normally propagates in a smooth-walled horn. If the modes are combined properly, the beam shape can be arbitrarily controlled to obtain a desired illumination. The advantages of the multi-mode horn are mechanical simplicity, low VSWR, and the potential for a wide variety of beam shapes including circular symmetry, broad illumination, sharp cutoff, and low sidelobes all in the same feed pattern. The disadvantages are the close mechanical tolerances required for multimode horns, difficulty during the design phase in assuring that the proper mode amplitudes and phases are produced, and an increased size compared with single-mode feeds. The diameter of a multimode feed horn must be larger than for a single mode horn to propagate the higher order modes. In effect, the gain of the multimode horn may be less than the gain of a single mode horn with the

same size aperture. Also the length of the multimode feed may be a disadvantage since small flare angles are required to control the mode amplitude and straight matching sections may be needed to control the phase dispersion between modes. Figure 1-1 illustrates the approach to generating and controlling higher order modes for a multimode feed horn.

The multimode feed horn is the best candidate for obtaining the desired goal of high efficiency and low sidelobes. Four circular waveguide modes, including the dominant mode, are sufficient to shape the feed pattern to practically any arbitrary distribution. The difficulty is achieving the exact combination of the desired modes. The resultant far field pattern for the multimode horn can be considered as a superposition of the radiation pattern for each individual mode as it exists in the feed aperture. [2] For example, Figure 1-2 shows the radiation pattern for the dominant TE_{11} mode in a circular aperture. The high sidelobes and narrow beamwidth are evident in the E-plane (vertical polarization is assumed). Figure 1-3 shows the primary pattern for a pure TM_{11} mode which is the first higher order mode. Notice in the principal plane of the H-field (elevation = 0°) the contribution is zero. The peaks of the TM_{11} mode can be added to the TE_{11} pattern to broaden the E-plane main beam. Also, the large sidelobes in the TM_{11} pattern add out-of-phase to effectively cancel or reduce the sidelobes in the E-plane.

The radiation patterns for two more higher order modes (TE_{12} and TM_{12}) are shown in Figures 1-4 and 1-5 respectively. These modes can be added to further shape the feed pattern. Figure 1-6 shows a combination of TE_{11} and TM_{11} modes which provides a circularly symmetric pattern suitable for illumination of a prime focus antenna. The addition of a third mode (TE_{12}) shows sharper skirts in the E-plane which reduces spillover energy as shown in Figure 1-7. Summing a fourth mode (TM_{12}) provides steep skirts in both planes and a higher efficiency "flat top" beam as shown in Figure 1-8. The primary pattern of a dual-mode feed suitable for a Cassegrain antenna is shown in Figure 1-9. Because of the restrictions on feed aperture size to avoid feed shadowing, it is difficult to accommodate more than two modes in a Cassegrain feed.

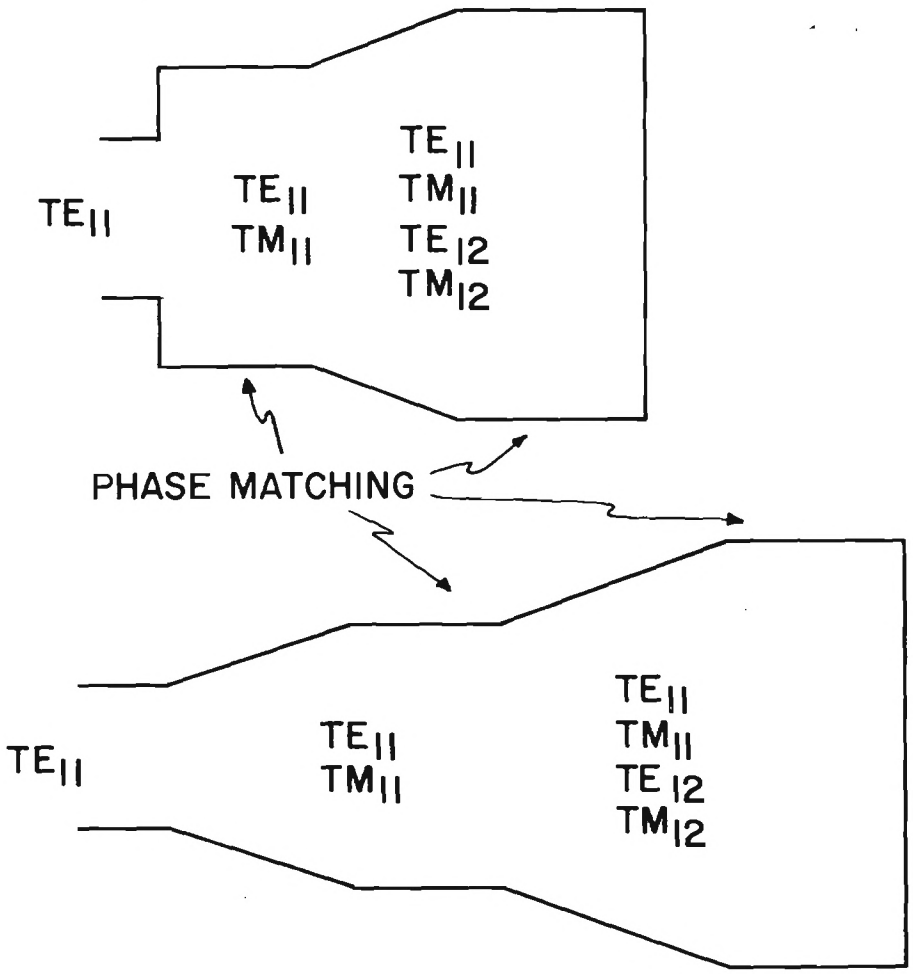

HIGHER ORDER MODES GENERATED BY STEP DISCONTINUITY OR FLARE ANGLE

ADVANTAGES

- SIDELOBE SUPPRESSION
- CIRCULARLY SYMMETRIC PATTERN
- COINCIDENT PHASE CENTERS
- SIMPLE CONSTRUCTION

DISADVANTAGES

- DIFFERENTIAL PHASE DISPERSION BETWEEN MODES
- DIFFICULTY OF MODE AMPLITUDE CONTROL
- CLOSE MANUFACTURING TOLERANCES

FIGURE 1-1

MULTIMODE FEED HORNS

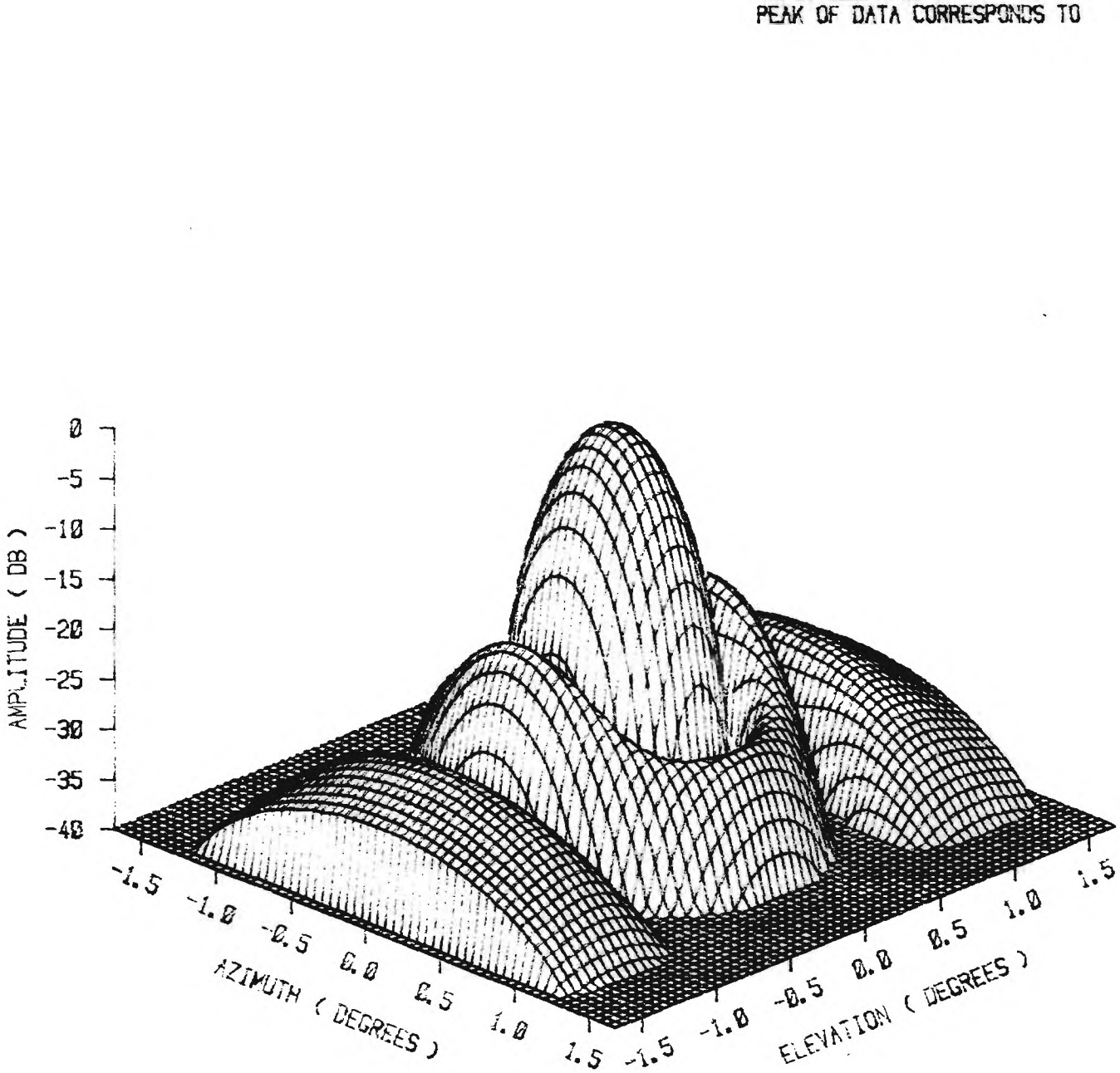

FIGURE 1-2 CIRCULAR TE_{11} MODE PATTERN

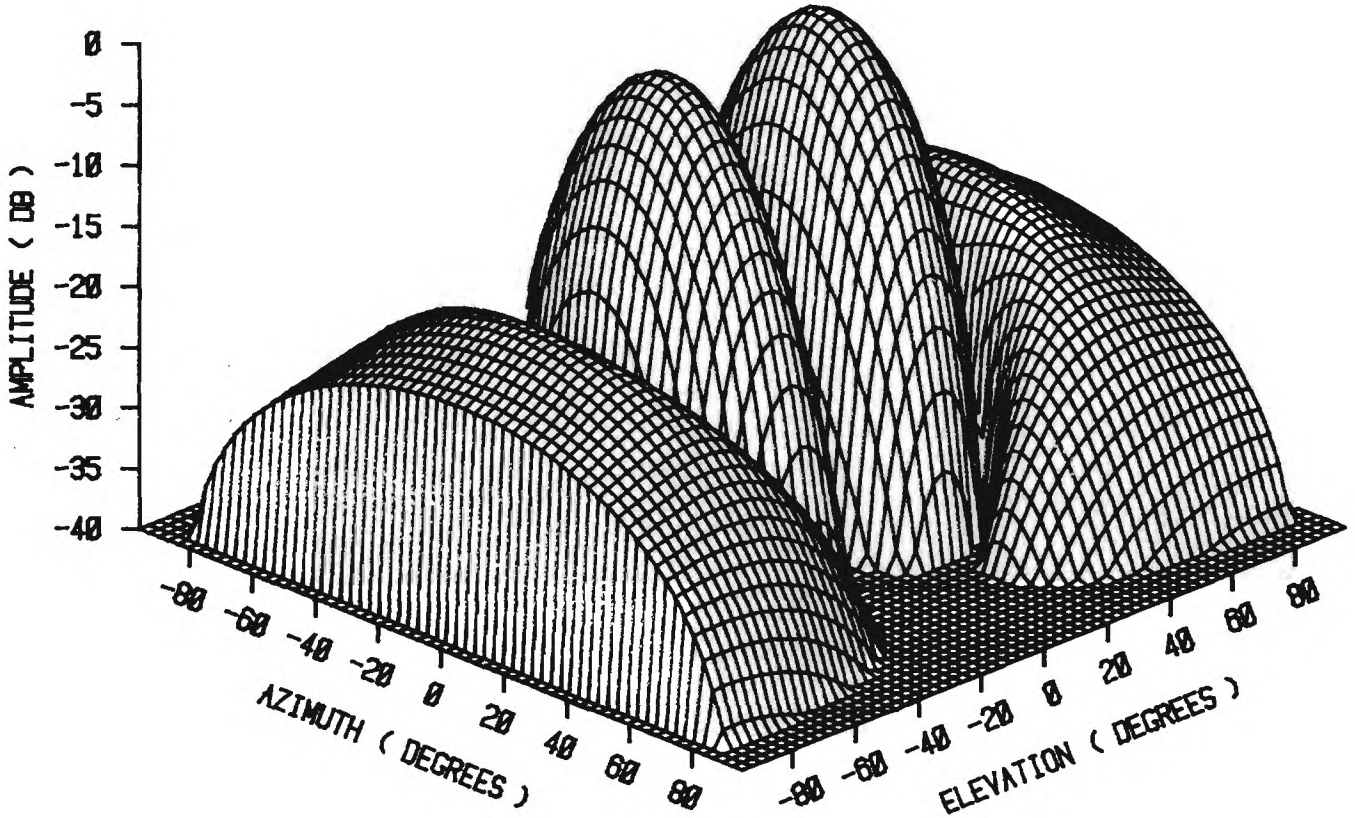

FIGURE 1-3 CIRCULAR TM_{11} MODE PATTERN

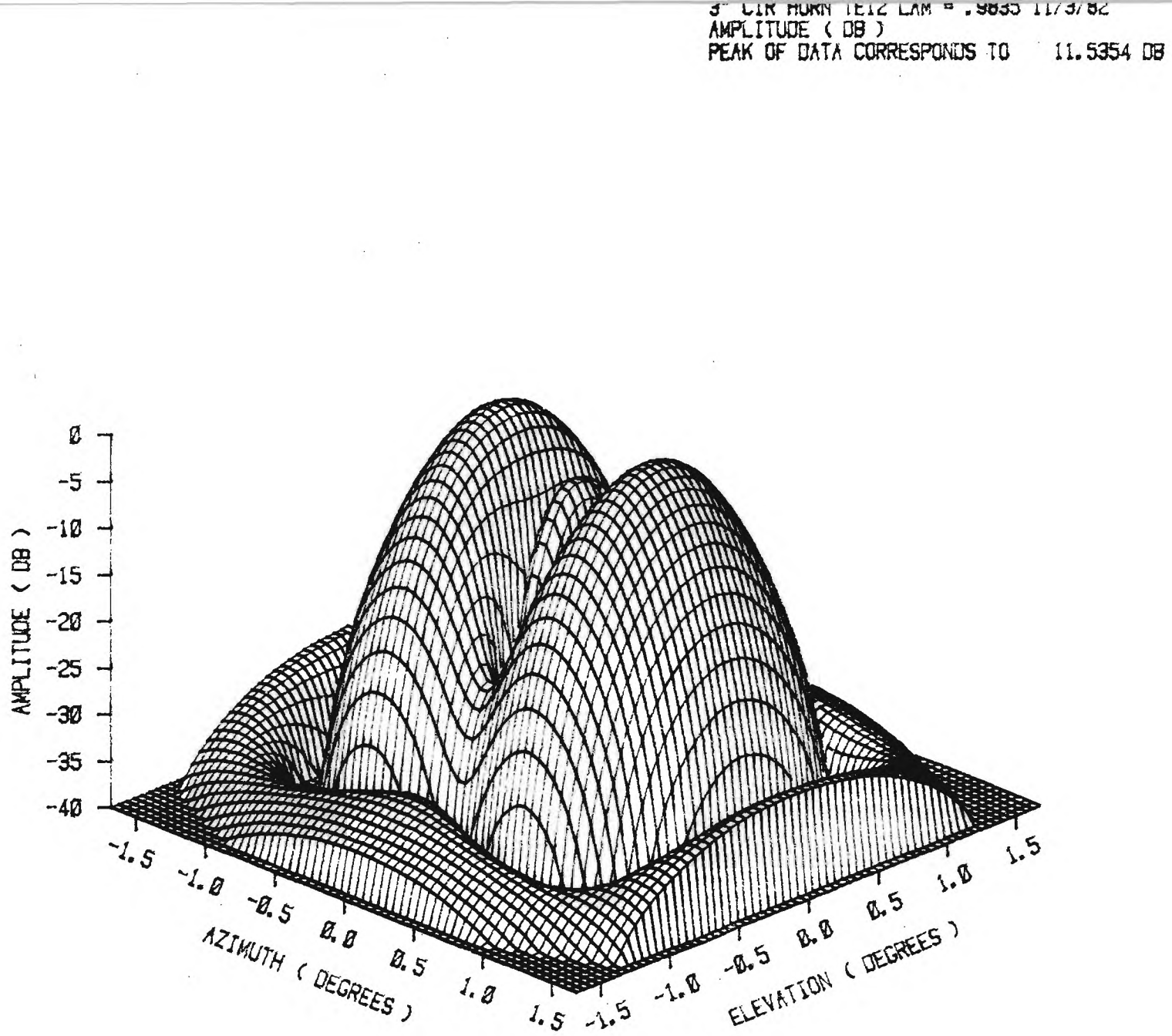

FIGURE 1-4 CIRCULAR TE_{12} MODE PATTERN

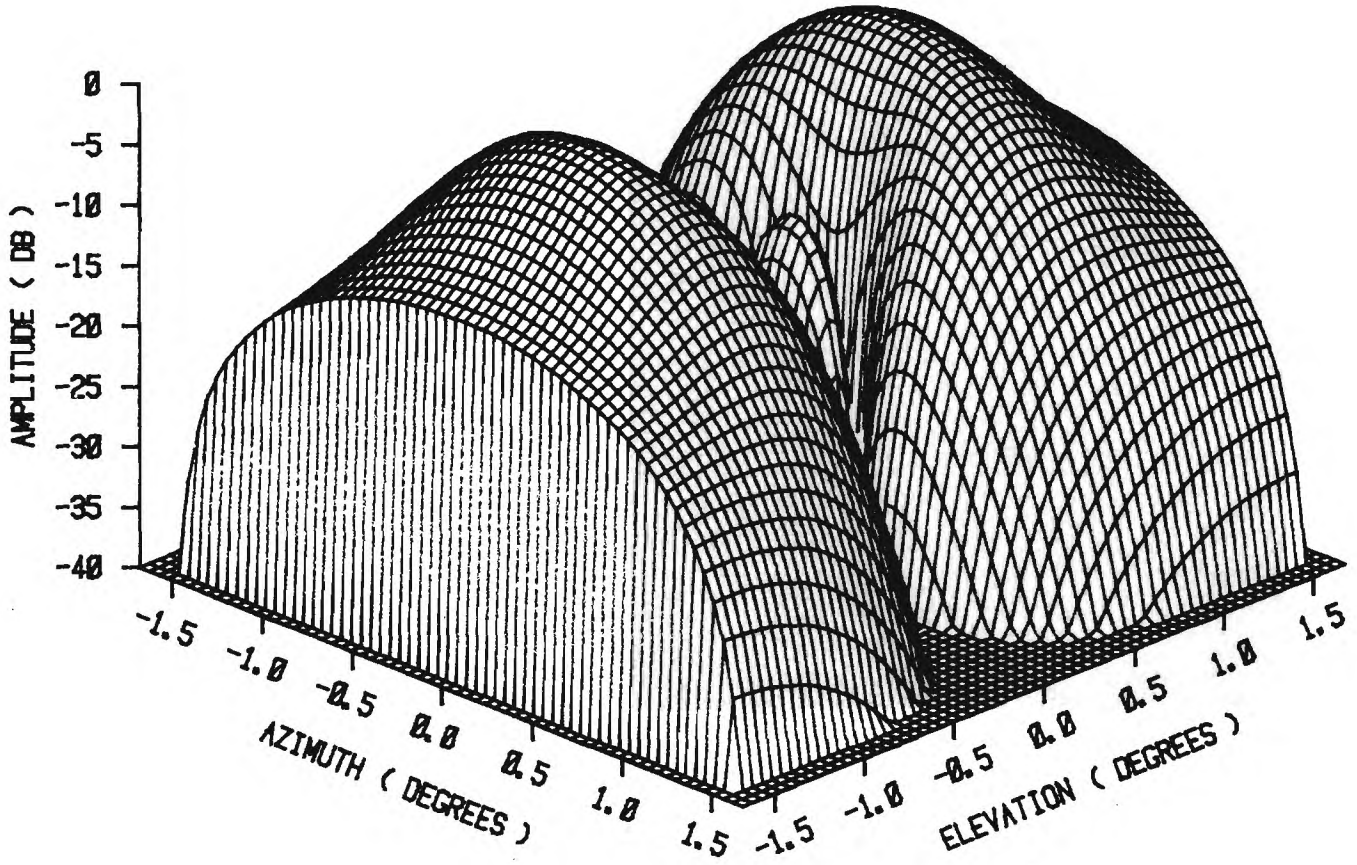

FIGURE 1-5 CIRCULAR TM_{12} MODE PATTERN

AMPLITUDE (DB)
PEAK OF DATA CORRESPONDS TO -12.6628 DB

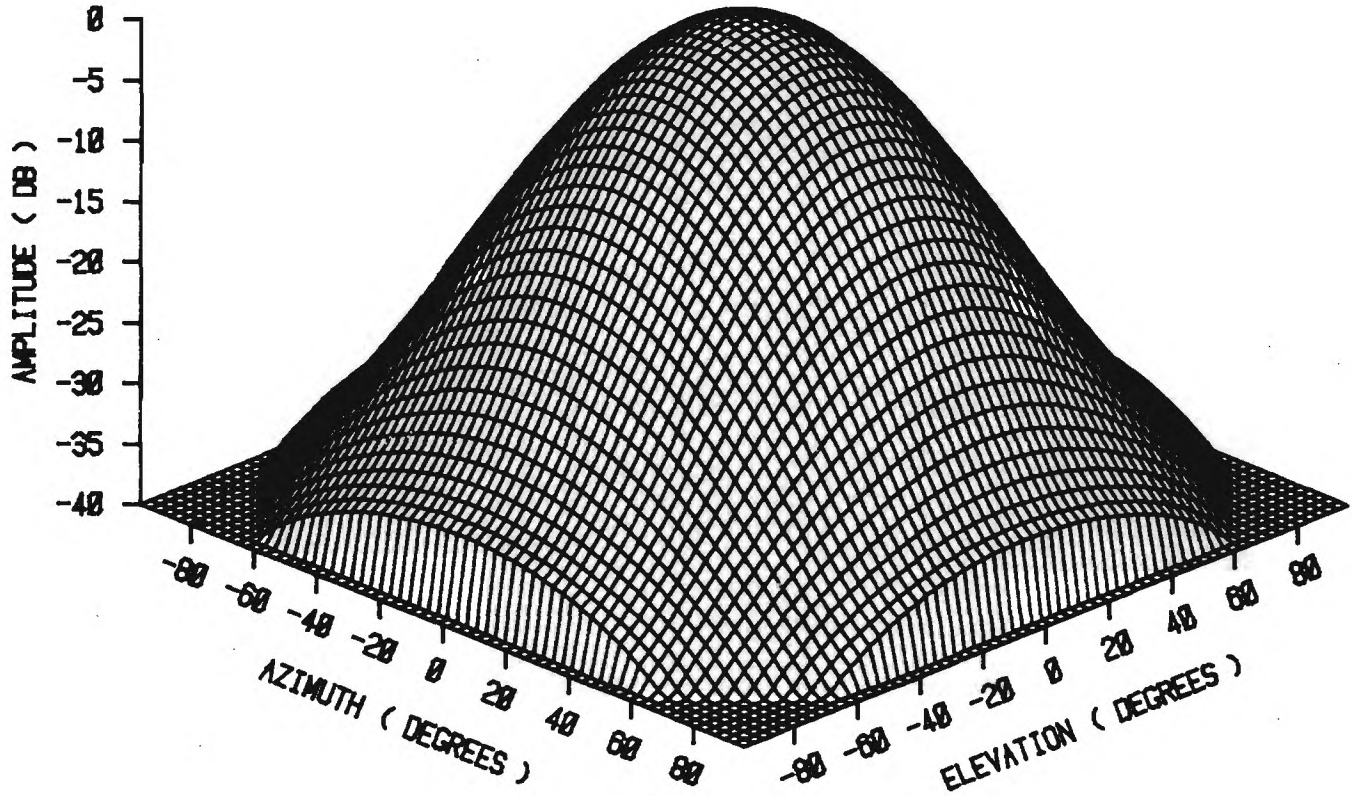

FIGURE 1-6 CIRCULAR DUAL-MODE FEED PATTERN

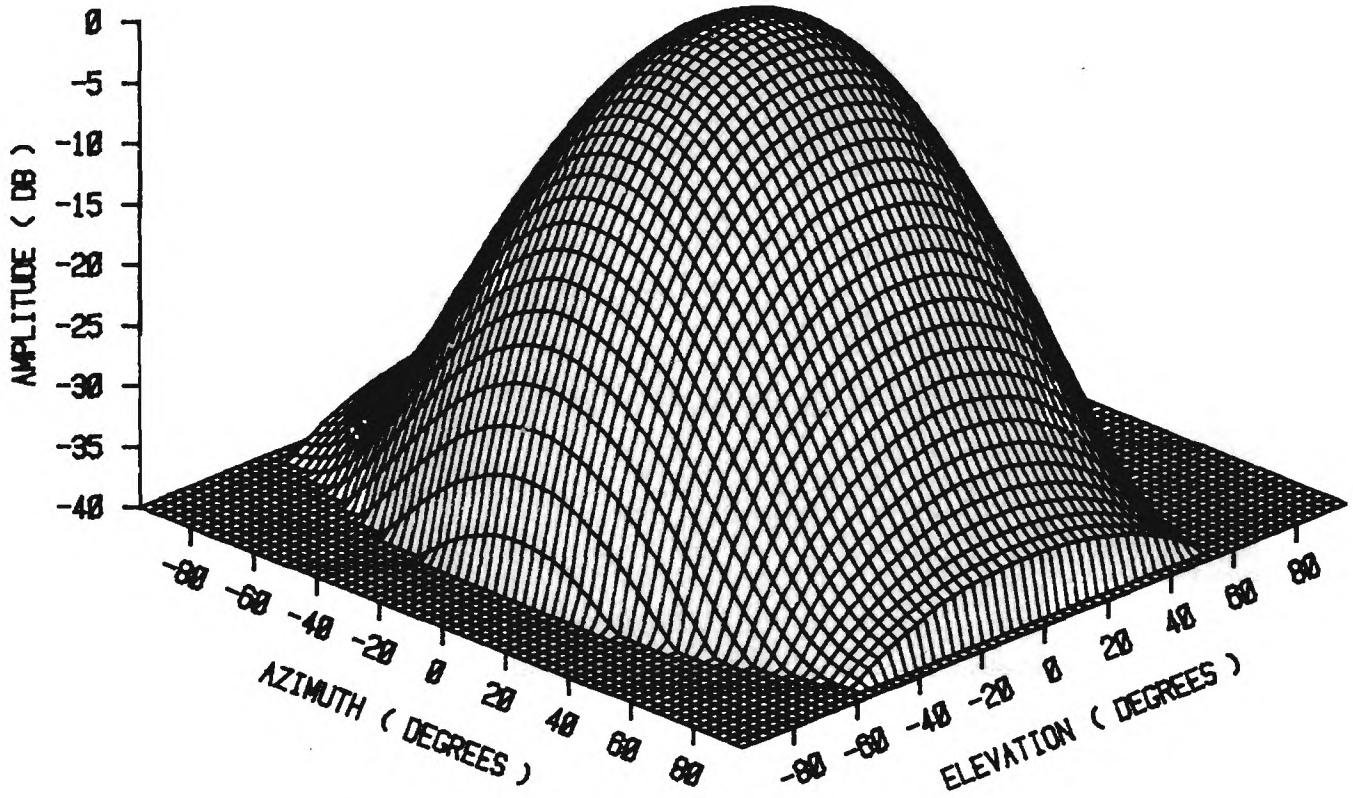

FIGURE 1-7 CIRCULAR THREE-MODE FEED PATTERN

AMPLITUDE (DB) 11.017#
PEAK OF DATA CORRESPONDS TO [illegible] DB

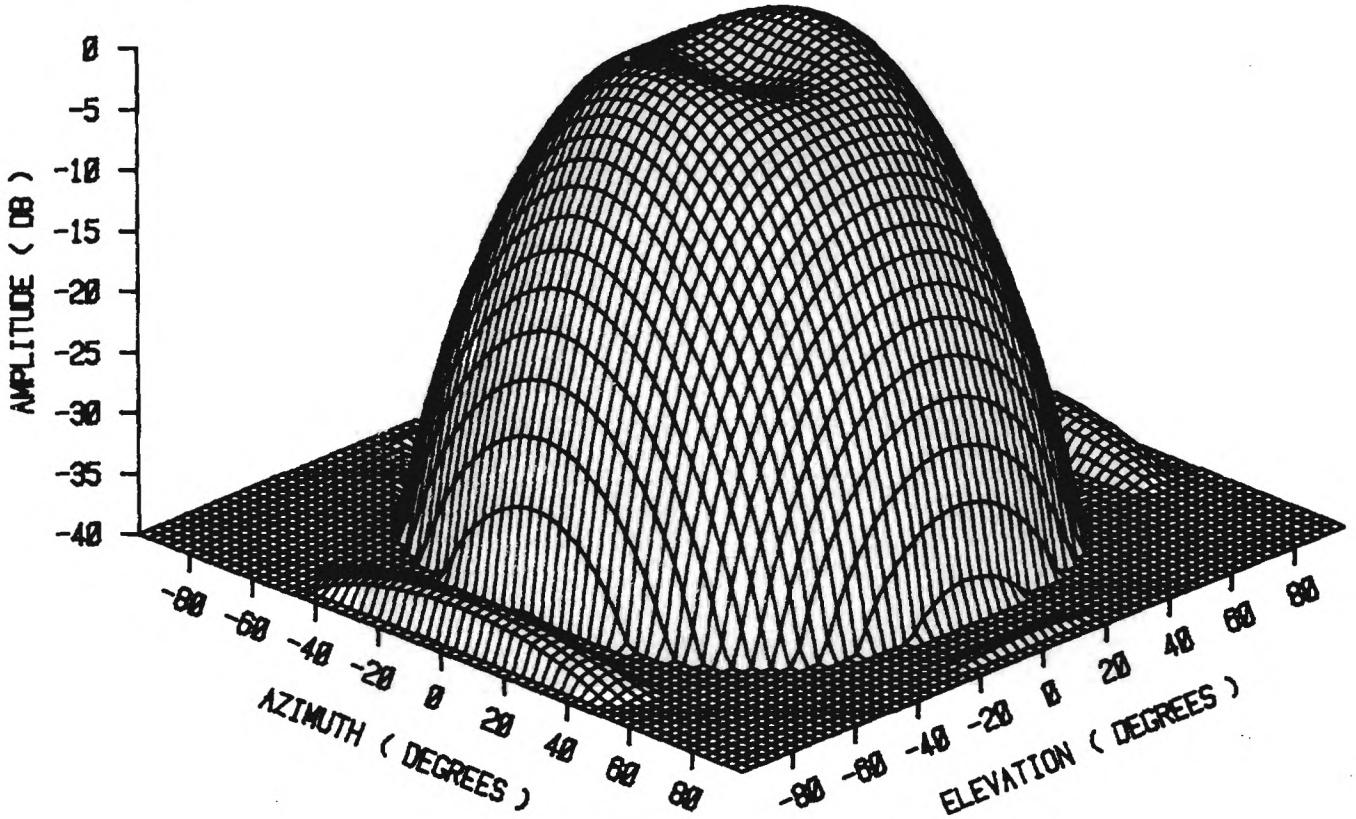

FIGURE 1-8 CIRCULAR FOUR-MODE FEED PATTERN

AMPLITUDE (DB)
PEAK OF DATA CORRESPONDS TO 17.2622 DB

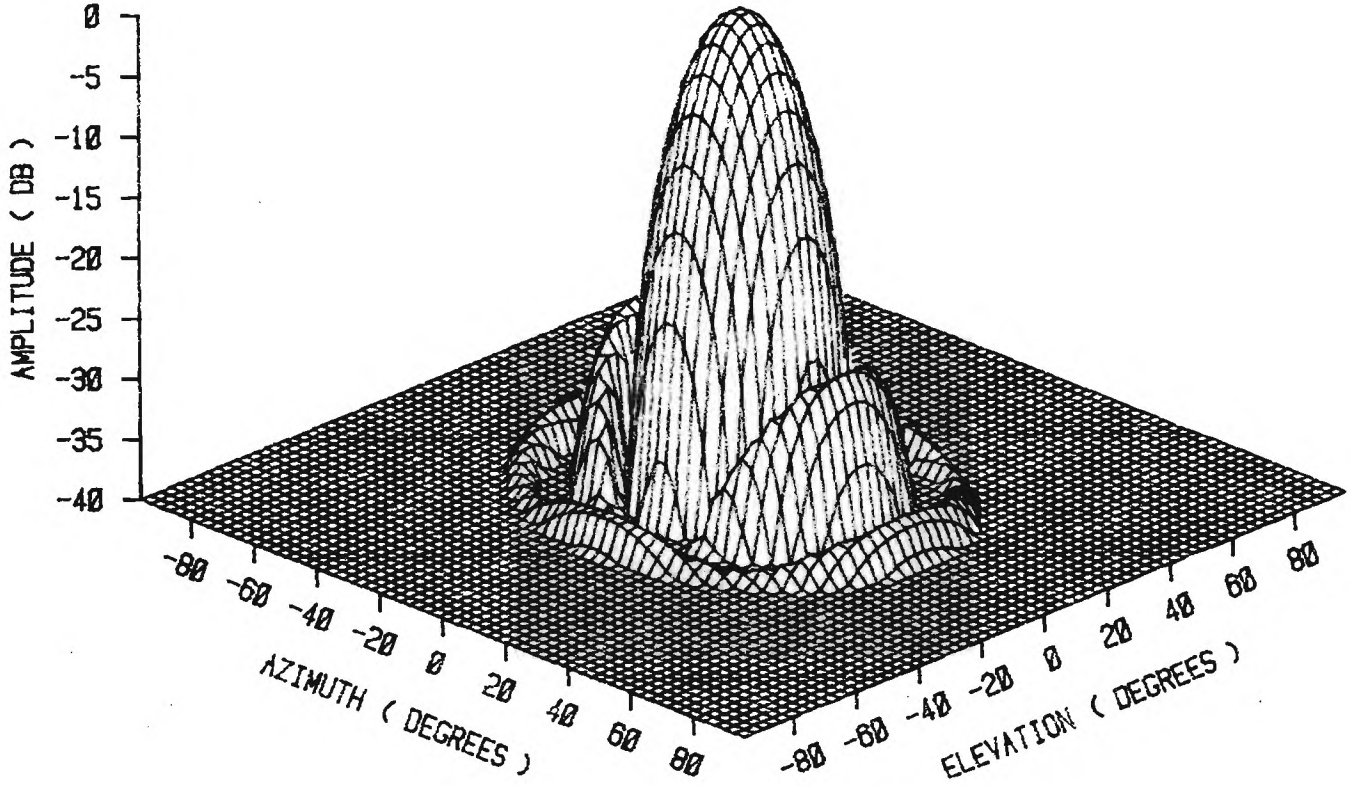

FIGURE 1-9 CIRCULAR HIGH-GAIN MULTIMODE FEED PATTERN

1.3.2 PRIME FOCUS ANTENNA DESIGN

A multimode feed with a primary pattern shown in Figure 1-8 is suitable for a high efficiency prime focus antenna. The beamwidth of the feed pattern is adjusted to provide a level of spillover energy which is consistent with the sidelobe requirements in the angular region (110°-120°). Also, the amount of edge illumination affects the first sidelobe level although in this case it is the rear spillover which determines the selection of edge taper.

The amount of aperture blockage also affects both the gain and the sidelobe levels. Figure 1-10 illustrates a prime focus antenna configuration. The aperture blockage can be divided into two parts, central or feed blockage (CB), and spar or feed support blockage (WS). The central blockage is determined by the diameter of the feed or of the part of the hub used for mounting the reflector panels and connecting to the backstructure. A circular portion of the main reflector with a diameter of approximately 10 inches sets the limit for the unuseable part of the reflector surface. This diameter is used for the central blockage dimension (CB). Spars or other feed supports are approximated as rectangular blockage areas with a width between 1/4 inches and 9/16 inches.

The secondary radiation patterns are calculated for a central blockage diameter of 10 inches and a spar width of 1/4 inches and 9/16 inches. Figures 1-11 and 1-12 show the individual contribution for central blockage and for a spar width of 1/4" in the E-plane and H-plane respectively. Figures 1-13 and 1-14 show similar comparisons for a spar width of 9/16 inches. Figures 1-15 and 1-16 show composite results in both planes. The required sidelobe envelope is approximated in each figure with a dotted line. The sidelobe levels from the two blockage sources are higher in the H-plane than the E-plane. A spar width of 1/4 inch meets the electrical specifications with a slight margin. However, 1/4 inch spars are not mechanically feasible. The case with 9/16 inch spars clearly does not meet the specifications for sidelobe levels. A potential compromise is the use of a button hook feed with thin guy wires. Even with a button hook though, there would be orientations of the antenna which would produce high sidelobes at some angles.

Another consideration in the design of a prime focus antenna is the length of the feed. Although a multimode feed horn offers the advantage of shaping the primary pattern, the feed itself is longer than a single-mode feed to maintain the proper phase relationship between modes and to accommodate individual stages of mode generation. Also, the flare of the feed is maintained at a small angle to prevent too high amplitude excitation of the modes. A complicated mechanical support may then be required for the feed. Because of the marginal sidelobe performance, primarily caused by the feed support blockage and because of the feed length required, a prime focus antenna is not suitable for the present application. An alternative consideration is to relax the sidelobe requirements in some planes and use three spars rather than the quadrapod of the existing reflector, or use a button hook support.

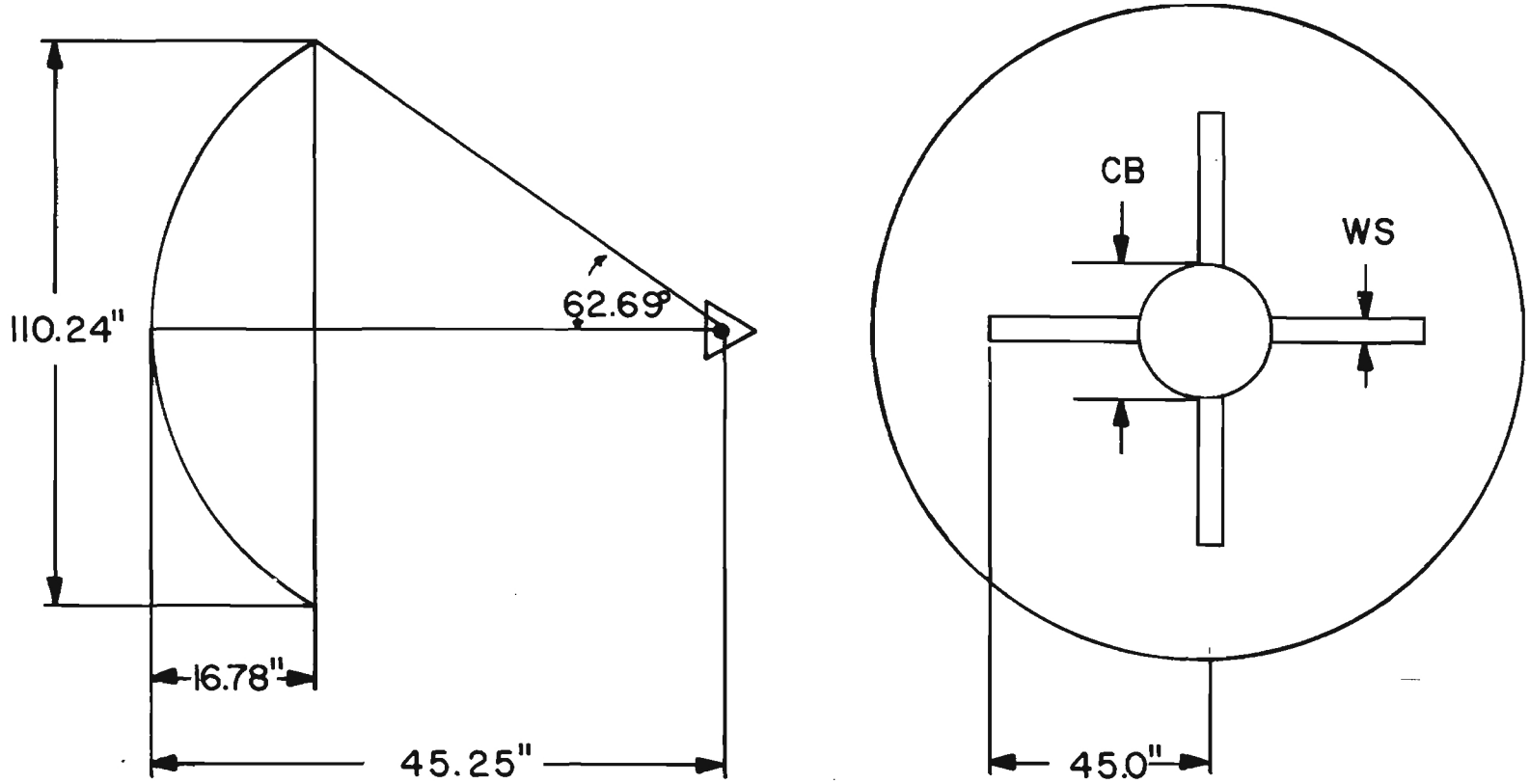

FIGURE 1-10
PRIME FOCUS ANTENNA CONFIGURATION

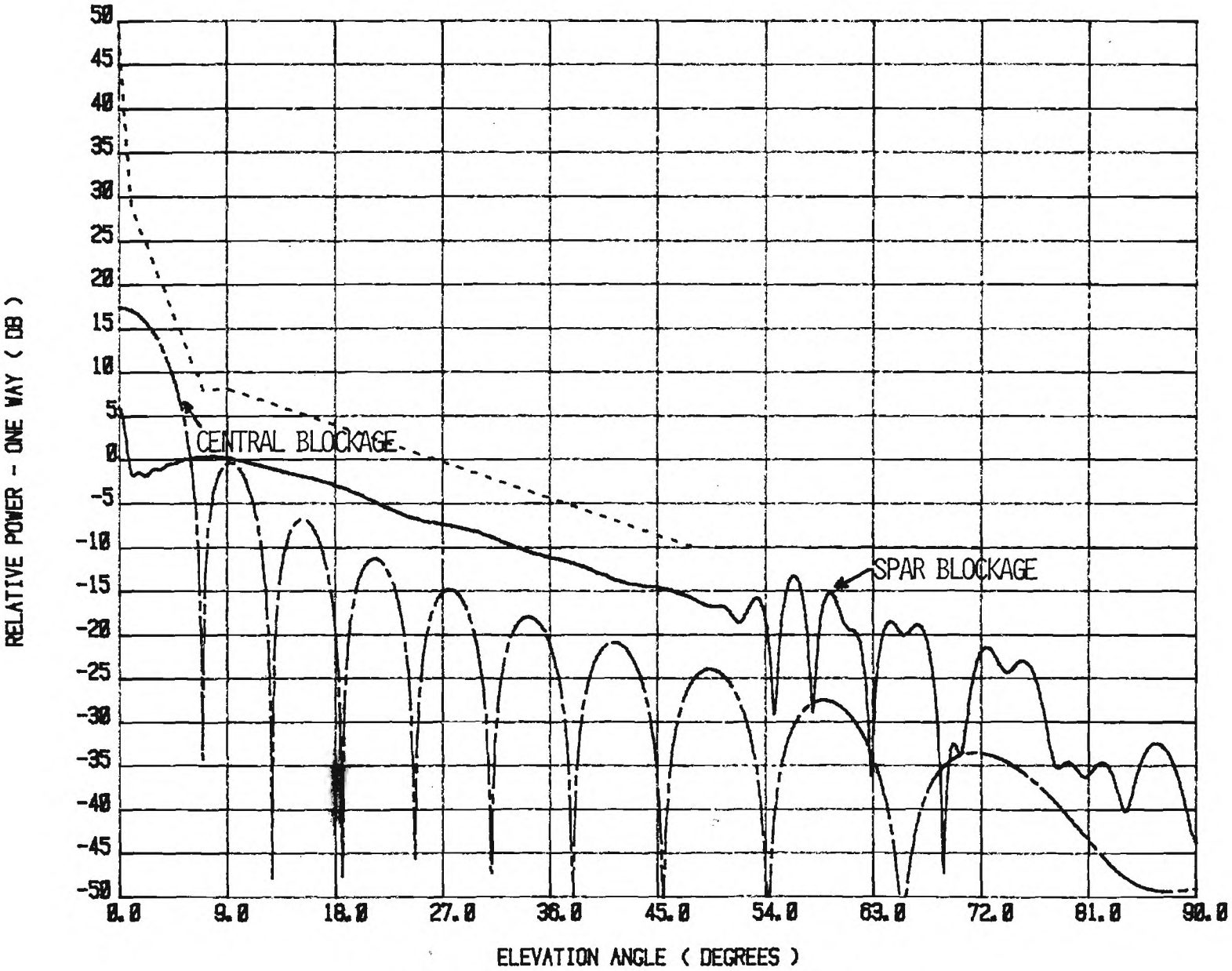

FIGURE 1-11 E-PLANE BLOCKAGE (1/4" SPARS)

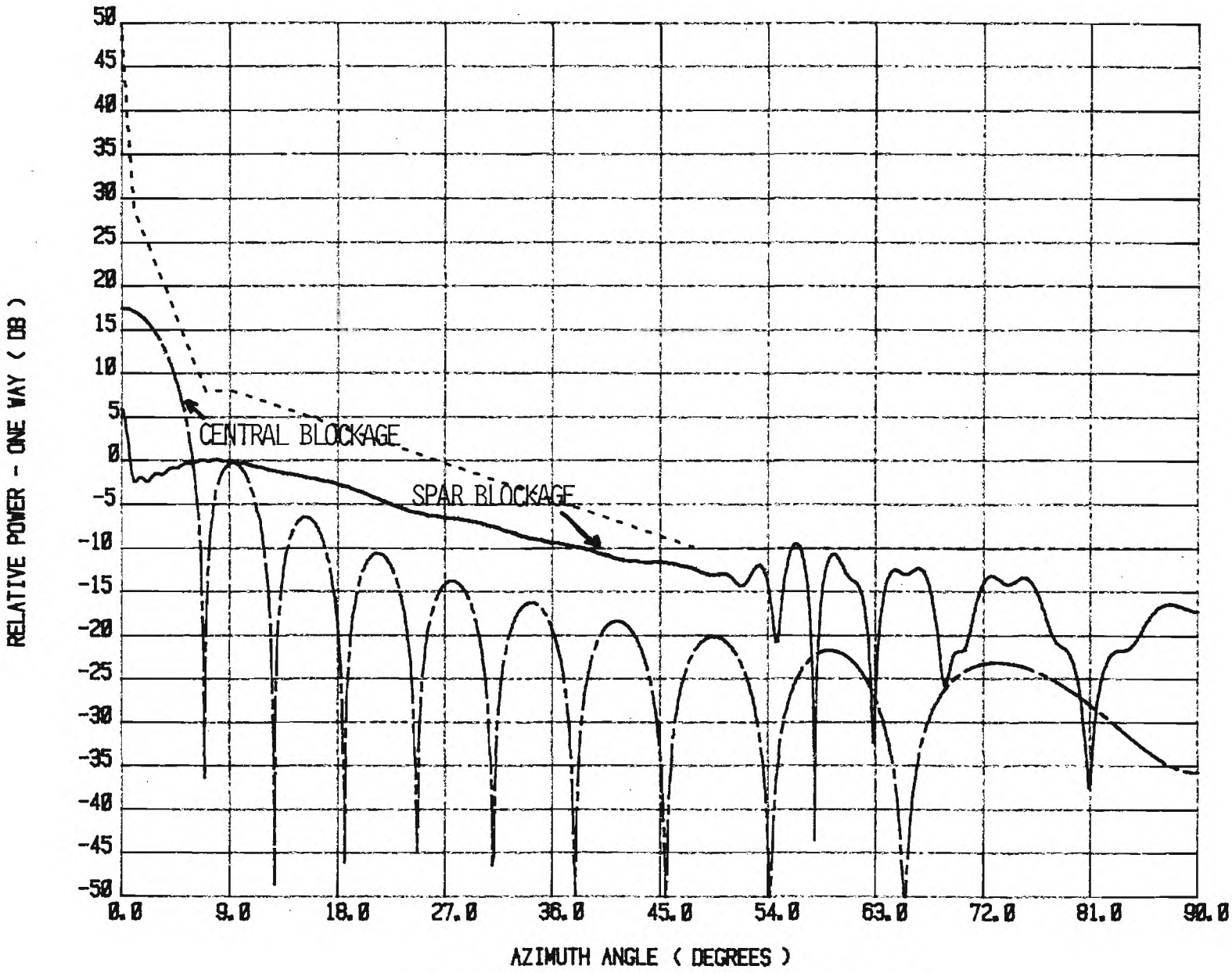

FIGURE 1-12 H-PLANE BLOCKAGE (1/4" SPARS)

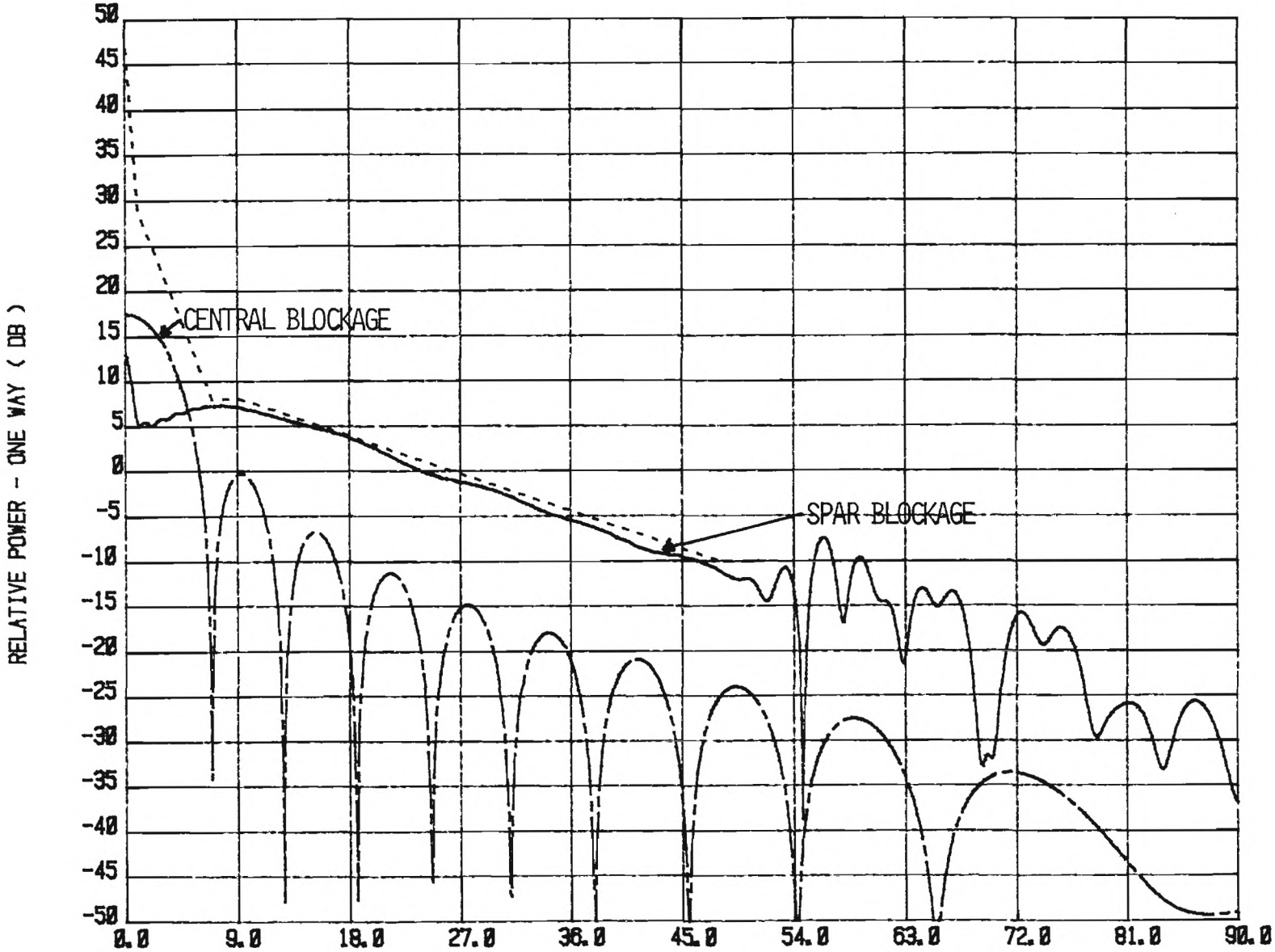

FIGURE 1-13 E-PLANE BLOCKAGE (9/16" SPARS)

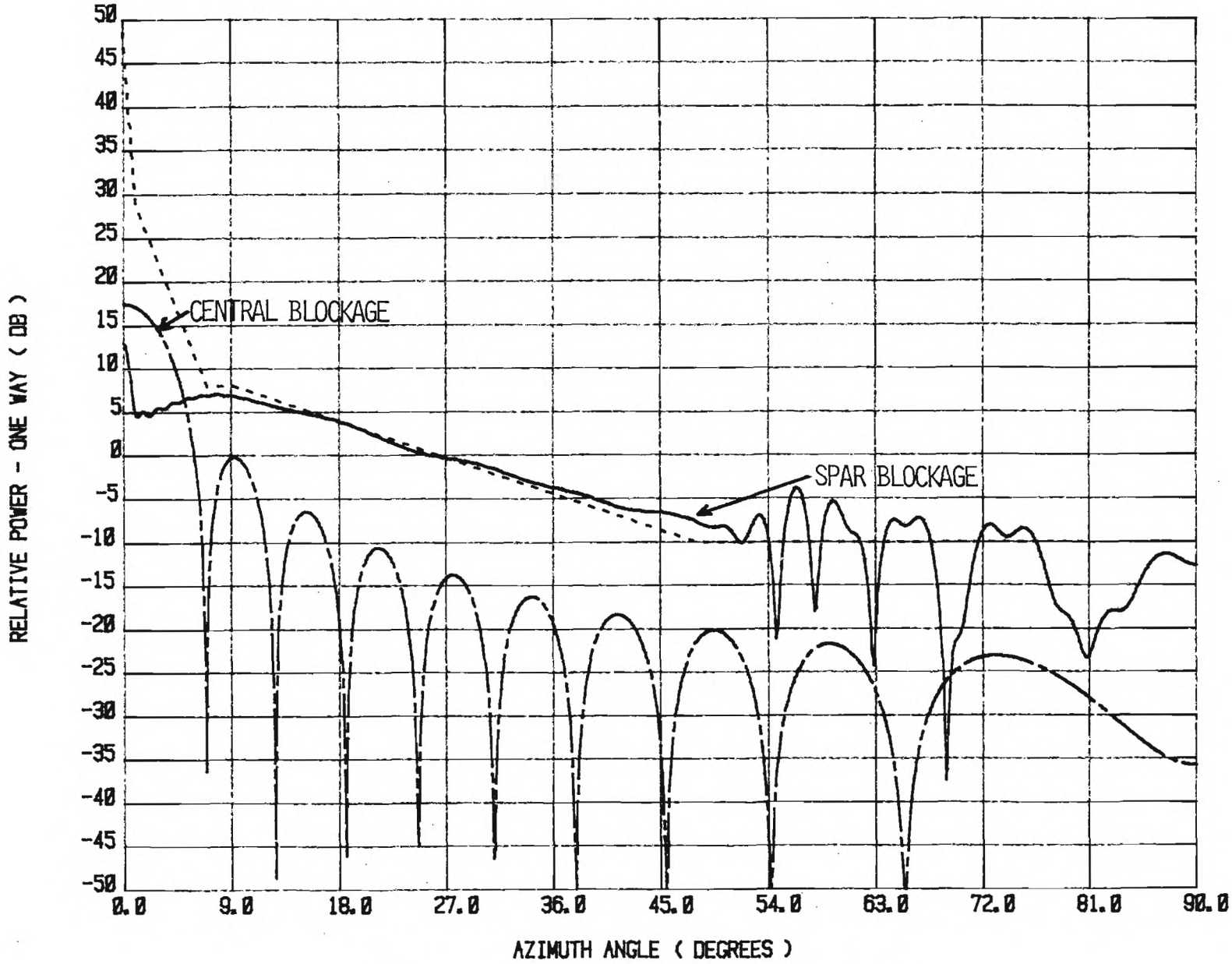

FIGURE 1-14 H-PLANE BLOCKAGE (9/16" SPARS)

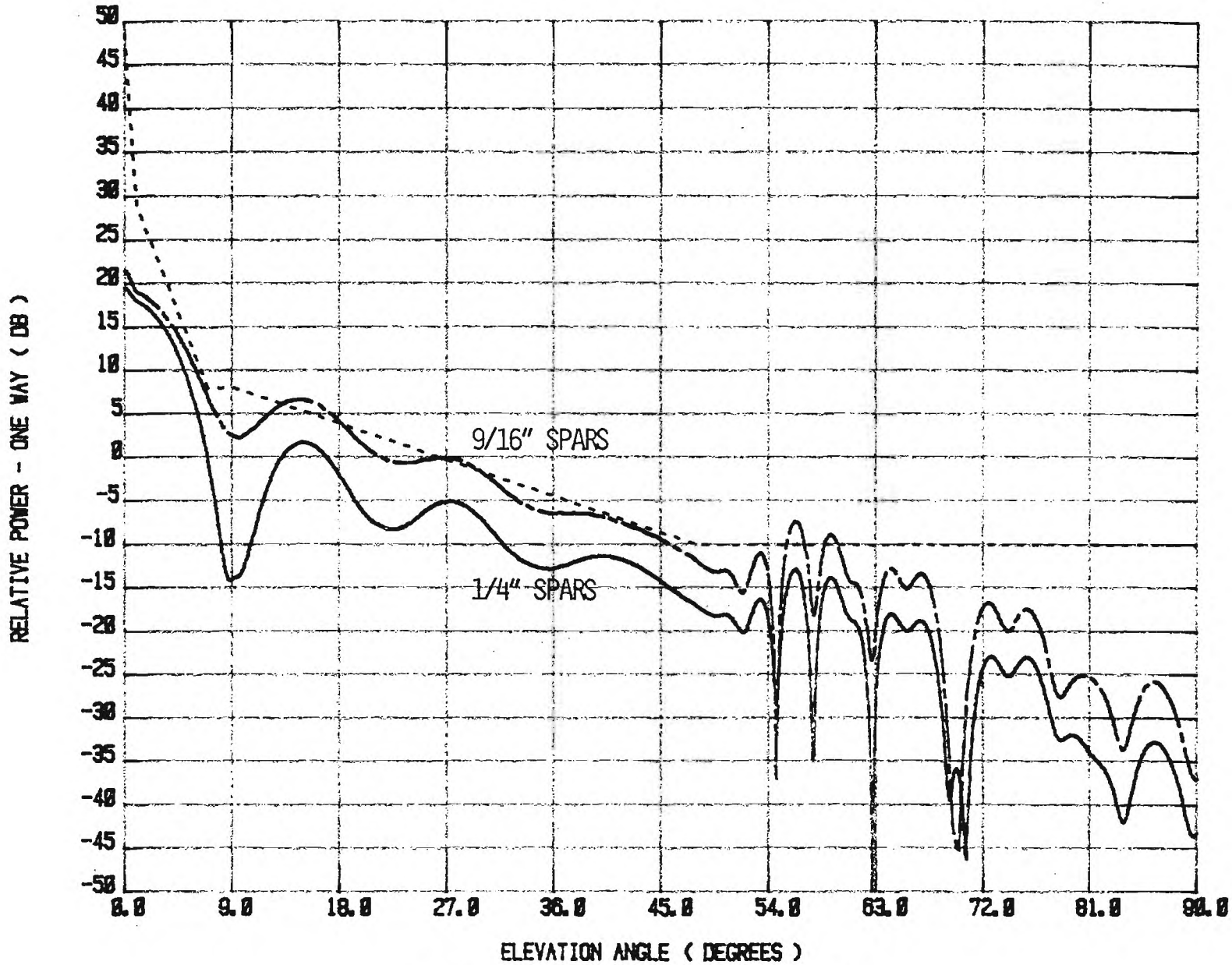

FIGURE 1-15 TOTAL E-PLANE BLOCKAGE

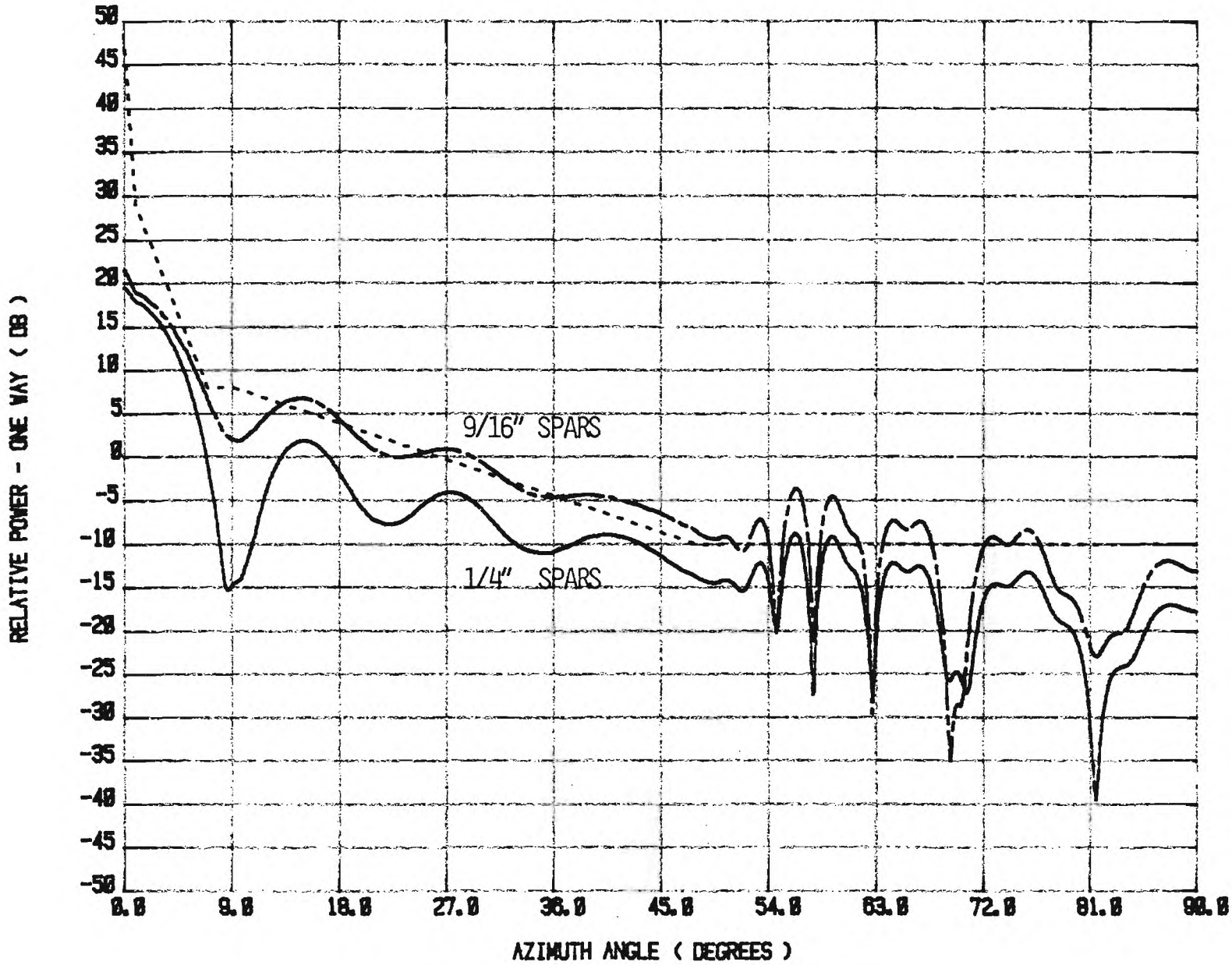

FIGURE 1-16 TOTAL H-PLANE BLOCKAGE

1.3.3 CASSEGRAIN ANTENNA DESIGN

A cassegrain antenna is useful when the feed is necessarily long or when it is desirable to attach electronics or a polarization rotation device directly to the feed. Also, if the subreflector can be supported from the feed itself (similar to a Cutler feed) or from the center of the main dish, the blockage produced by spars or other feed support can be eliminated. Because of these advantages the dual-reflector approach with the subreflector supported from the feed is selected for the present application.

A disadvantage of the traditional Cassegrain geometry is that the edge illumination at the main reflector is essentially the same as the edge taper on the subreflector. If low feed spillover past the subreflector is required, then the edge illumination on the main reflector also is low. The aperture illumination can be controlled independently if the reflector surfaces are allowed to vary from the traditional paraboloid and hyperboloid of the Cassegrain antenna. As a result synthesized, dual-reflector surfaces are popular for achieving arbitrary aperture illuminations with a given feed pattern incident on the subreflector. However, in this application the main reflector is constrained to be a paraboloid. Figure 1-17 shows the basic Cassegrain geometry and lists three design options.

Table 1-2 draws a comparison for the three Cassegrain antenna options. Option 1 is closest to meeting the desired edge taper since the subreflector taper is within .5dB of desired and the achieved main dish taper is within 3 dB of desired. However, the desired gain is not achieved. Option 2 meets the desired gain but misses the subreflector taper by slightly over 3 dB and the main reflector taper by approximately 12.7dB without considering any additional contributions to the sidelobes in this angular region (110°-120°). Option 3 meets the desired gain marginally. The subreflector taper is within 2 dB of desired which meets the requirement. The main dish taper is within 9.4 dB of desired which is marginal considering the design goal of 10 dB limit for sidelobes exceeding the envelope. In addition to direct feed spillover at the subreflector half angle, all three options are marginal in the region of 48° to 54° as the feed sidelobes appear at these angles with an intensity almost equal to the required envelope. The interpretation of "marginal" implies that the specification is achieved theoretically, but in practice unforeseen conditions or events make the theoretical specification physically unattainable with a high level of confidence. For example, many experiments work in the laboratory under controlled conditions but are not able to be duplicated under field conditions. It is therefore desirable to have sufficient margin in the theoretical predictions to allow for this discrepancy. Table 1-3 summarizes the specification compliance for each Cassegrain option. Option 3 is selected for the prototype design since it is the only option which meets all the specifications although the gain and the sidelobe levels are marginal.

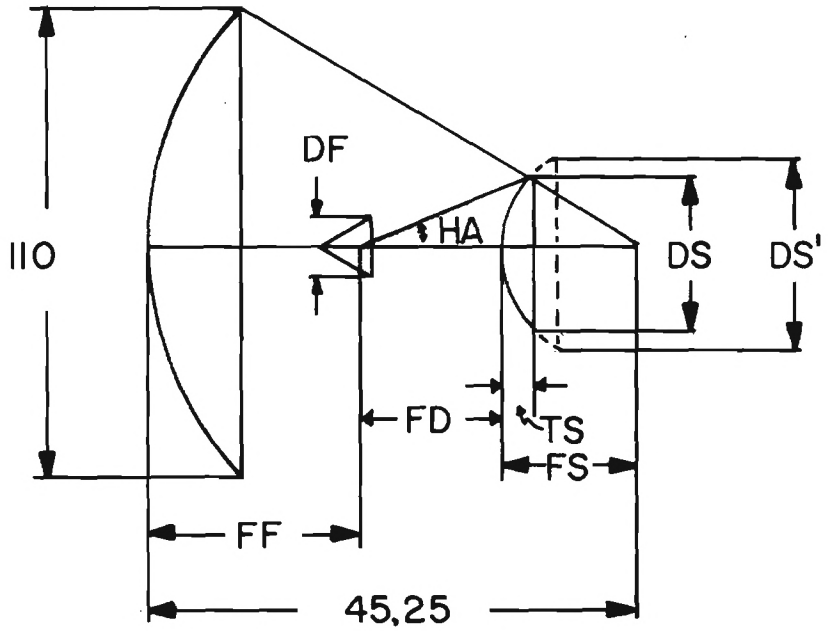

DIMENSION	OPTION 1	OPTION 2	OPTION 3
HA	38.25°	20.0°	22°
DS	11.5	11.0	11.5
DS'	12.0	11.5	11.5
FF	34.97	27.29	28.04
FD	6.54	13.92	13.04
FS	3.73	4.04	4.17
TS	.75	1.19	1.19
DF	2.4	4.0	4.0

NOTE: ALL DIMENSIONS ARE IN INCHES
UNLESS OTHERWISE SPECIFIED

FIGURE 1-17

CASSEGRAIN ANTENNA OPTIONS

Table 1-2 Comparison of Illumination Properties of Cassegrain Antenna Options

	Option 1	Option 2	Option 3
Feed Gain (dBi)	16.3	20.7	20.7
Subreflector/Main Dish Edge Taper (dB)	-23.5	-18.0	-21.3
Subreflector Desired Taper (dB)	-23.9	-21.2	-22.3
Main Dish Desired Taper (dB)	-26.3	-30.7	-30.7

TABLE 1-3 Ku-Band Feed Compliance

SPECIFICATION		Option 1	Option 2	Option 3
Frequency 11.7-12.2 GHz		Yes	Yes	Yes
VSWR 1.3:1		*	Yes	Yes
Gain 48.5 dBi at 11.95 GHz		No	Yes	*
Sidelobes	0° - 10°	Yes	Yes	Yes
	10° - 48°	*	Yes	Yes
	48° - 180°	*	No	*
Polarization (Dual-Linear)		Yes	Yes	Yes
Axial Ratio 35 dB on axis		Yes	Yes	Yes
Isolation (Port-to-Port) 30 dB		Yes	Yes	Yes
Feed Interface WR-75		Yes	Yes	Yes
G/T at 20° Elev. 22 dB/°K		*	No	*

* The specification is met theoretically but with no margin.

Aperture blockage is another design consideration for the Cassegrain antenna, as with a prime focus antenna. Spars are not used in the proposed design; rather, a light-weight subreflector supported by a low-loss, low-dielectric material is envisioned. Central blockage is therefore the only concern. Aperture blockage affects both the gain and the first sidelobe level. In a Cassegrain geometry the blockage caused by the feed diameter must be compared with the blockage of the subreflector. For a given geometry the feed may actually shadow a larger portion of the main reflector than the subreflector. For a multimode feed horn the diameter of the feed typically is larger than for a single-mode horn because higher order modes must be supported in the feed aperture. Therefore, the normal tradeoff between subreflector diameter and feed diameter becomes even more critical.

A feed diameter of four inches shadows approximately the same diameter on the main reflector as a 12 inch diameter subreflector. The size of the feed shadow depends on the distance of the feed from the subreflector, as well as the diameter of the aperture. The closer the feed is to the subreflector, the greater the angle of the reflected ray intercepted (or blocked) by the feed and consequently the larger the shadow. However, the farther the feed is from the subreflector, the larger the feed aperture must be to maintain the same edge taper on the subreflector and consequently the shadow can not be decreased simply by moving the feed farther away. Both factors (distance and diameter) must be considered simultaneously for a given set of illumination conditions.

A parameter which also influences the distance of the feed from the subreflector is the location of the phase center inside the feed. If the phase center is coincident with the feed aperture, the shadow diameter is simply

$$D_B = \frac{8F}{d} S[\frac{1}{cos(\alpha)} - 1].$$

where F is the focal length of the paraboloid, d is the diameter of the feed, S is the distance from the focal point to the feed aperture , and 2α is the angle subtended by the feed measured from the focal point. If the phase center is inside the feed by a distance P, the shadow diameter is then

$$D_B = \frac{8F}{d} (S+P)[\frac{1}{cos(\alpha)} - 1].$$

The feed is effectively moved closer to the subreflector by a distance equal to the distance the phase center is inside the feed. Therefore, the farther inside the feed the phase center is, the larger the area shadowed by the feed.

2.0 TEST AND EVALUATION OF THE PROTOTYPE DESIGN

2.1 DESCRIPTION OF THE PROTOTYPE DESIGN

The prototype design is a Cassegrain antenna with a multimode feed horn and a subreflector supported by a dielectric cone. Table 2-1 gives the dimensions and coordinates for the Cassegrain geometry. Three types of subreflector support are considered. Type 1 is a 0.038-inch thick fiberglass cone which clamps around the feed and flares out to the diameter of the subreflector. Slots are cut in the narrow end of the cone to allow focus adjustment for the subreflector. Type 2 is identical to Type 1 with the exception that the fiberglass layer is 0.013 inch thick. Type 3 is a polyurethane foam cylindrical block which is hollowed out at one end for the feed diameter and cut out at the other end to conform to the shape of the subreflector.

Based on preliminary test results, a requirement exists for a vertex tuning plate on the subreflector to meet the VSWR specification. Since the distance between the feed and the subreflector is small (approximately ten wavelengths) a large reflection is produced at the subreflector which is directed back into the feed. The vertex plate cancels a significant portion of the reflection by adding a 180° phase shift to part of the returned energy. The phase shift is accomplished by adjusting the distance between the plate and the subreflector to approximately a quarter of a wavelength.

Another modification to the prototype design is a subreflector diffraction skirt. The skirt acts to block some of the subreflector spillover energy and to scatter the energy diffusely by using triangular edges (i.e., serrations) on the skirt.

TABLE 2-1 PROTOTYPE CASSEGRAIN ANTENNA DIMENSIONS AND COORDINATES

CASSEGRAIN ANTENNA OUTPUT

IAMETER OF MAIN REFLECTOR = 110.000
IAMETER OF SUBREFLECTOR = 11.5000
UBREFLECTOR HALF ANGLE = 22.0000
NGLE TO EDGE OF MAIN REFLECTOR = 62.9726
EPTH OF MAIN REFLECTOR = 16.8430
EPTH OF SUBREFLECTOR = 1.20202
OCAL LENGTH = 44.9000

EED DIAMETER = 4.00000
ISTANCE OF FEED PHASE CENTER BEHIND FEED APERTURE = .000000
ISTANCE OF FEED PHASE CENTER BEHIND DISH APERTURE = -10.8920
ISTANCE FROM FEED PHASE CENTER TO SUBREFLECTOR = 13.0298
ISTANCE FROM FOCAL POINT TO FEED PHASE CENTER = 17.1650
ISTANCE FROM FOCAL POINT TO SUBREFLECTOR EDGE = 2.93324
ISTANCE OF FEED PHASE CENTER FROM VERTEX = 27.7350
EED SHADOW DIAMETER = 10.4268

X2	Y2	X1	Y1	T1	T2
55.0000	.0000	5.7500	.0000	22.000	62.973
50.0000	2.9231	5.1076	.2314	20.043	58.217
45.0000	5.5679	4.5034	.4318	18.073	53.232
40.0000	7.9343	3.9315	.6043	16.093	48.020
35.0000	10.0223	3.3868	.7515	14.103	42.587
30.0000	11.8318	2.8644	.8754	12.104	36.946
25.0000	13.3630	2.3606	.9777	10.099	31.114
20.0000	14.6158	1.8715	1.0598	8.086	25.112
15.0000	15.5902	1.3938	1.1226	6.069	18.966
10.0000	16.2862	.9246	1.1669	4.048	12.708
5.0000	16.7038	.4609	1.1933	2.025	6.374
.0000	16.8430	.0000	1.2020	.073	-.027

2.2 PROTOTYPE TEST DATA

Figures 2-1 through 2-5 show E-plane far field patterns for the prototype design configurations. Figures 2-6 through 2-10 show H-plane patterns for the same configurations. Figures 2-11 through 2-20 show the radiation patterns on an expanded scale for each design configuration so the beamwidth and near-in sidelobe levels can be determined more accurately. Figures 2-21 through 2-24 show the primary patterns for the multimode feed. Figure 2-25 shows the return loss as the feed is moved ± 1 inch to allow for changes in position due to focusing of the subreflector.

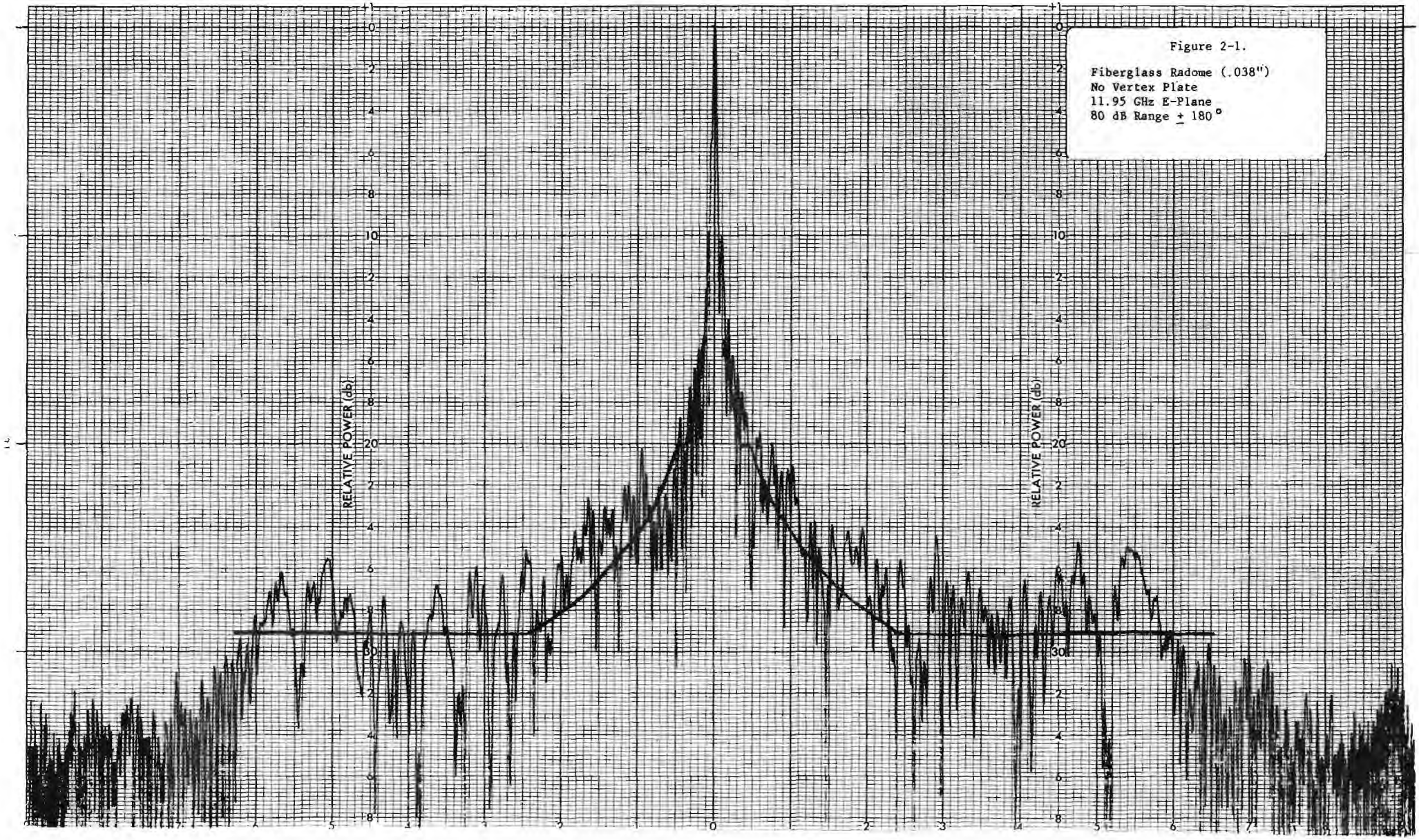

Figure 2-1.

Fiberglass Radome (.038")
No Vertex Plate
11.95 GHz E-Plane
80 dB Range ± 180°

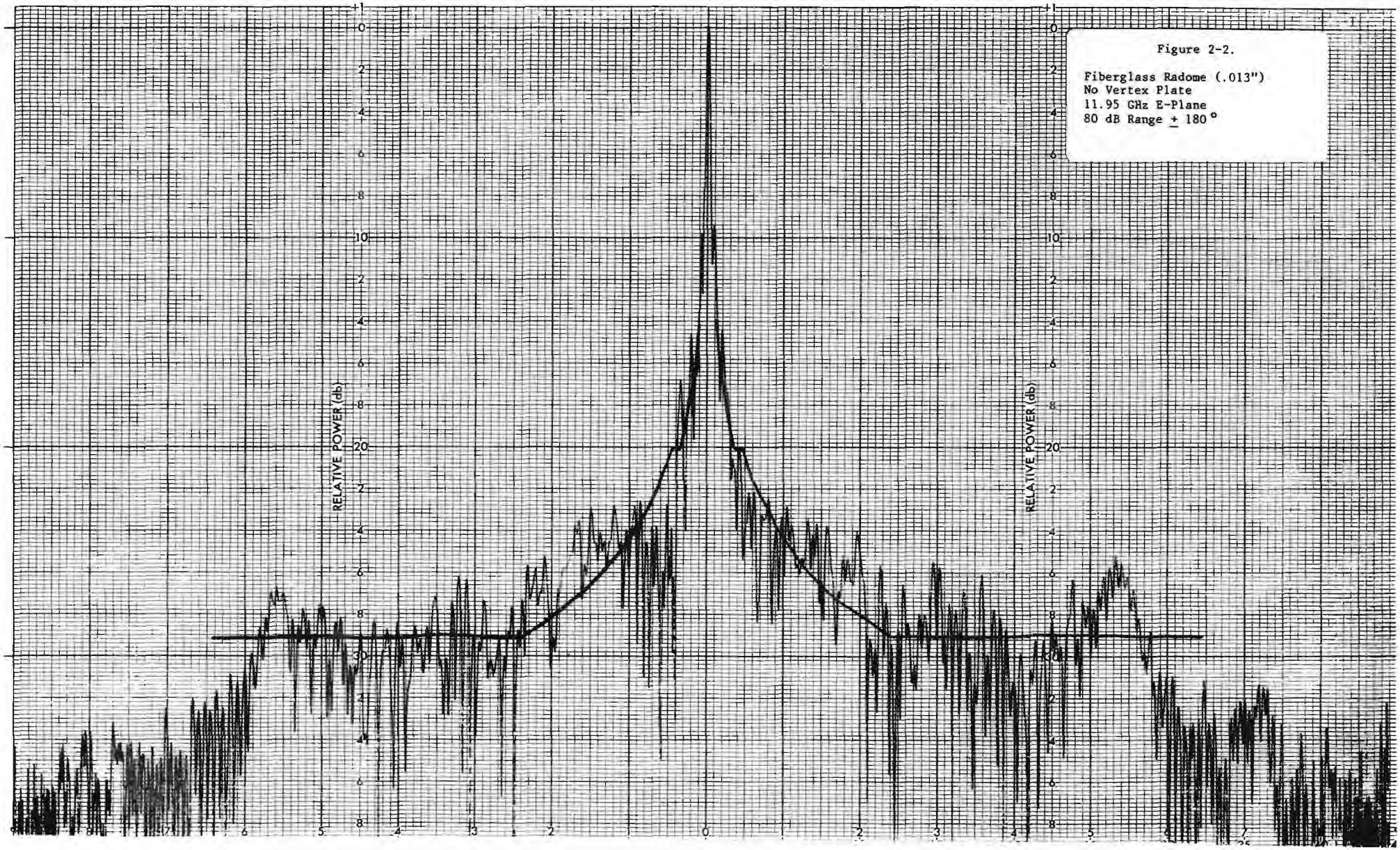

Figure 2-2.

Fiberglass Radome (.013")
No Vertex Plate
11.95 GHz E-Plane
80 dB Range ± 180°

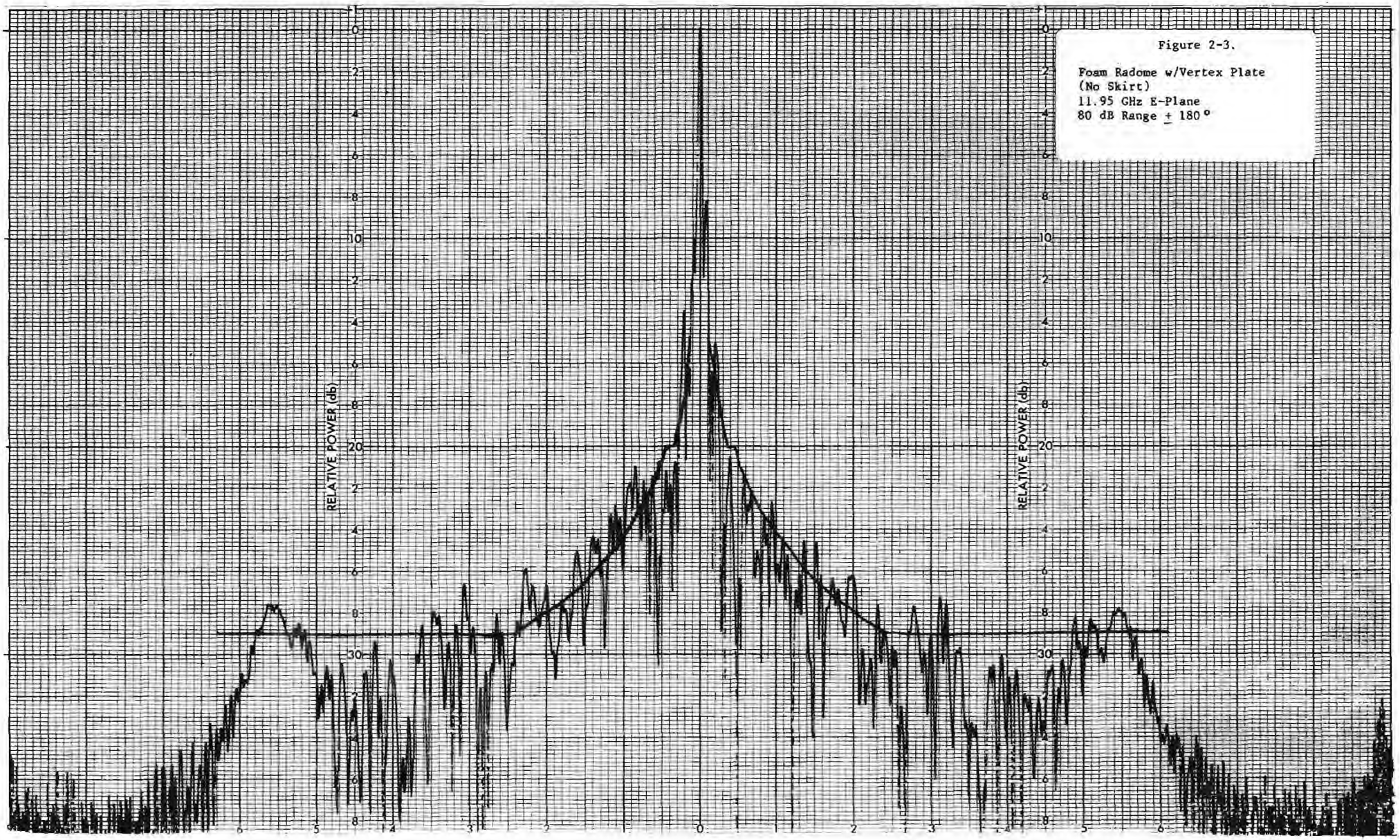

Figure 2-3.

Foam Radome w/Vertex Plate
(No Skirt)
11.95 GHz E-Plane
80 dB Range ± 180°

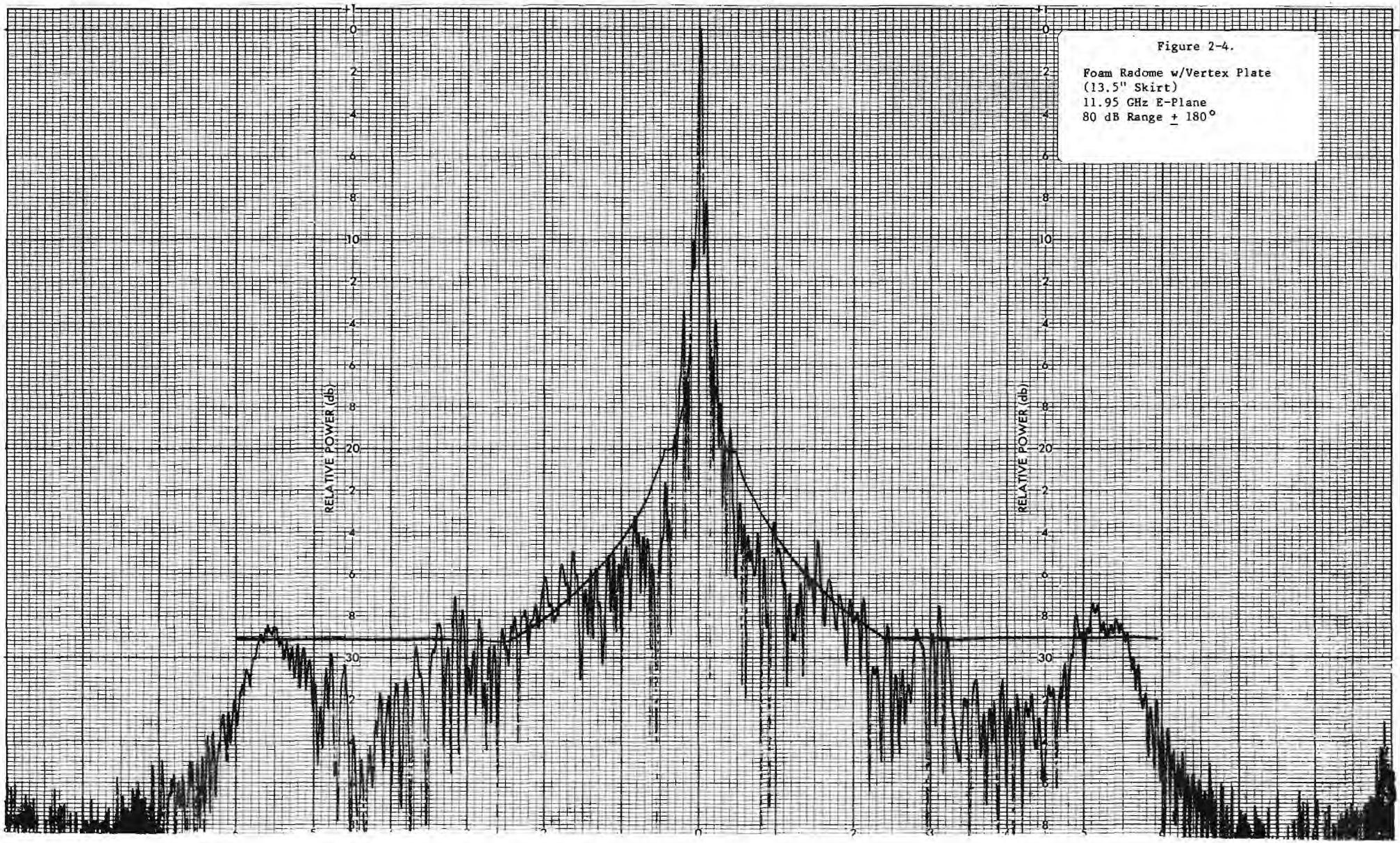

Figure 2-4.

Foam Radome w/Vertex Plate
(13.5" Skirt)
11.95 GHz E-Plane
80 dB Range ± 180°

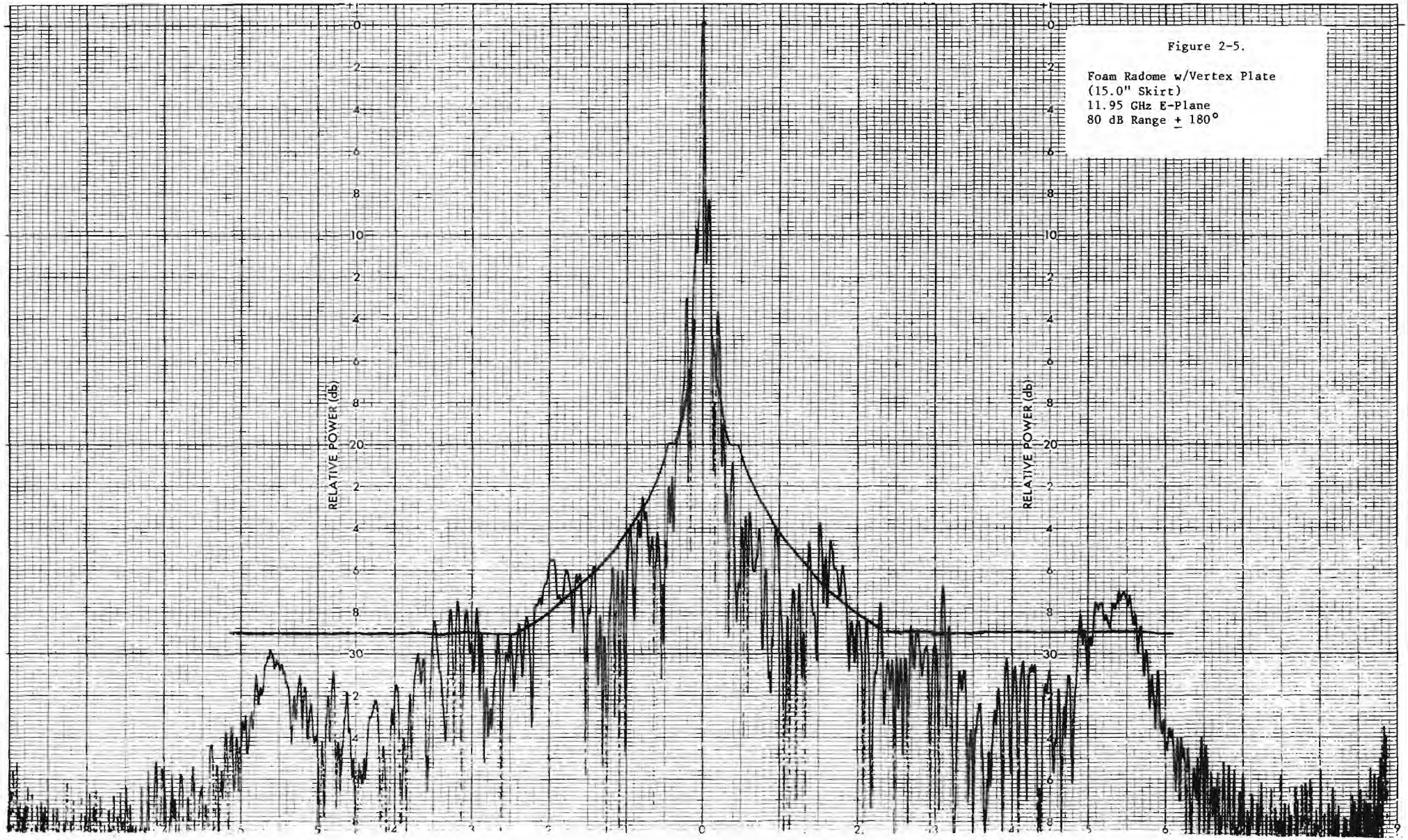

Figure 2-5.

Foam Radome w/Vertex Plate
(15.0" Skirt)
11.95 GHz E-Plane
80 dB Range ± 180°

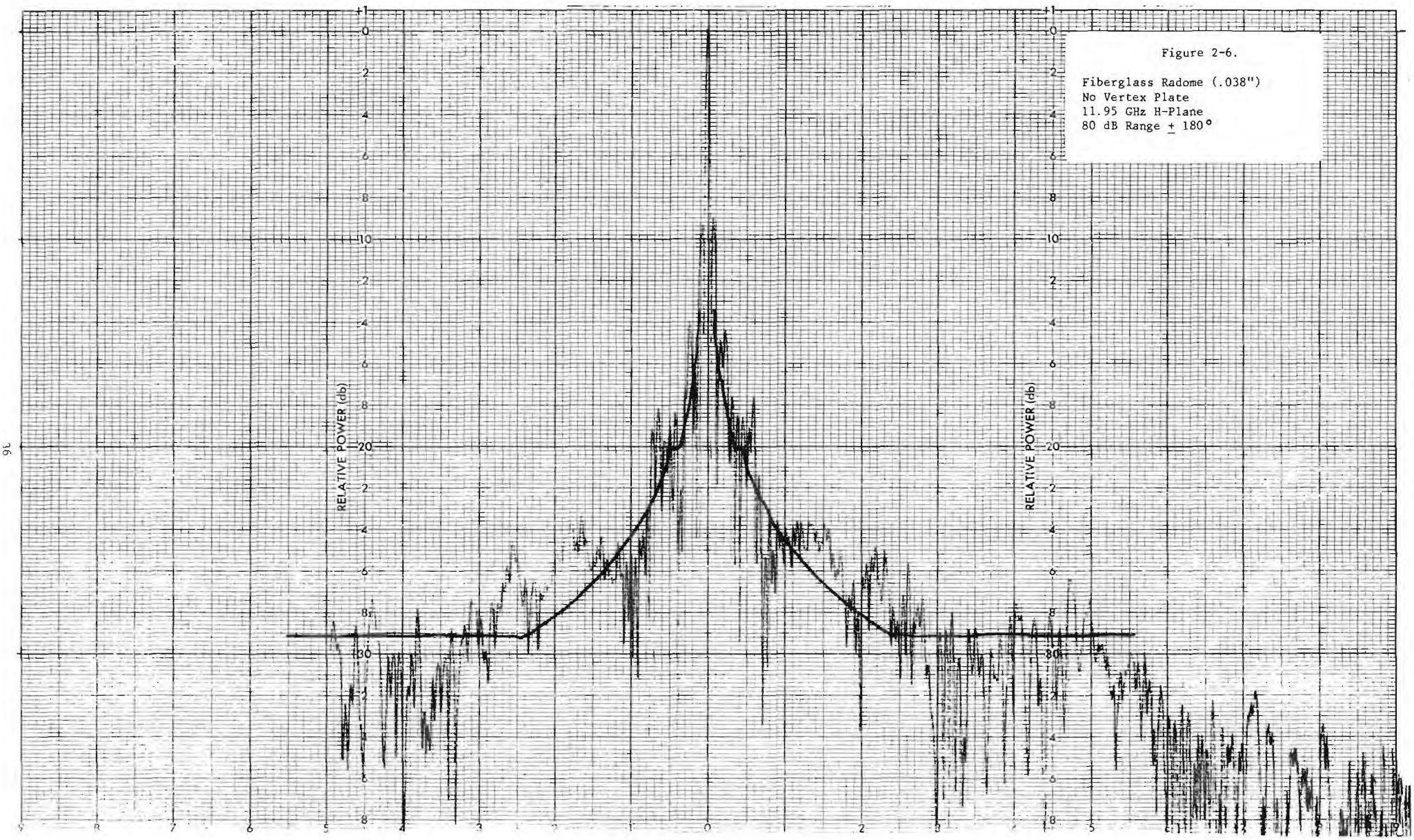

Figure 2-6.

Fiberglass Radome (.038")
No Vertex Plate
11.95 GHz H-Plane
80 dB Range ± 180°

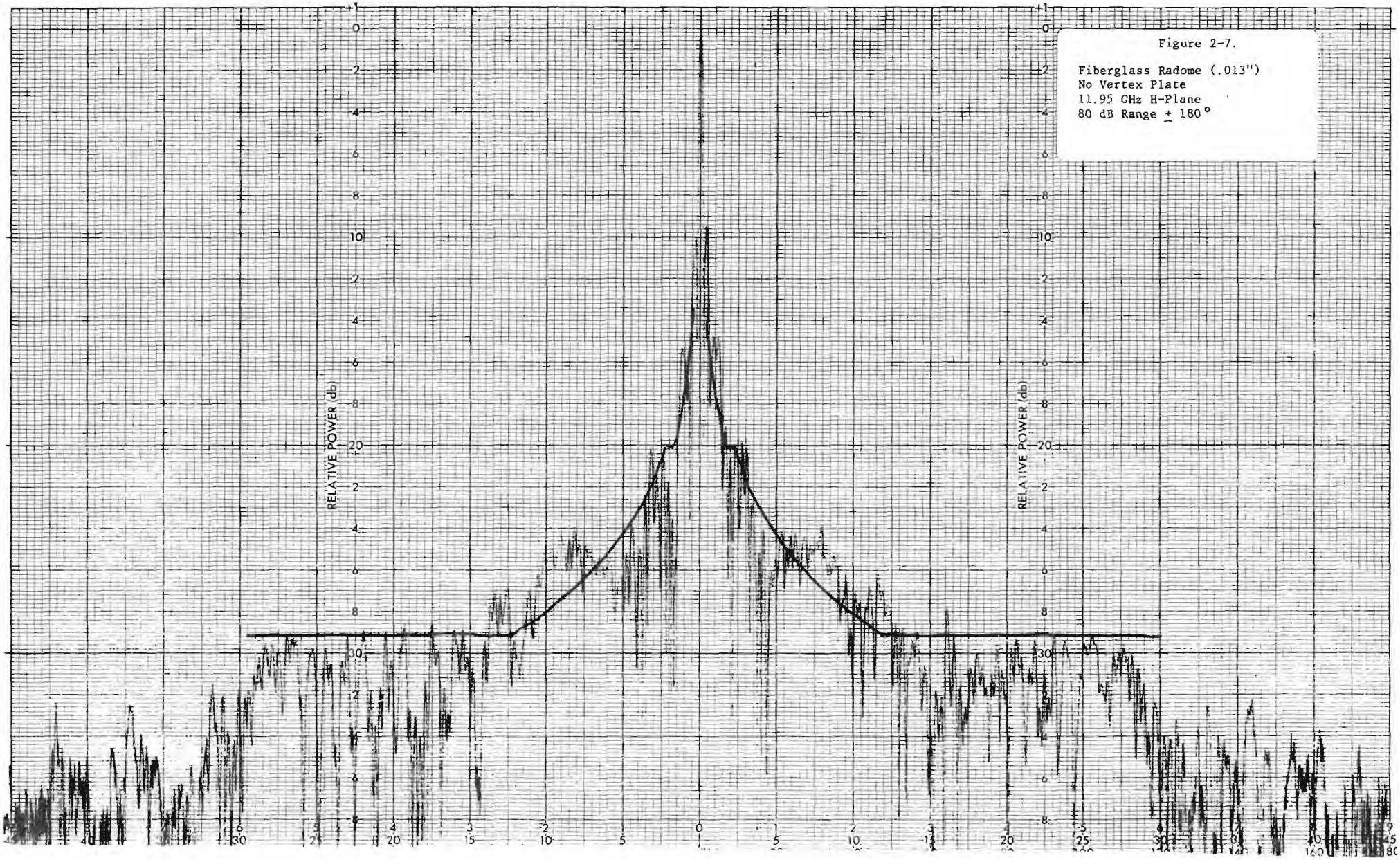

Figure 2-7.

Fiberglass Radome (.013")
No Vertex Plate
11.95 GHz H-Plane
80 dB Range ± 180°

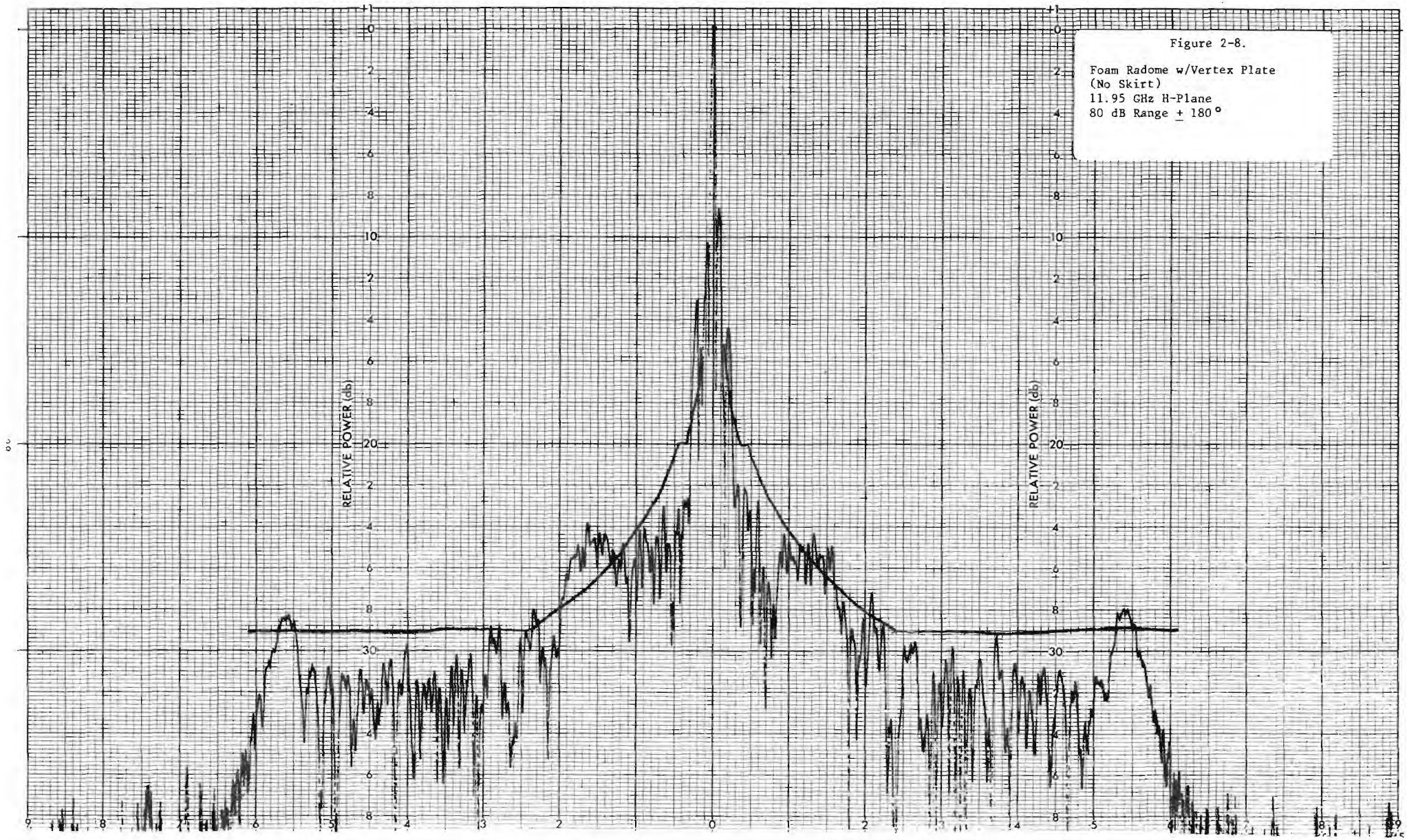

Figure 2-8.

Foam Radome w/Vertex Plate
(No Skirt)
11.95 GHz H-Plane
80 dB Range ± 180°

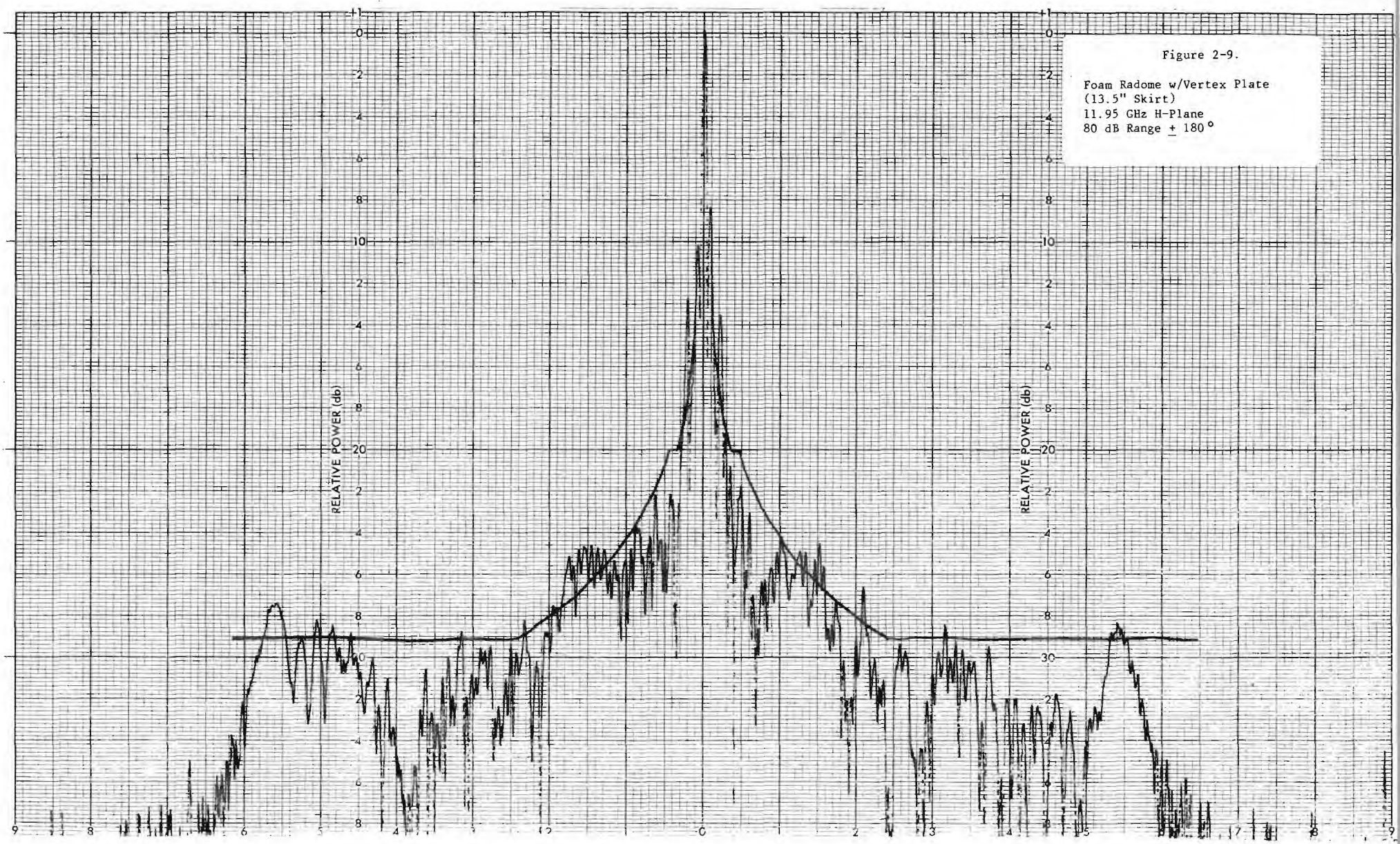

Figure 2-9.

Foam Radome w/Vertex Plate
(13.5" Skirt)
11.95 GHz H-Plane
80 dB Range ± 180°

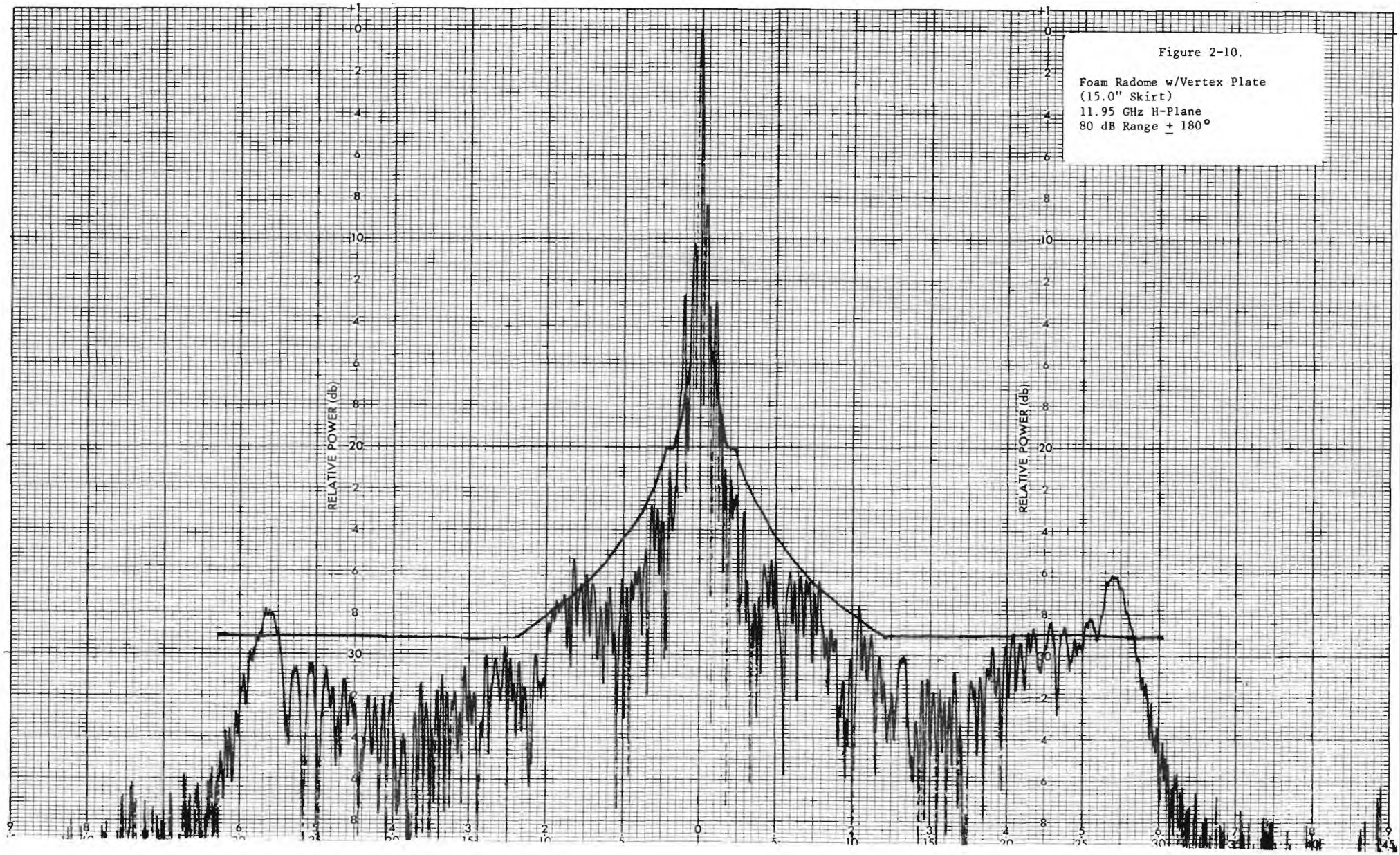

Figure 2-10.

Foam Radome w/Vertex Plate
(15.0" Skirt)
11.95 GHz H-Plane
80 dB Range ± 180°

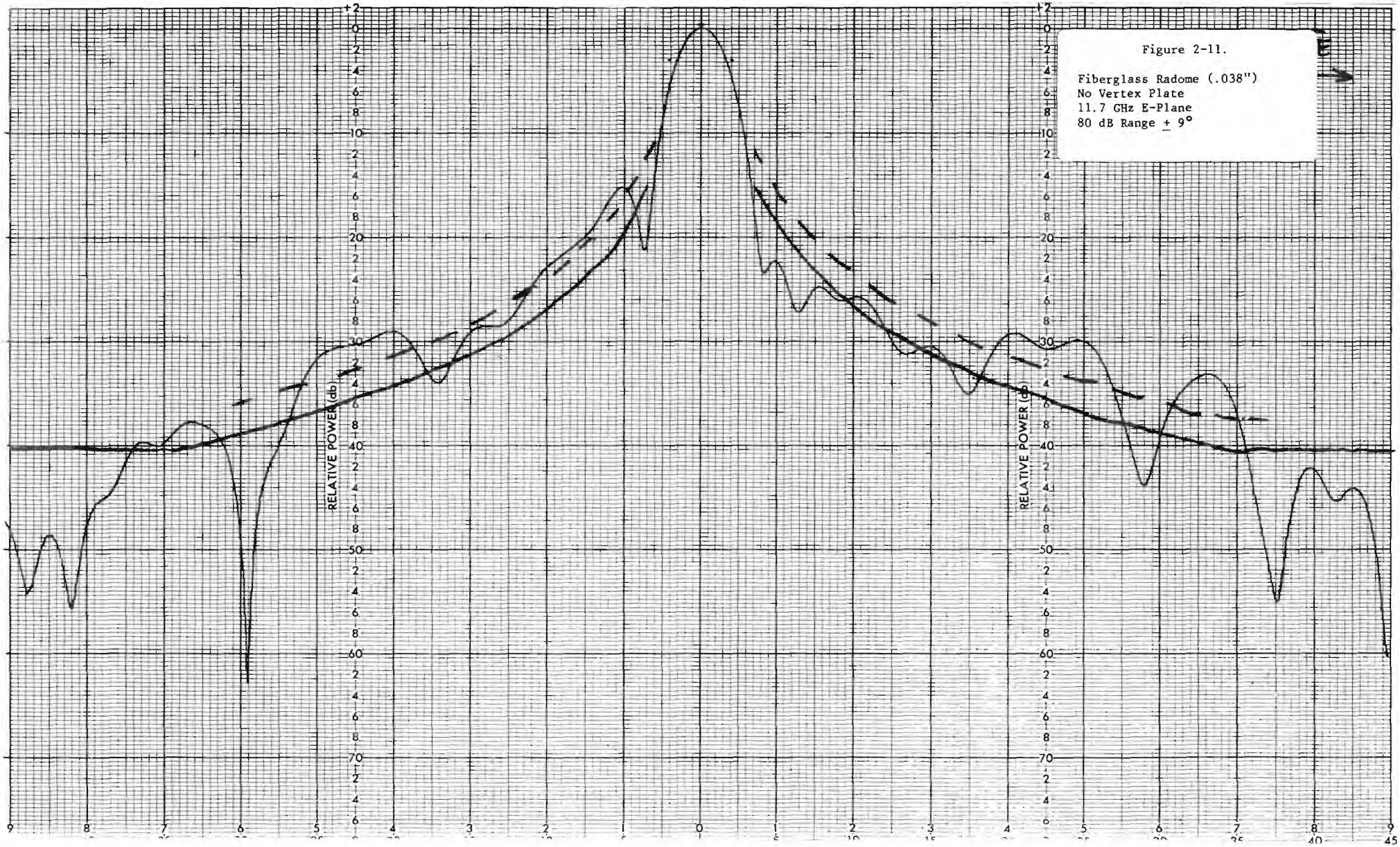

Figure 2-11.

Fiberglass Radome (.038")
No Vertex Plate
11.7 GHz E-Plane
80 dB Range ± 9°

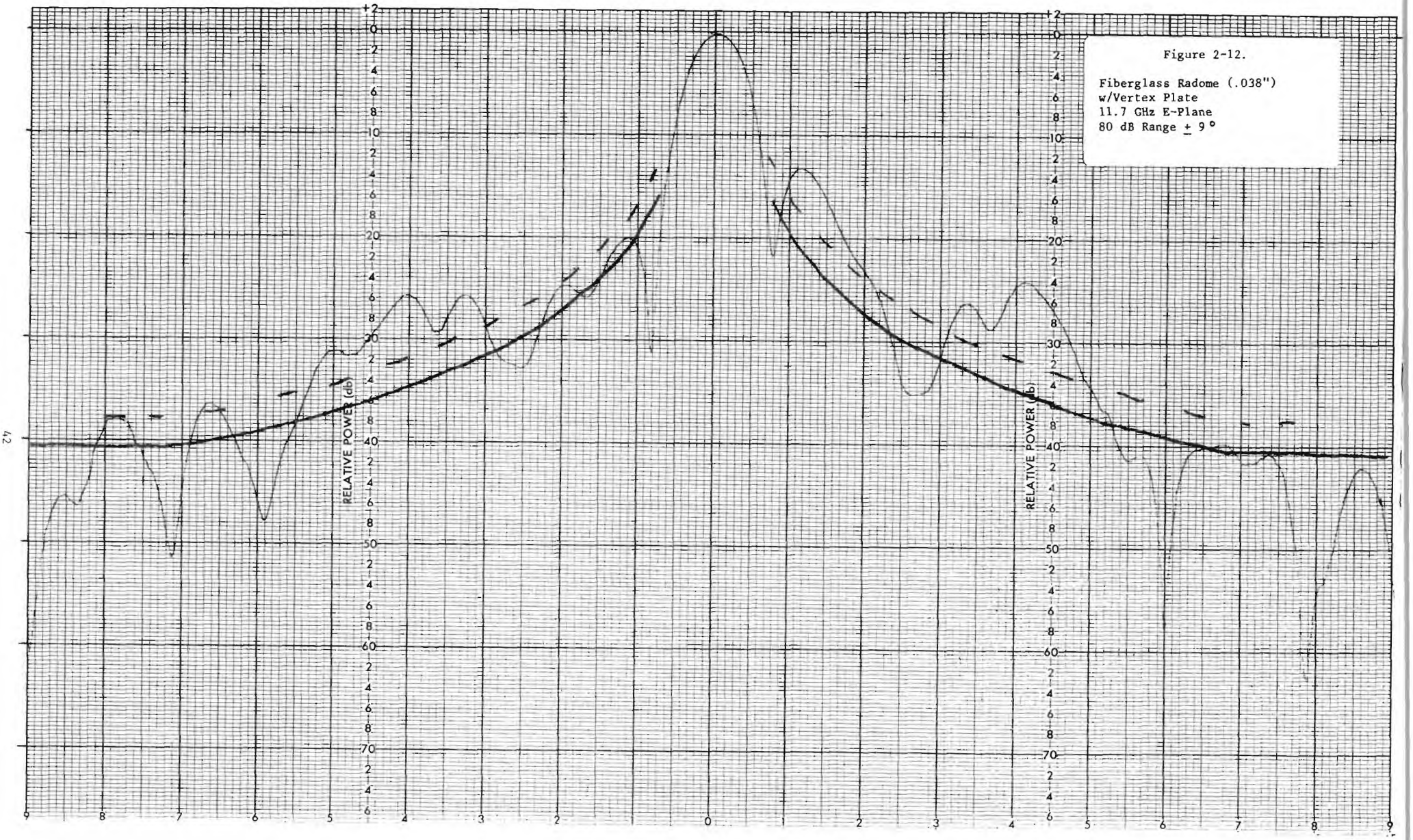

Figure 2-12.

Fiberglass Radome (.038")
w/Vertex Plate
11.7 GHz E-Plane
80 dB Range ± 9°

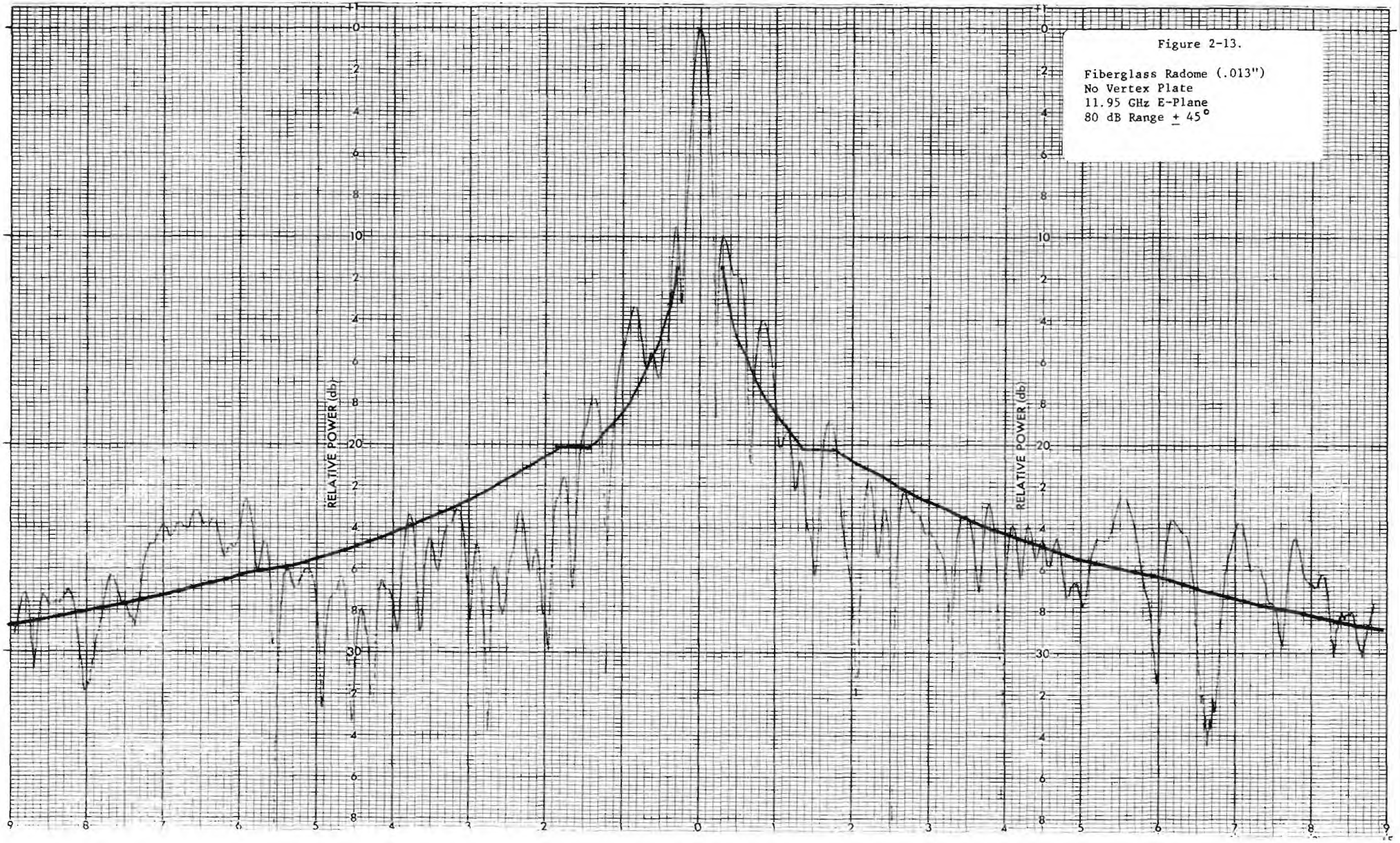

Figure 2-13.

Fiberglass Radome (.013")
No Vertex Plate
11.95 GHz E-Plane
80 dB Range ± 45°

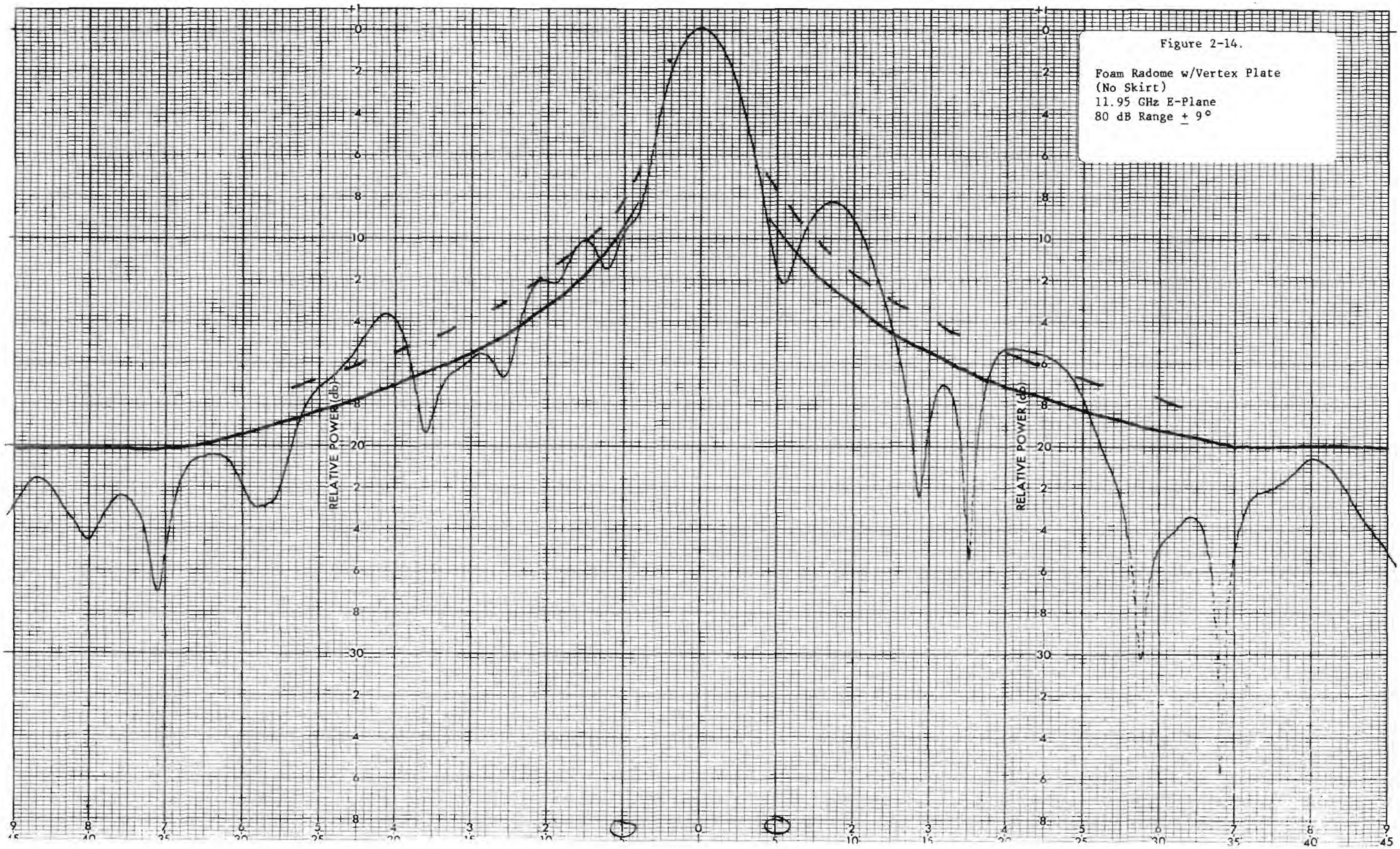

Figure 2-14.

Foam Radome w/Vertex Plate
(No Skirt)
11.95 GHz E-Plane
80 dB Range ± 9°

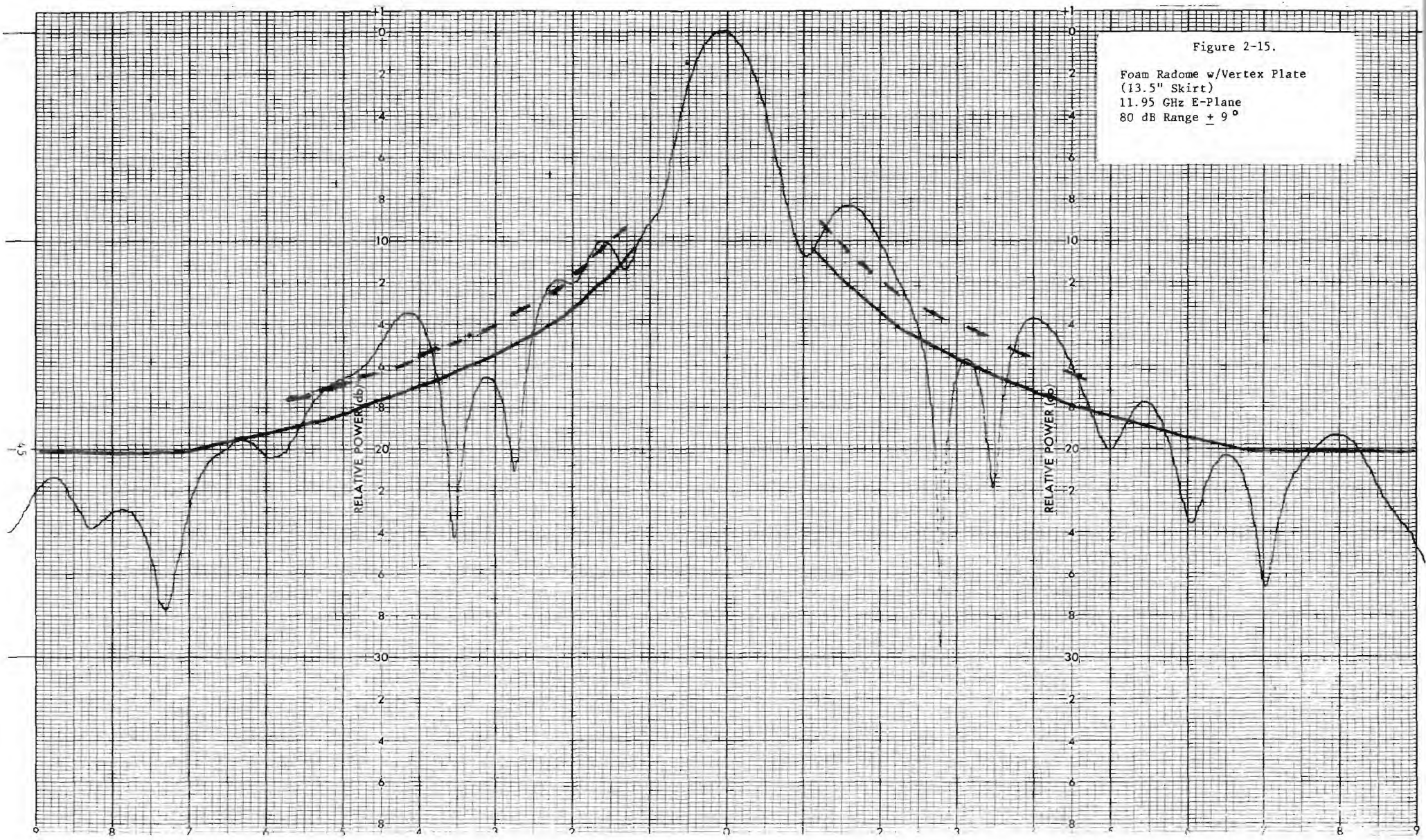

Figure 2-15.

Foam Radome w/Vertex Plate
(13.5" Skirt)
11.95 GHz E-Plane
80 dB Range ± 9°

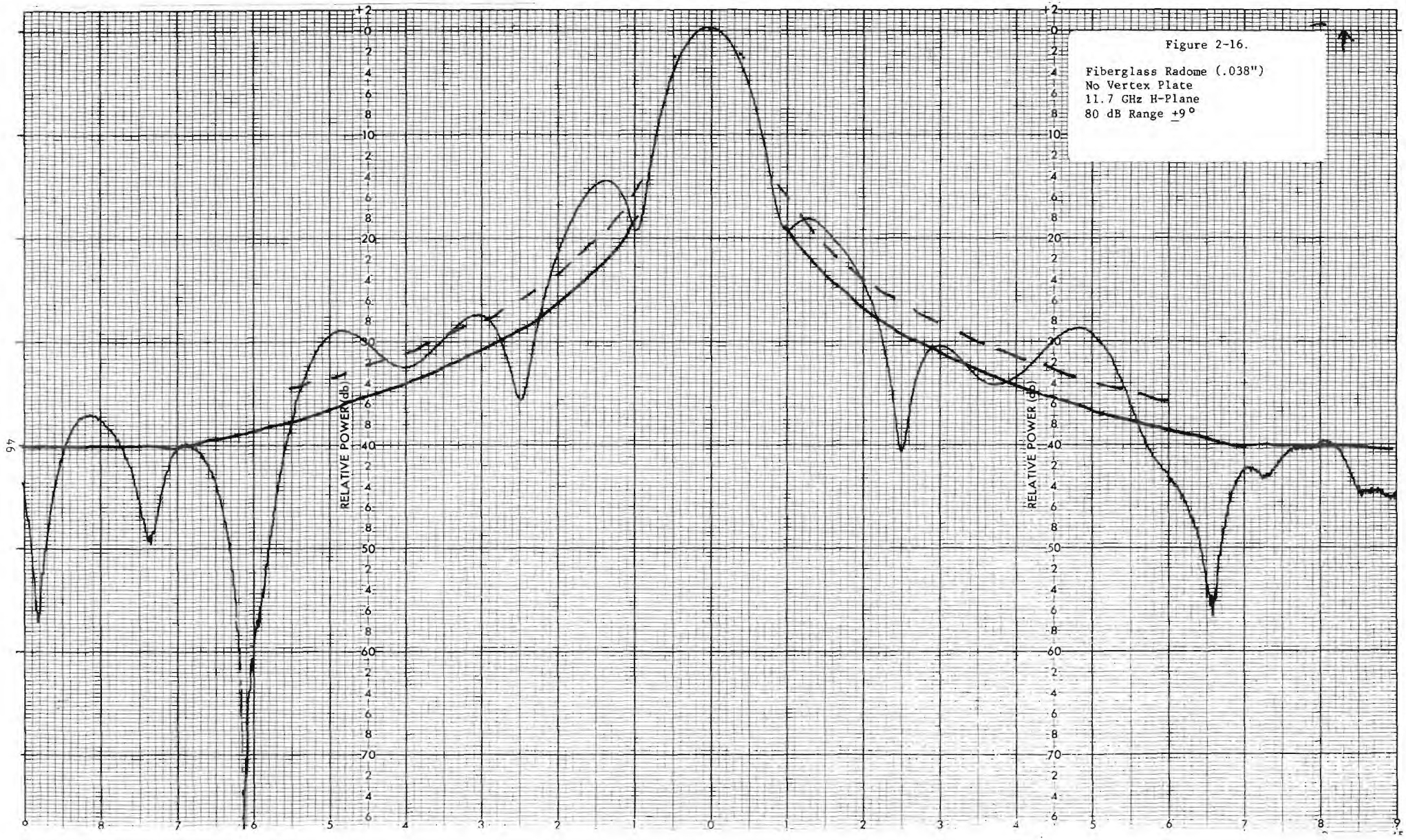

Figure 2-16.

Fiberglass Radome (.038")
No Vertex Plate
11.7 GHz H-Plane
80 dB Range ±9°

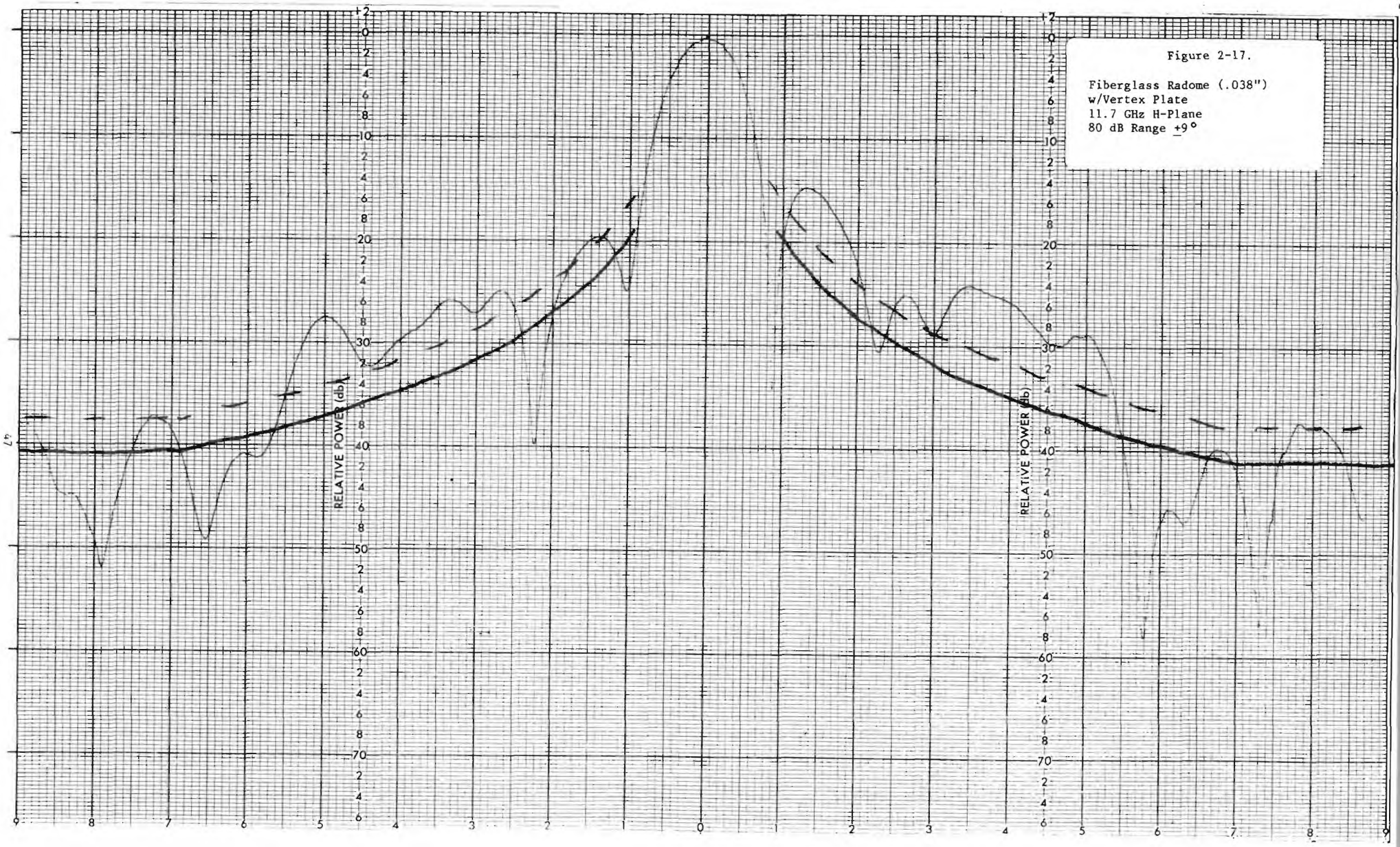

Figure 2-17.

Fiberglass Radome (.038")
w/Vertex Plate
11.7 GHz H-Plane
80 dB Range ±9°

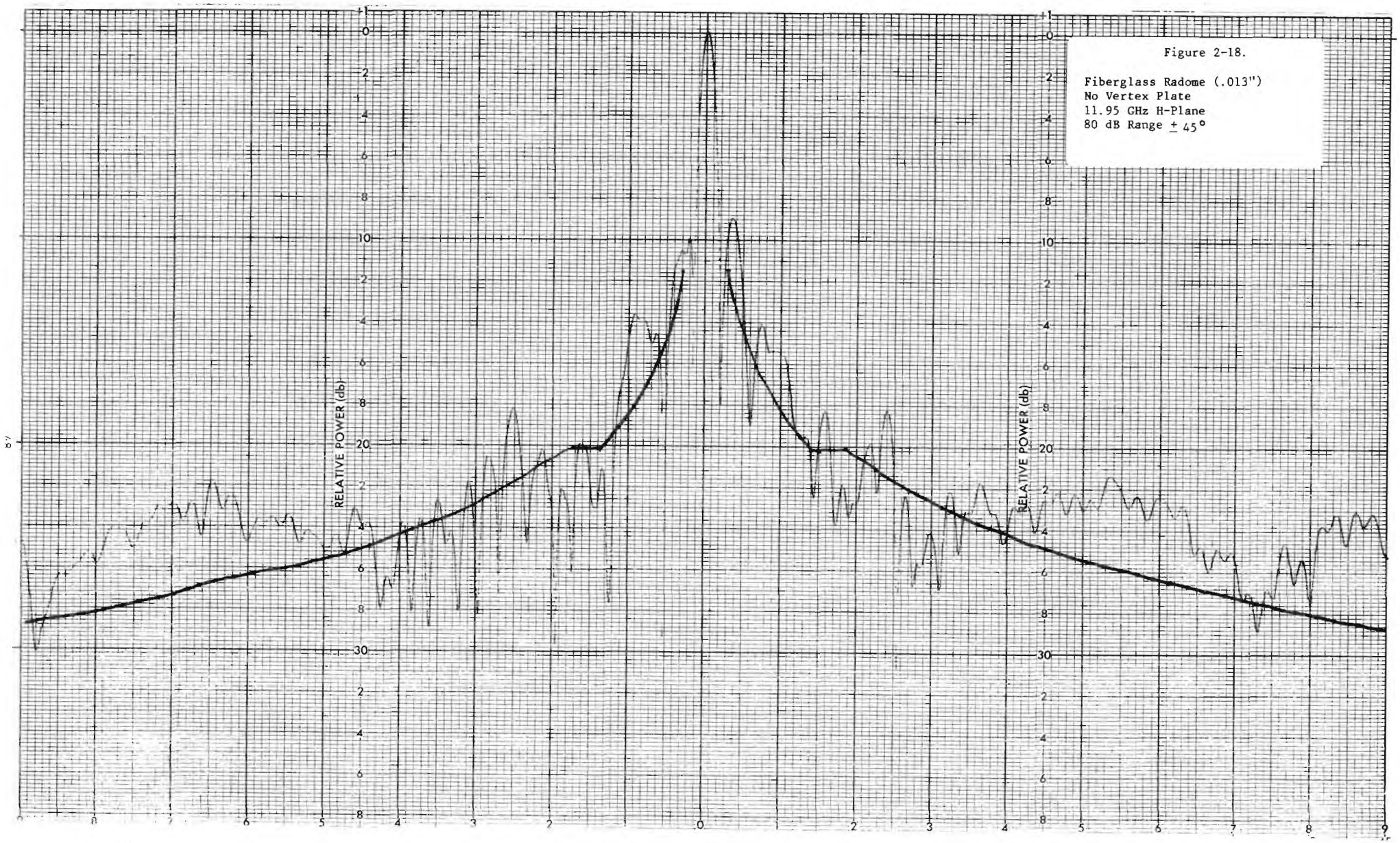

Figure 2-18.

Fiberglass Radome (.013")
No Vertex Plate
11.95 GHz H-Plane
80 dB Range ± 45°

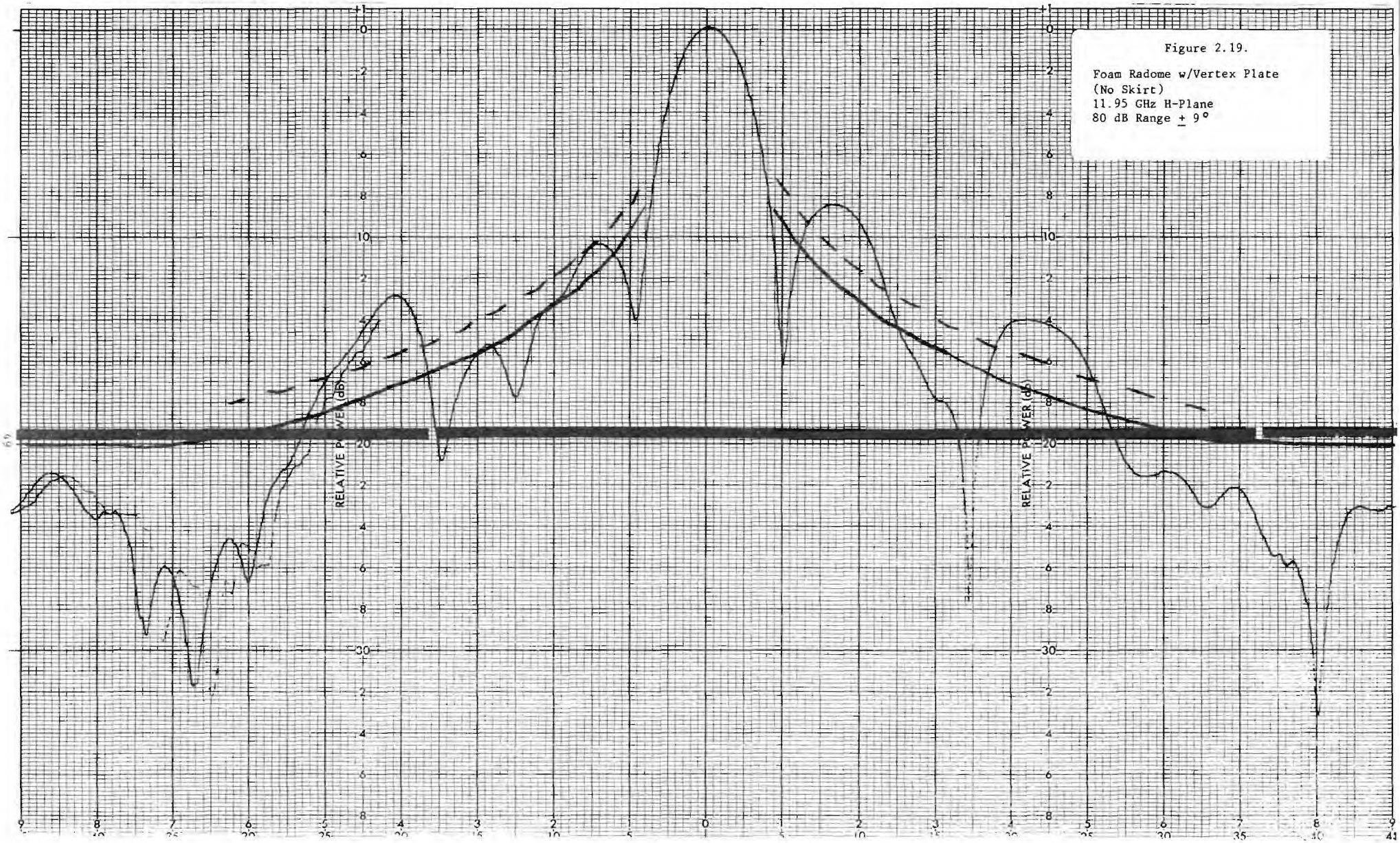

Figure 2.19.

Foam Radome w/Vertex Plate
(No Skirt)
11.95 GHz H-Plane
80 dB Range ± 9°

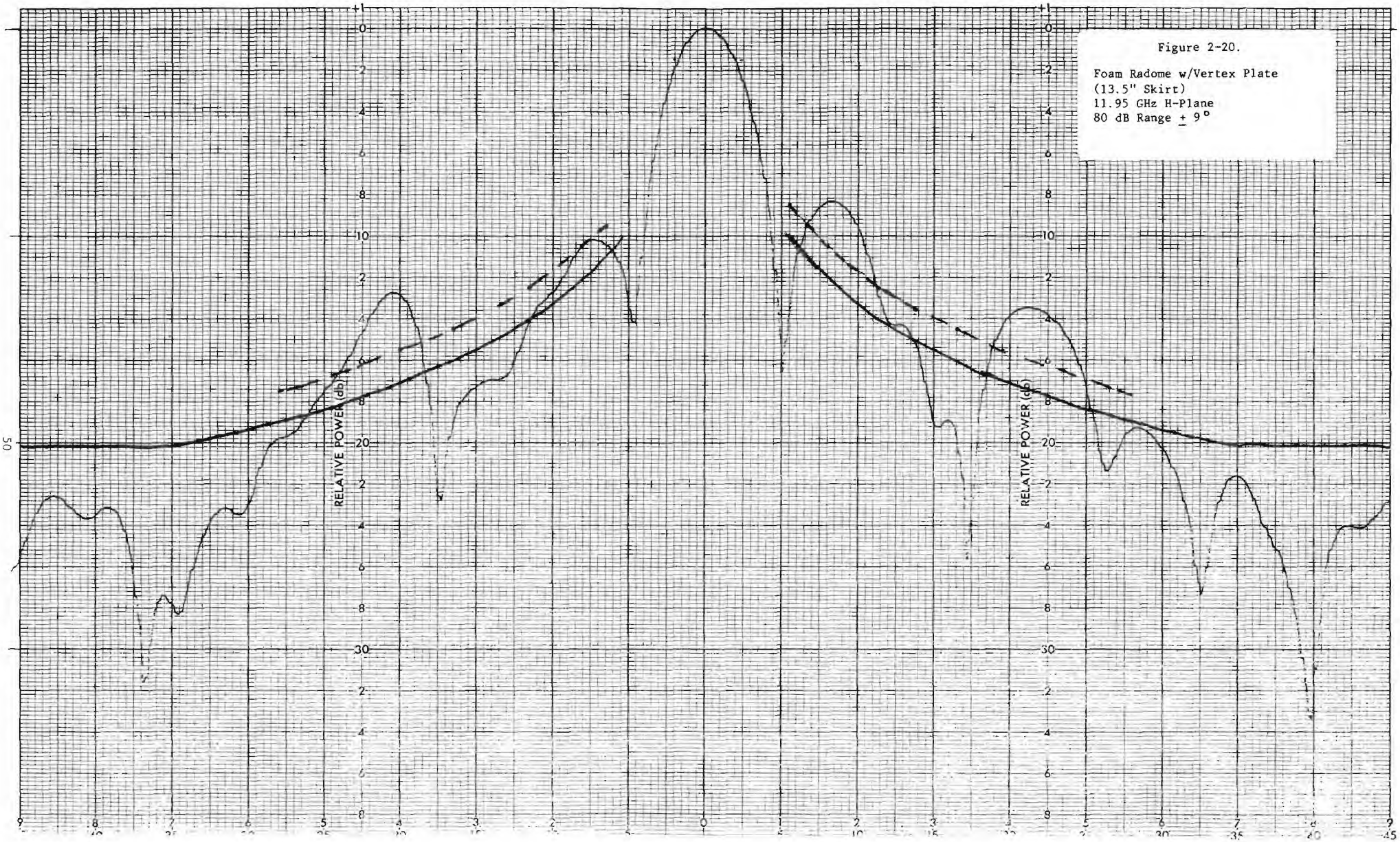

Figure 2-20.

Foam Radome w/Vertex Plate
(13.5" Skirt)
11.95 GHz H-Plane
80 dB Range ± 9°

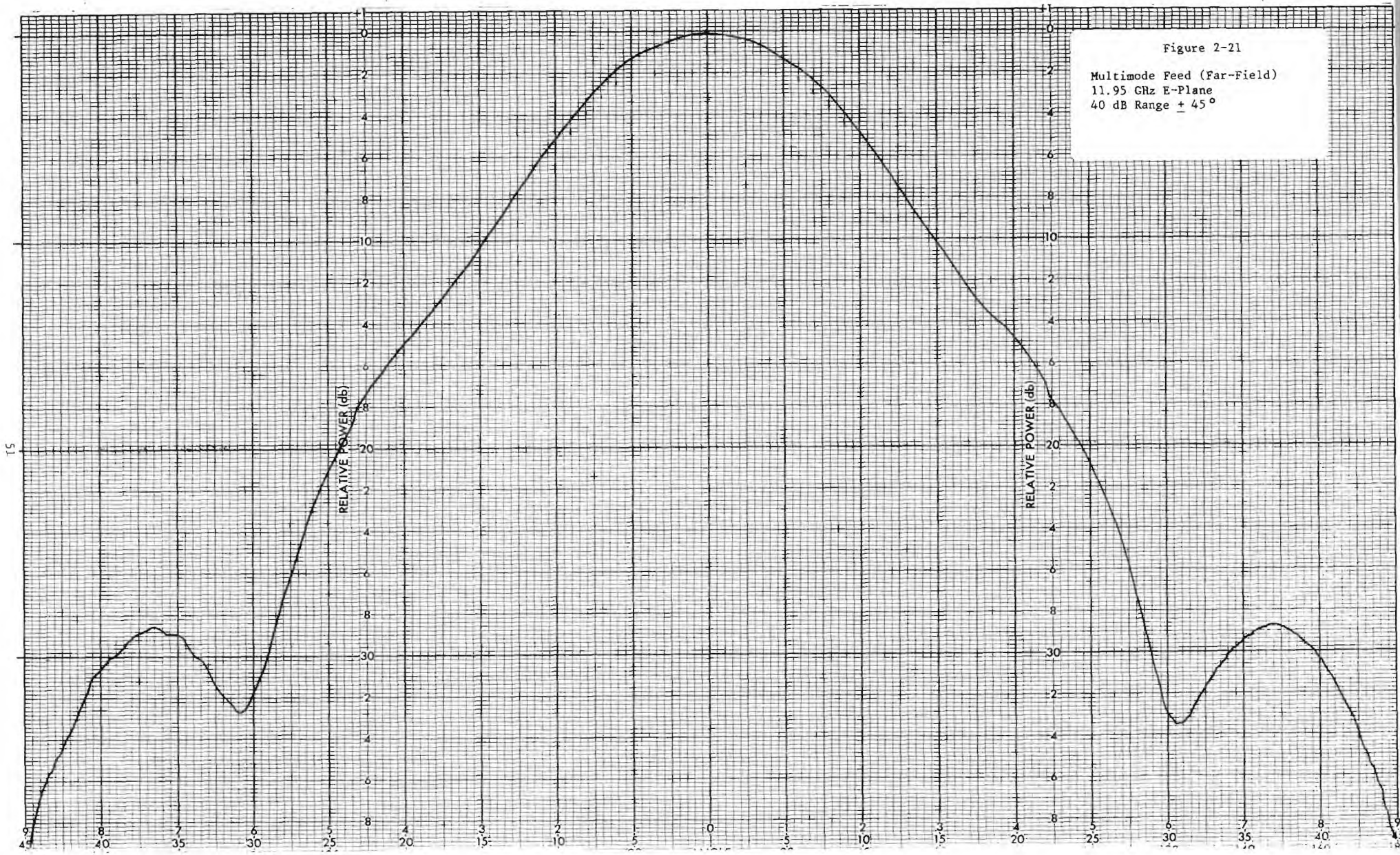

Figure 2-21

Multimode Feed (Far-Field)
11.95 GHz E-Plane
40 dB Range ± 45°

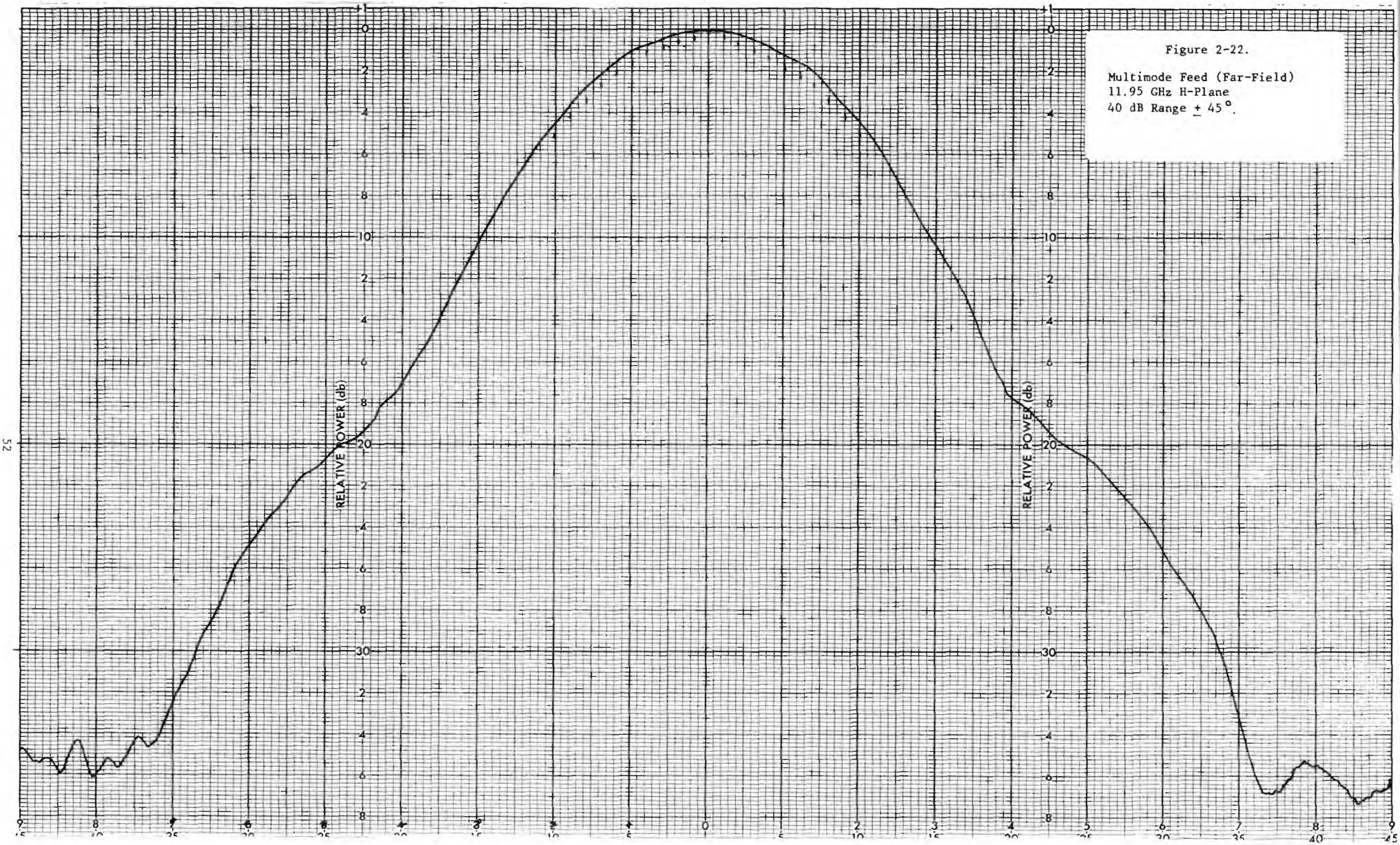

Figure 2-22.

Multimode Feed (Far-Field)
11.95 GHz H-Plane
40 dB Range ± 45°.

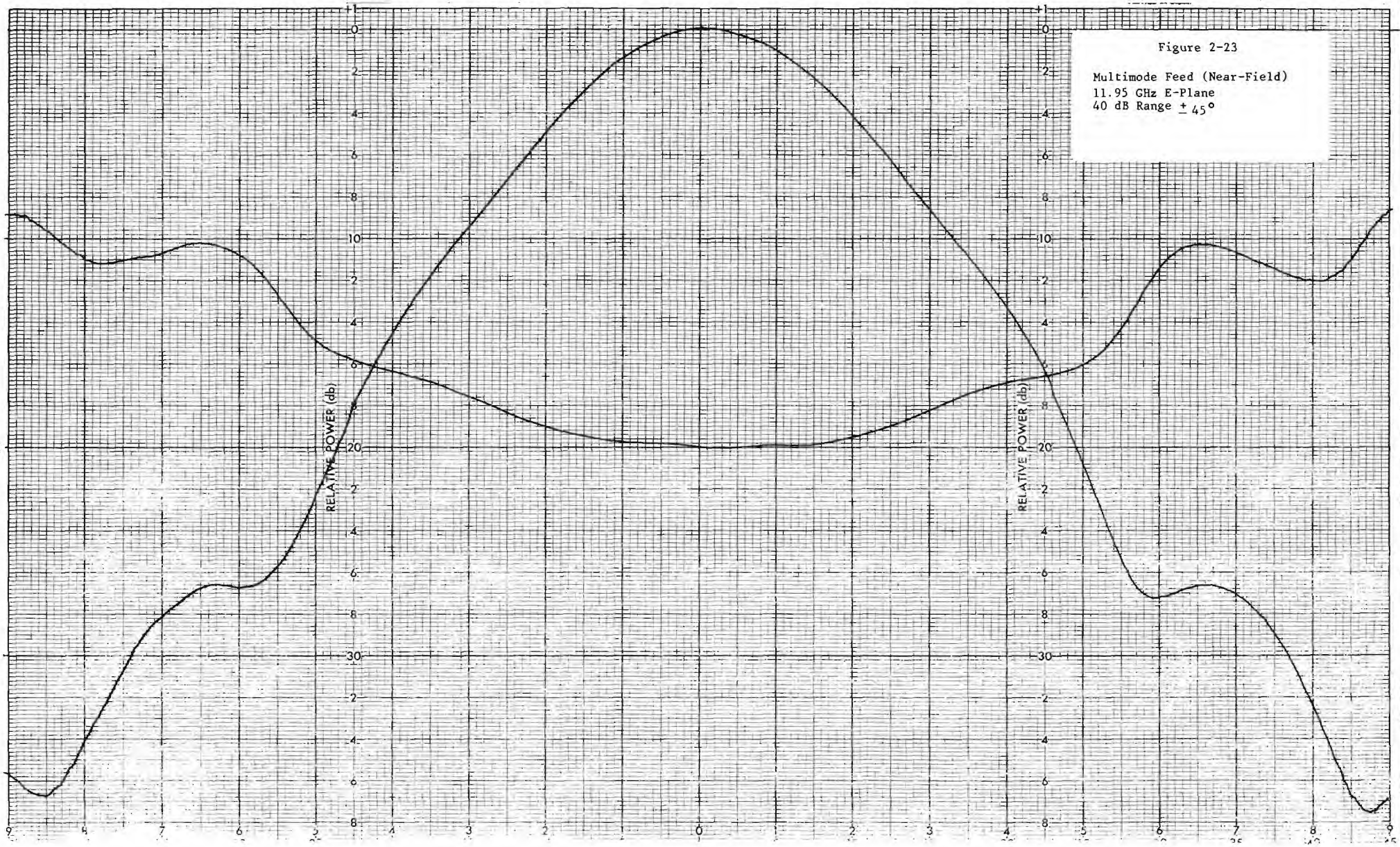

Figure 2-23

Multimode Feed (Near-Field)
11.95 GHz E-Plane
40 dB Range ± 45°

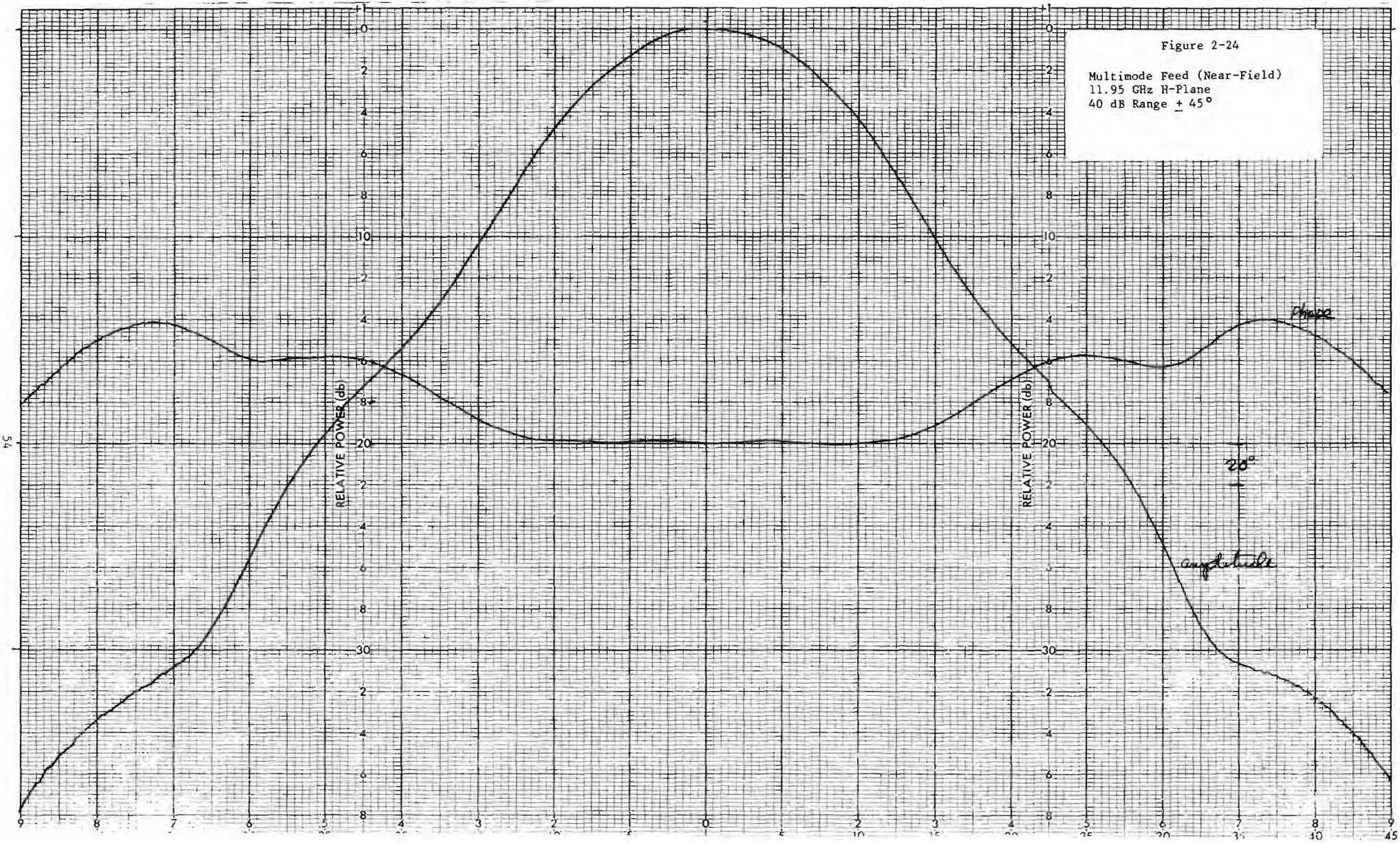

Figure 2-24

Multimode Feed (Near-Field)
11.95 GHz H-Plane
40 dB Range ± 45°

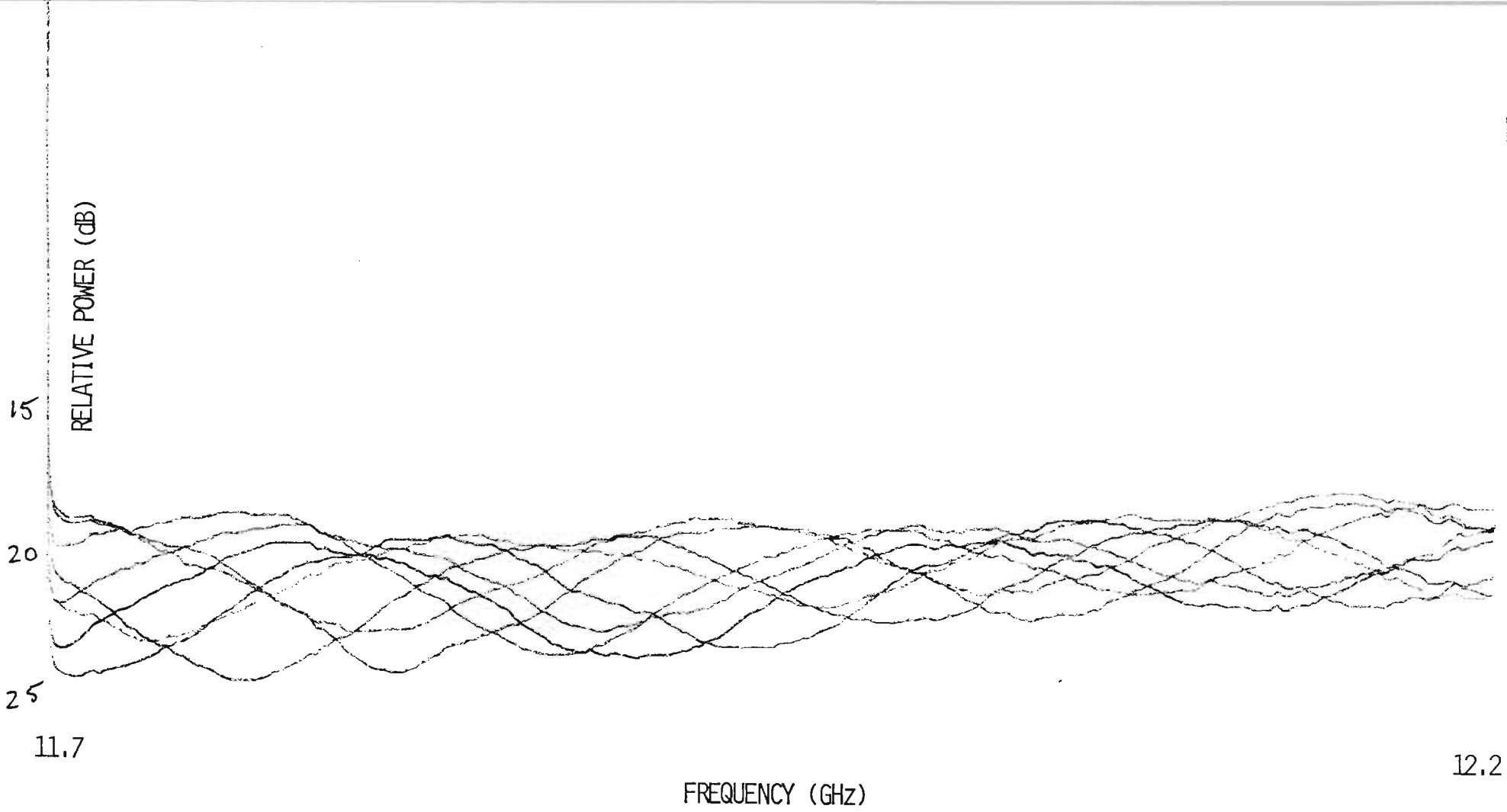

FIGURE 2-25 FEED AND SUBREFLECTOR RETURN LOSS

2.3 EVALUATION OF THE PROTOTYPE TEST RESULTS

Table 2-2 presents a summary of the test data for each of the prototype design configurations. Table 2-3 describes the performance of each configuration with respect to gain and sidelobe criteria. The recommended approach for further testing is a foam-supported subreflector or a thin-walled radome support. Since a thin-walled structure is too weak to support the subreflector, the foam support is preferred. Also, the thin walled radome is susceptible to internal reflections which appear as randomly scattered energy in the far-field pattern.

A comparison of the measured feed pattern with a predicted feed pattern is shown in Figure 2-26 for the E-plane and in Figure 2-27 for the H-plane. The ideal feed pattern is shown in Figure 2-28. The feed design could be improved by eliminating the phase dispersion between the TE_{11} and TM_{11} modes and by further attenuating the TE_{12} mode. The predicted feed patterns are based on far-field pattern calculations for modes in a circular aperture [4]. A more thorough analysis which involves greater complexity of formulation considers the finite flare angle of the horn and the related phase error in the feed aperture [5]. However, the difficulty of predicting the exact amplitude and phase of the higher order modes is not treated in either of these cases. The potential exists for further reseach in this area.

Table 2-2

Comparison of Measured Data for SA Ku-Band Antennas

Feed: Multimode Stepped

Date: March 10, 1983

RADOME	VERTEX PLATE	SKIRT	H.P.B.W. (Degrees)		SIDELOBE LEVELS*						GAIN (dB)
					E			H			
			E	H	1^{o}-10^{o}	10^{o}-48^{o}	48^{o}-180^{o}	1^{o}-10^{o}	10^{o}-48^{o}	48^{o}-180^{o}	
Fiberglass (.038")	N	N	.64	.75	5	5	5	5	5	4	47.7
	Y	N	.67	.75	5	5	5	5	5	4	47.65
Fiberglass (.013")	N	N	.65	.725	4	4	4	3	4	1	48.35
Foam	Y	N	.70	.725	3	3	1	3	3	1	47.1
	Y	13.5"	.72	.725	3	2	1	3	2	1	47.1
	Y	15.0"	.725	.75	3	2	1	3	1	1	47.0

* 5 - 90% of sidelobes do not meet the specified envelope by as much as 10 dB.

4 - The majority of sidelobes do not meet the specified envelope by as much as 8 dB.

3 - The majority of sidelobes meet the specified envelope. The remaining sidelobes exceed the envelope by as much as 6 dB.

2 - 60% - 80% of sidelobes meet the specified envelope. The remaining sidelobes exceed the envelope by as much as 4 dB.

1 - 90% of sidelobes meet the specified envelope.

Table 2-3

Performance Summary for SA Ku-Band Antennas

1. Gain

   A. The Fiberglass radome produces reflection loss of 1.0 dB for .038" radome and 0.4 dB for .013" radome.

   B. The foam radome eliminates reflection loss. The particular foam used in the prototype model has 10 times more ohmic loss than given in handbooks. Loss from the foam is approximately 1.5 dB. This loss could be eliminated by choice of better foam.

   C. Subreflector location is critical for peak gain.

2. Sidelobes

   A. 1^{o} - 10^{o} Region

      a. Sidelobes in this region are higher than predicted levels (primarily caused by reflector surface errors).

      b. The sidelobes are partially improved with the foam radome.

   B. 10^{o} - 48^{o} Region

      a. Both fiberglass radomes produce high sidelobes in this region due to radome reflections.

      b. These sidelobes are substantially improved by the substitution of foam.

   C. 48^{o} - 180^{o} Region

      a. The 0.038" radome produces excessive sidelobes in this region.

      b. The 0.013" fiberglass and foam radomes produce acceptable sidelobe levels.

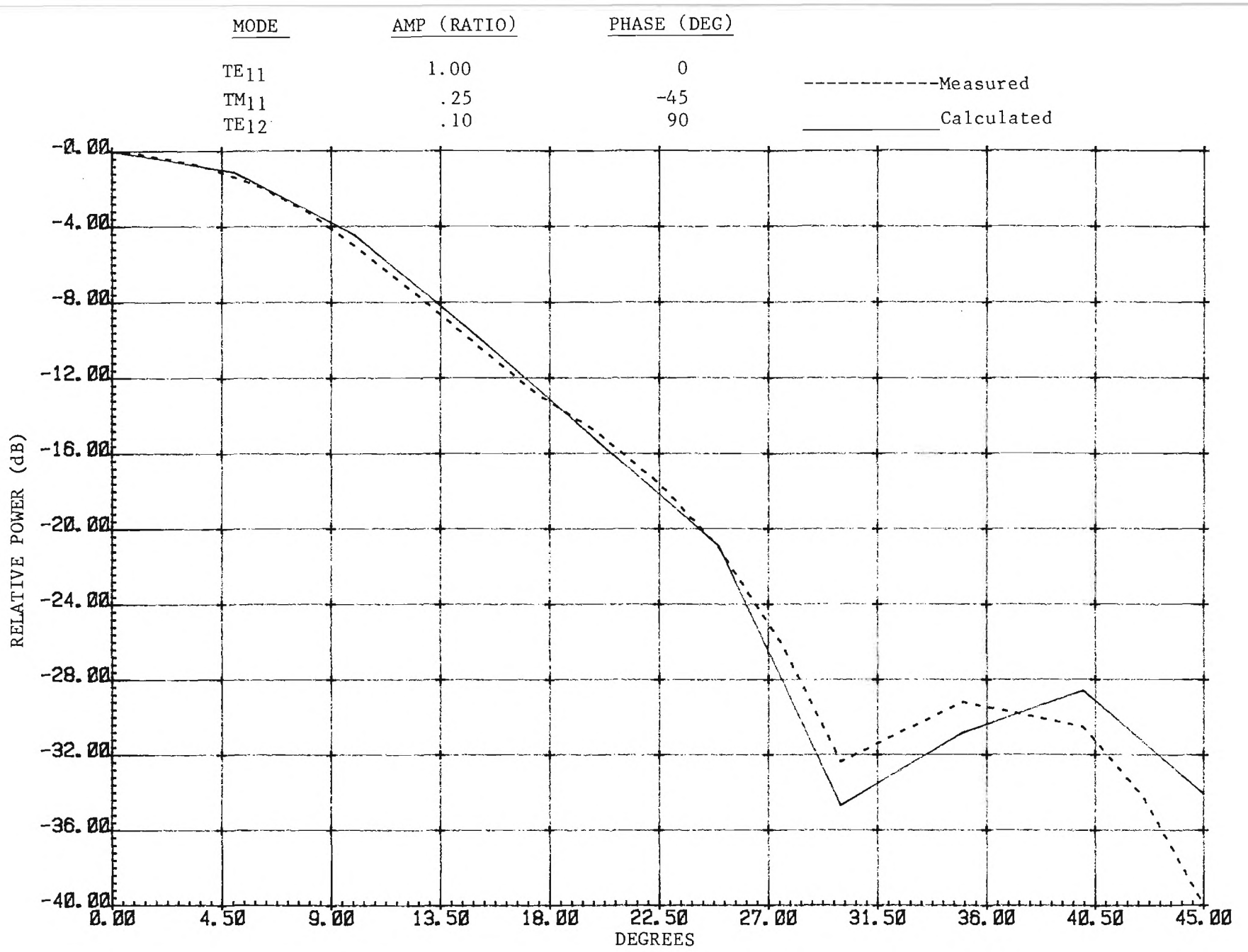

FIGURE 2-26

MULTIMODE FEED PATTERN (E-PLANE)

MODE	AMP (RATIO)	PHASE (DEG)
TE_{11}	1.00	0
TM_{11}	0.25	-45
TE_{12}	0.10	90

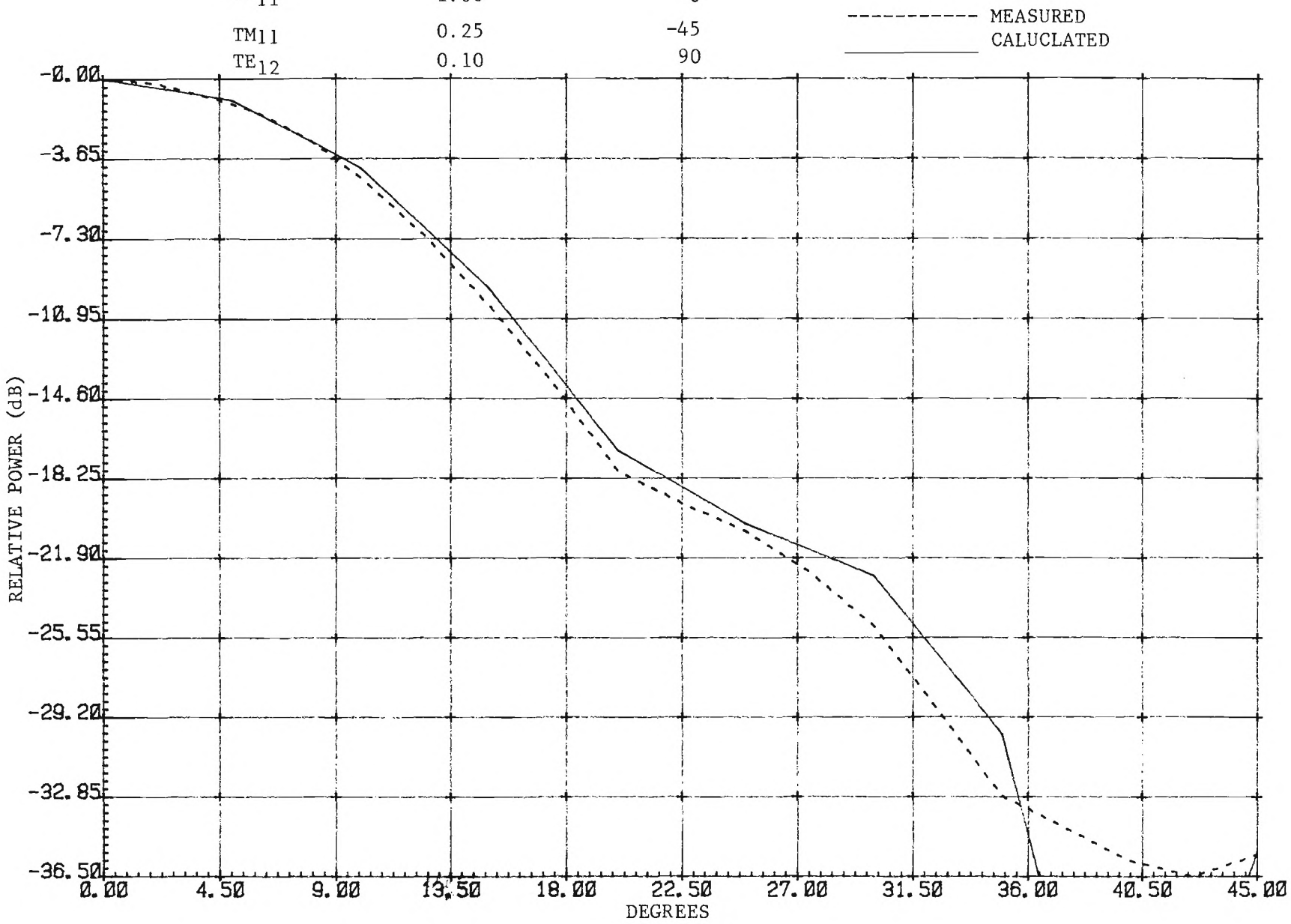

FIGURE 2-27

MULTIMODE FEED PATTERN (H-PLANE)

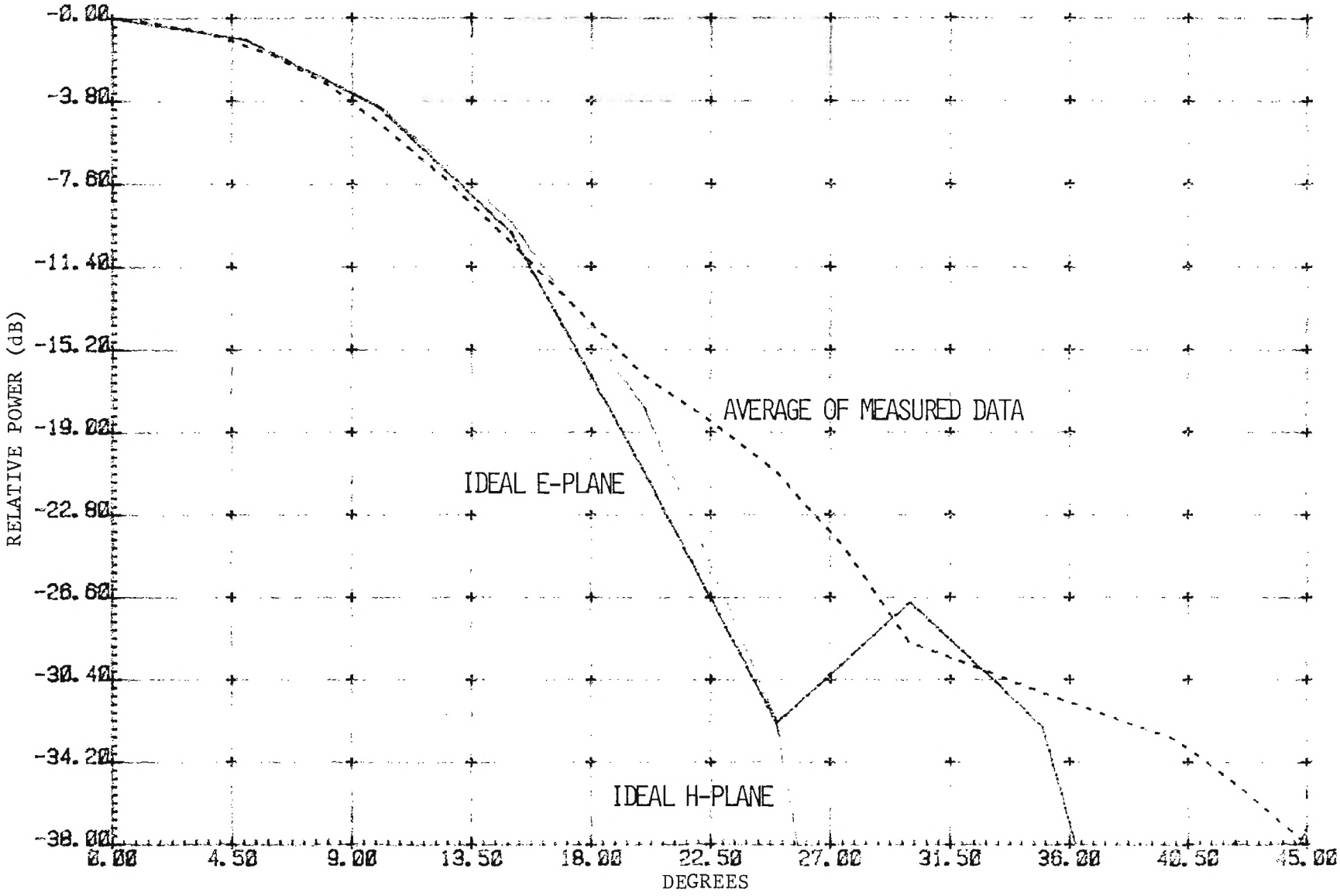

FIGURE 2-28 COMPARISON OF MEASURED AND IDEAL FEED PATTERNS

3.0 TEST AND EVALUATION OF THE PRODUCTION UNIT

3.1 DESCRIPTION OF THE PRODUCTION UNIT

Two configurations are considered for the production unit. One configuration implements the thin-walled fiberglass radome as a subreflector support. The other configuration uses a solid styrofoam cone to support the subreflector. The focal length of the production unit is slightly different from the prototype unit (i.e., 46.138 inches instead of 45.25 inches). Table 3-1 lists the parameters and coordinates for the reflector geometry.

TABLE 3-1 PRODUCTION UNIT ANTENNA DIMENSIONS AND COORDINATES

CASSEGRAIN ANTENNA OUTPUT

IAMETER OF MAIN REFLECTOR = 110.000
IAMETER OF SUBREFLECTOR = 11.4590
UBREFLECTOR HALF ANGLE = 22.0000
NGLE TO EDGE OF MAIN REFLECTOR = 61.5931
EPTH OF MAIN REFLECTOR = 16.3910
EPTH OF SUBREFLECTOR = 1.15066
OCAL LENGTH = 46.1380

EED DIAMETER = 4.00000
ISTANCE OF FEED PHASE CENTER BEHIND FEED APERTURE = .000000
ISTANCE OF FEED PHASE CENTER BEHIND DISH APERTURE = -12.4671
ISTANCE FROM FEED PHASE CENTER TO SUBREFLECTOR = 13.0304
ISTANCE FROM FOCAL POINT TO FEED PHASE CENTER = 17.2799
ISTANCE FROM FOCAL POINT TO SUBREFLECTOR EDGE = 3.09882
ISTANCE OF FEED PHASE CENTER FROM VERTEX = 28.8582
EED SHADOW DIAMETER = 10.6445

X2	Y2	X1	Y1	T1	T2
55.0000	.0000	5.7295	.0000	22.000	61.593
50.0000	2.8447	5.0929	.2209	20.043	56.902
45.0000	5.4185	4.4932	.4124	18.073	51.994
40.0000	7.7214	3.9247	.5774	16.093	46.872
35.0000	9.7533	3.3823	.7184	14.103	41.543
30.0000	11.5144	2.8618	.8372	12.104	36.020
25.0000	13.0045	2.3591	.9353	10.098	30.318
20.0000	14.2236	1.8707	1.0140	8.086	24.458
15.0000	15.1719	1.3936	1.0743	6.069	18.466
10.0000	15.8492	.9246	1.1169	4.048	12.370
5.0000	16.2556	.4610	1.1422	2.025	6.203
.0000	16.3910	.0000	1.1507	.074	-.027

3.2 PRODUCTION UNIT TEST DATA

Figures 3-1 through 3-9 show the secondary E-plane patterns for the thin-walled fiberglass cone configuration at three different frequencies. Figures 3-10 through 3-18 show the same configuration in the H-plane. Figures 3-19 through 3-27 show the E-plane antenna patterns for the foam-supported subreflector. Figures 3-28 through 3-36 show the foam configuration in the H-plane.

Table 3-2 shows the gain and noise temperature results computed from a measured pattern. Table 3-3 lists the measured surface error data. Figure 3-37 shows a graph of the results from the mechanical surface tolerance measurement. The measurement shows significant correlation in peak errors from one panel segment to the next panel. The measurement is based on a relatively few number of physical points on the reflector surface and may not accurately represent the exact surface error. However, sufficient data is available to establish a trend.

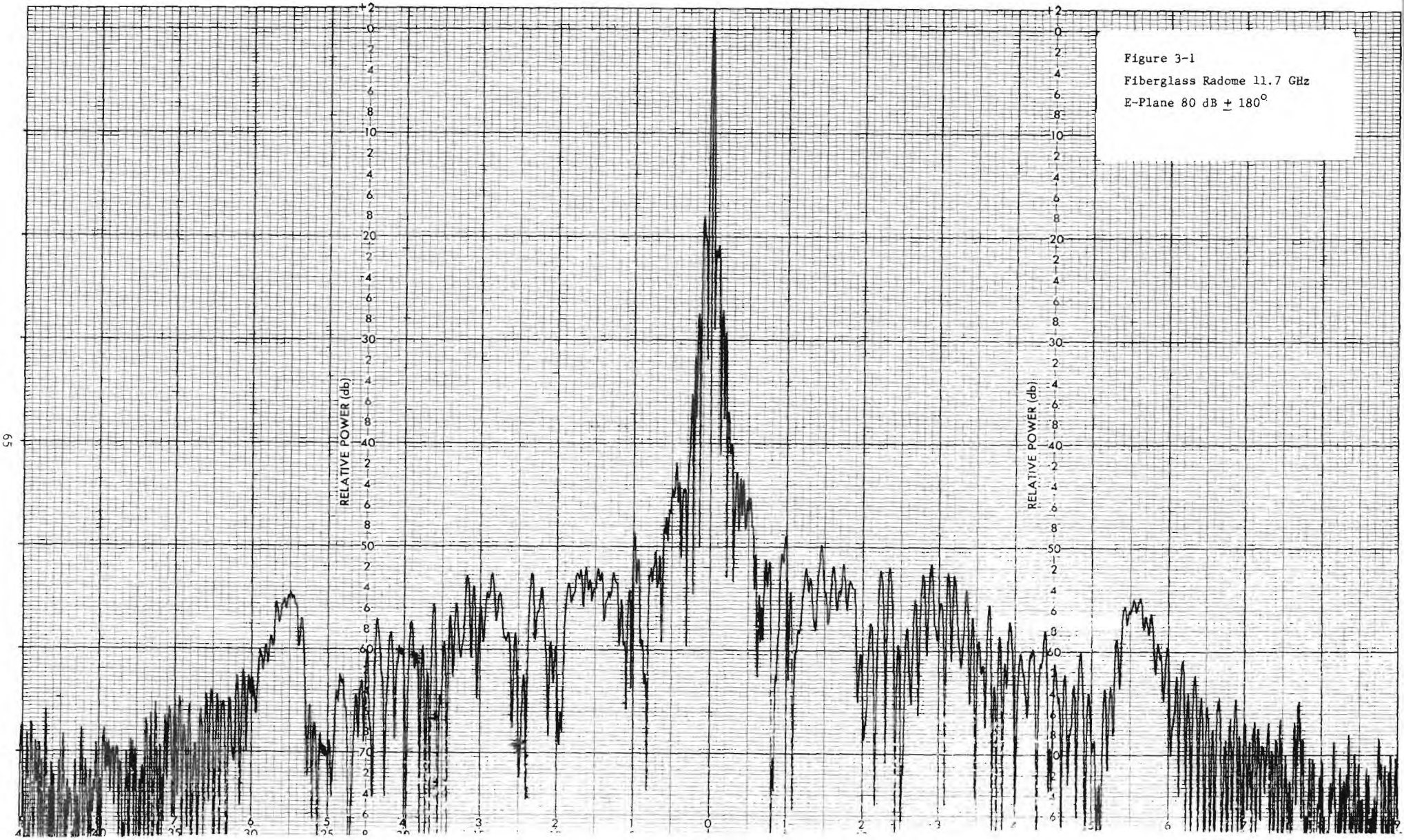

Figure 3-1
Fiberglass Radome 11.7 GHz
E-Plane 80 dB ± 180°

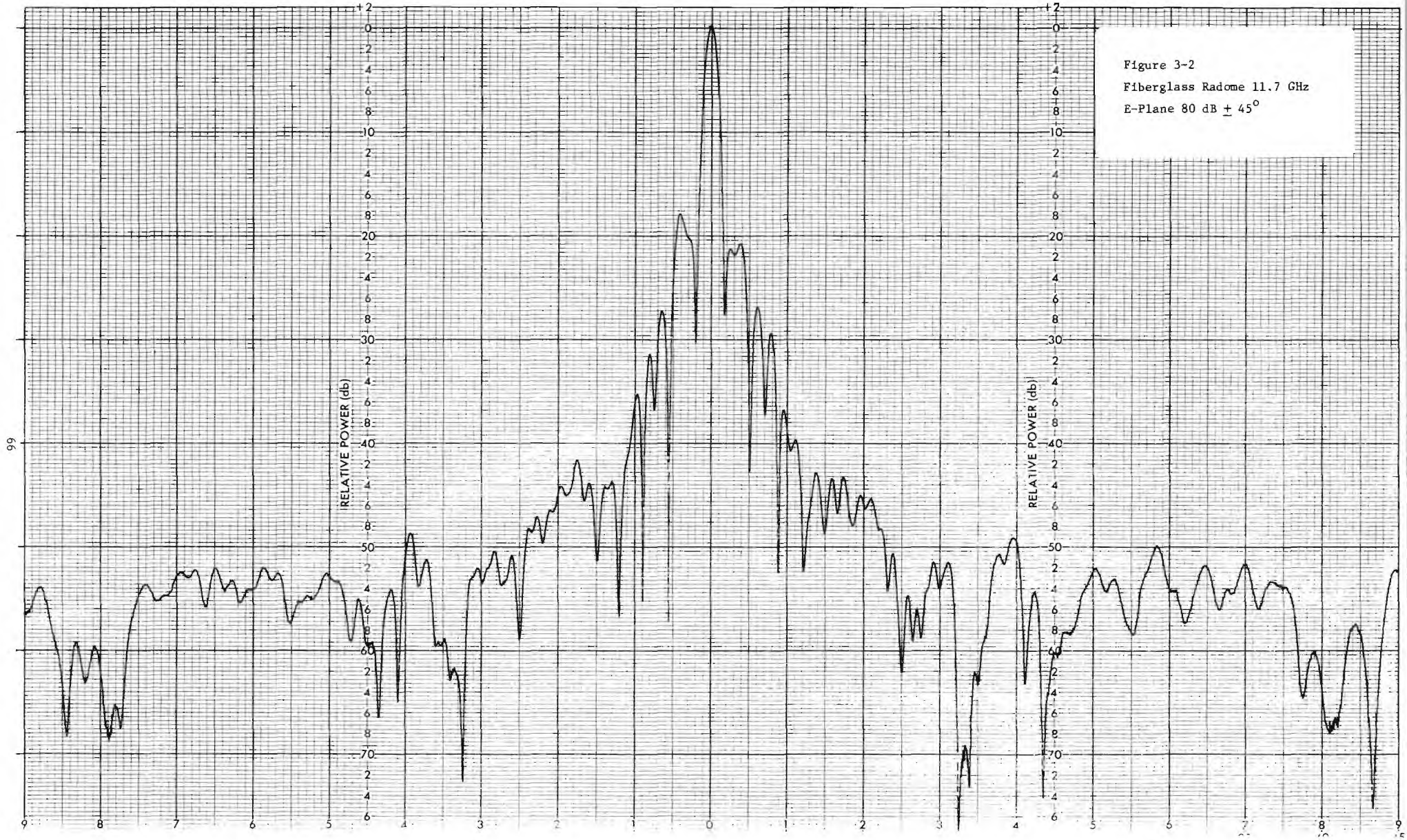

Figure 3-2
Fiberglass Radome 11.7 GHz
E-Plane 80 dB ± 45°

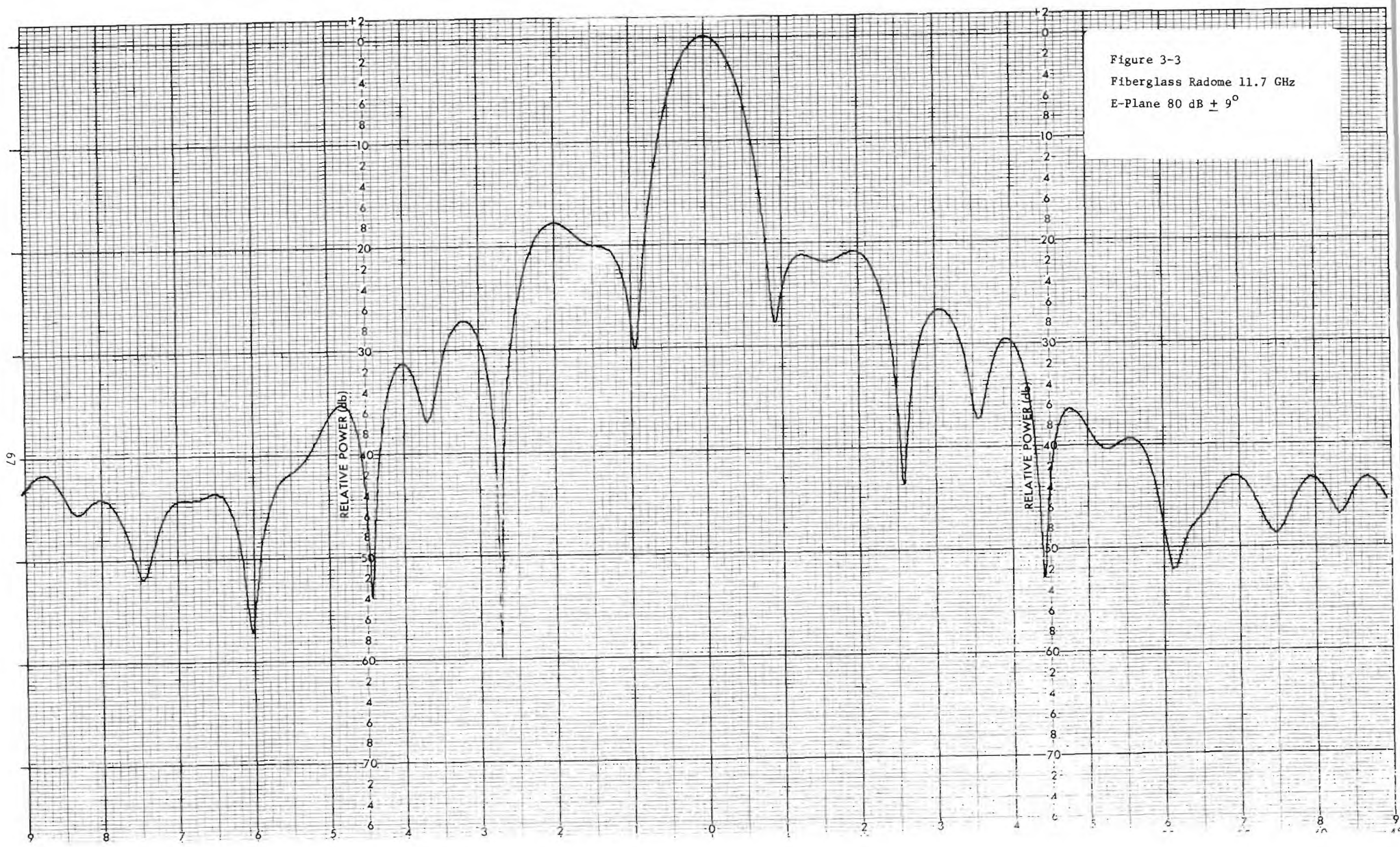

Figure 3-3
Fiberglass Radome 11.7 GHz
E-Plane 80 dB $\pm$ 9°

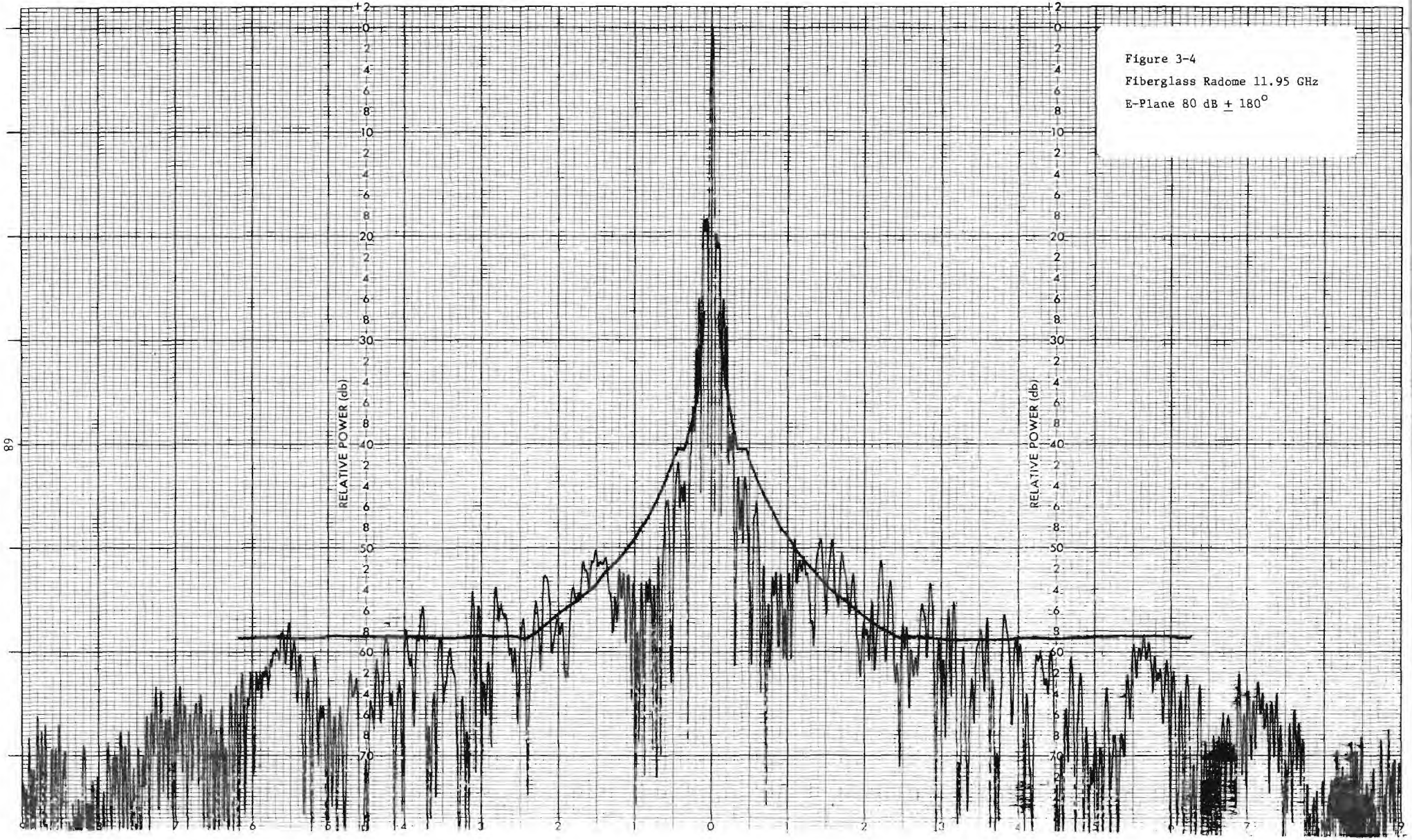

Figure 3-4
Fiberglass Radome 11.95 GHz
E-Plane 80 dB ± 180°

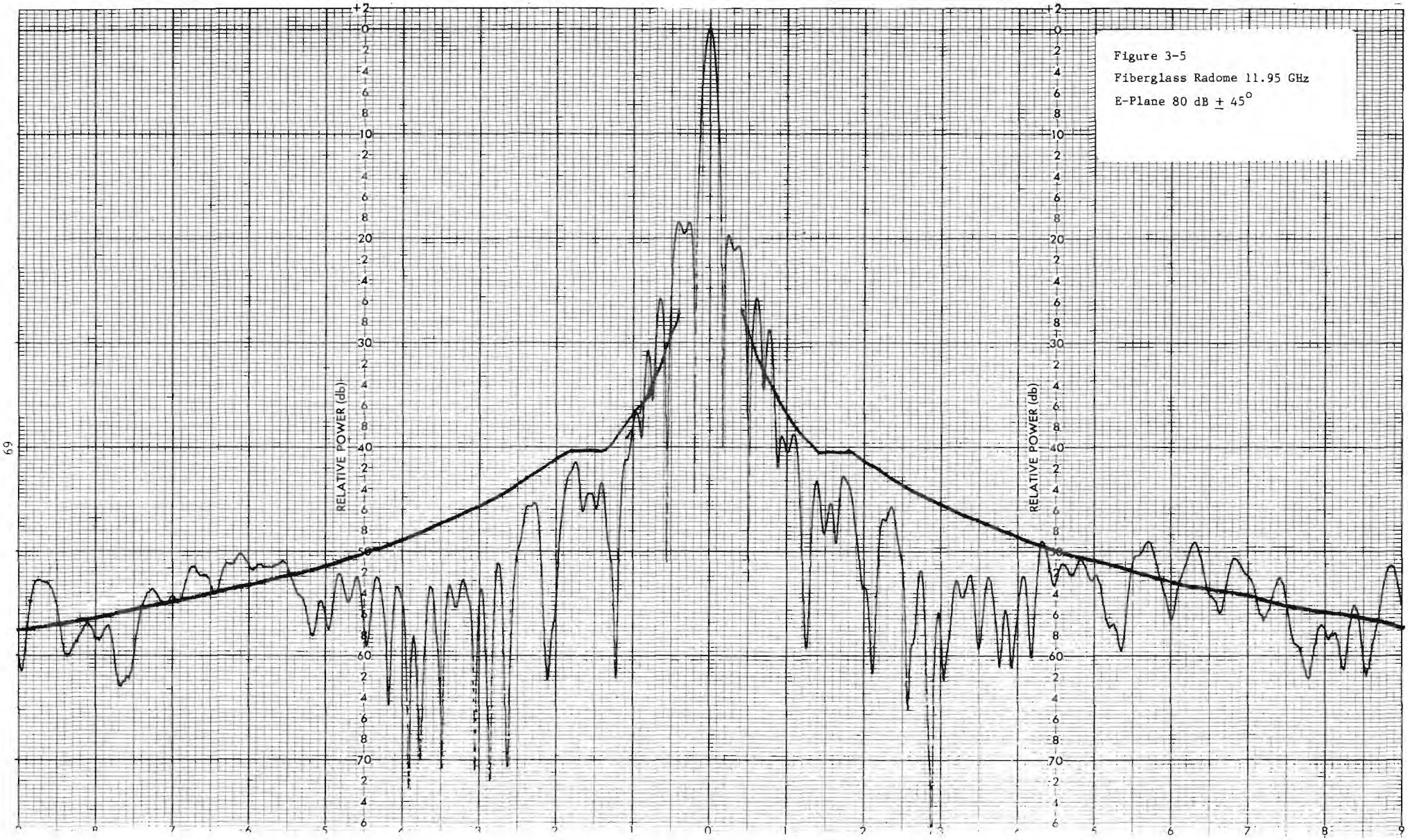

Figure 3-5
Fiberglass Radome 11.95 GHz
E-Plane 80 dB $\pm$ 45°

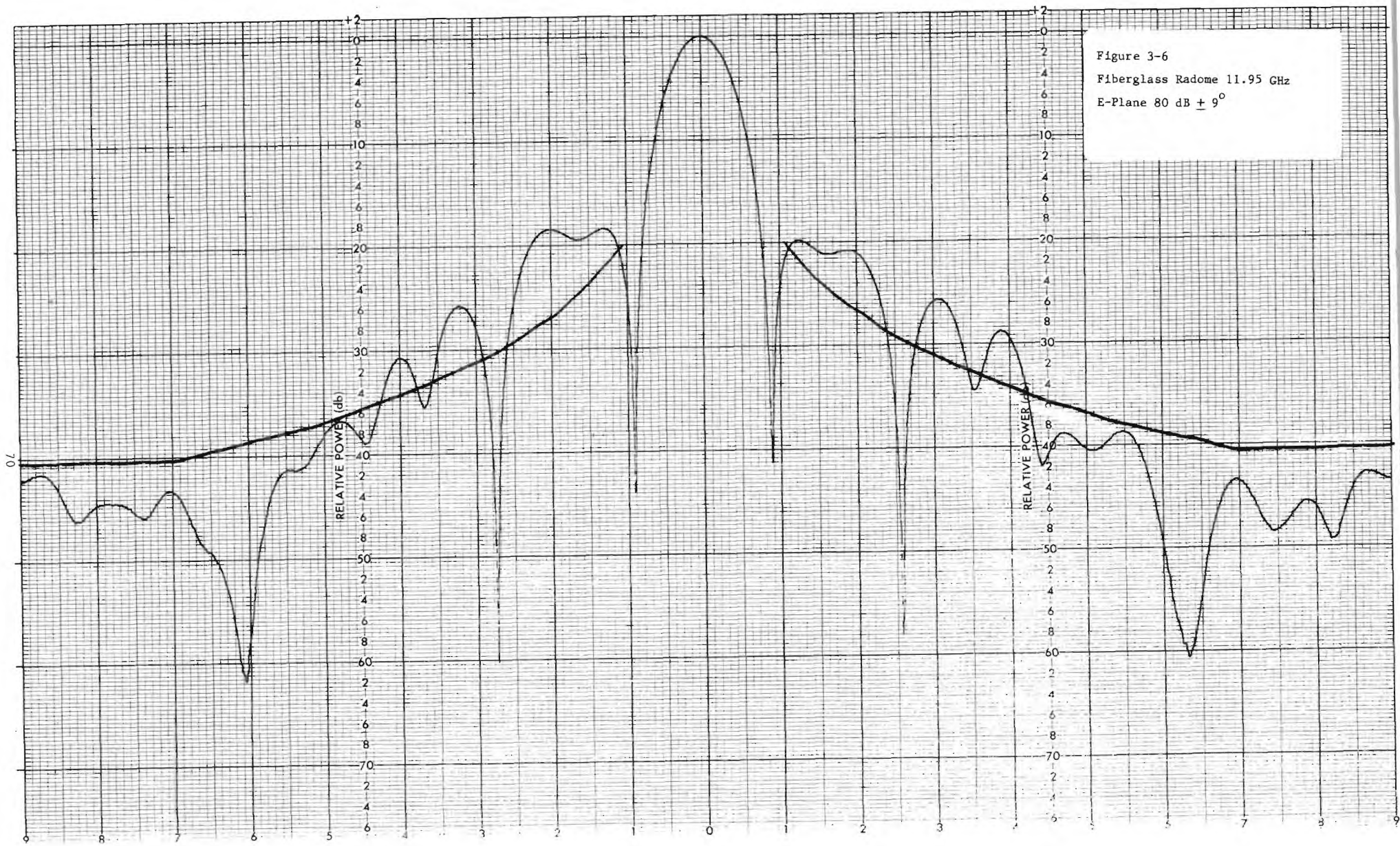

Figure 3-6
Fiberglass Radome 11.95 GHz
E-Plane 80 dB $\pm$ 9°

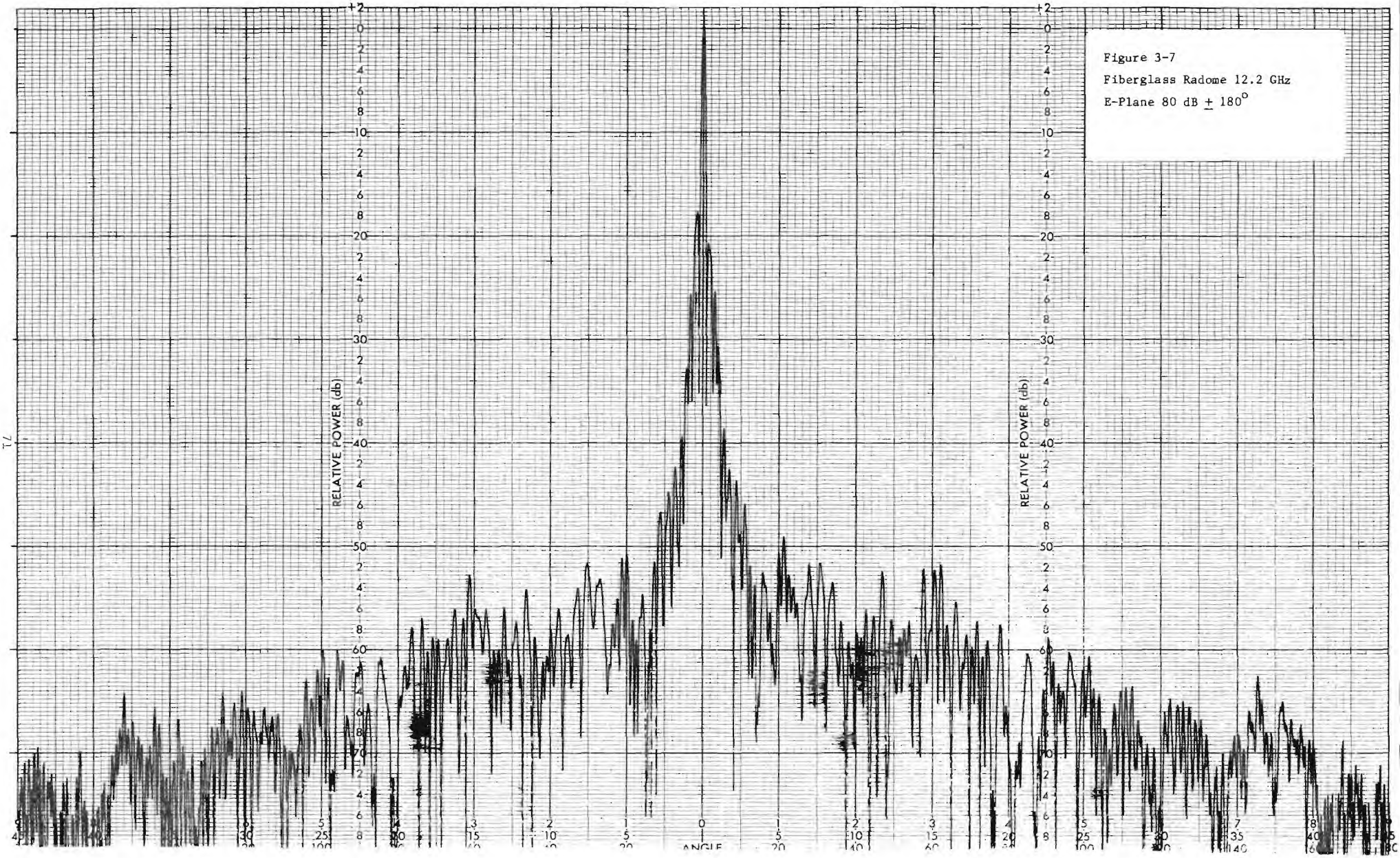

Figure 3-7
Fiberglass Radome 12.2 GHz
E-Plane 80 dB $\pm$ 180°

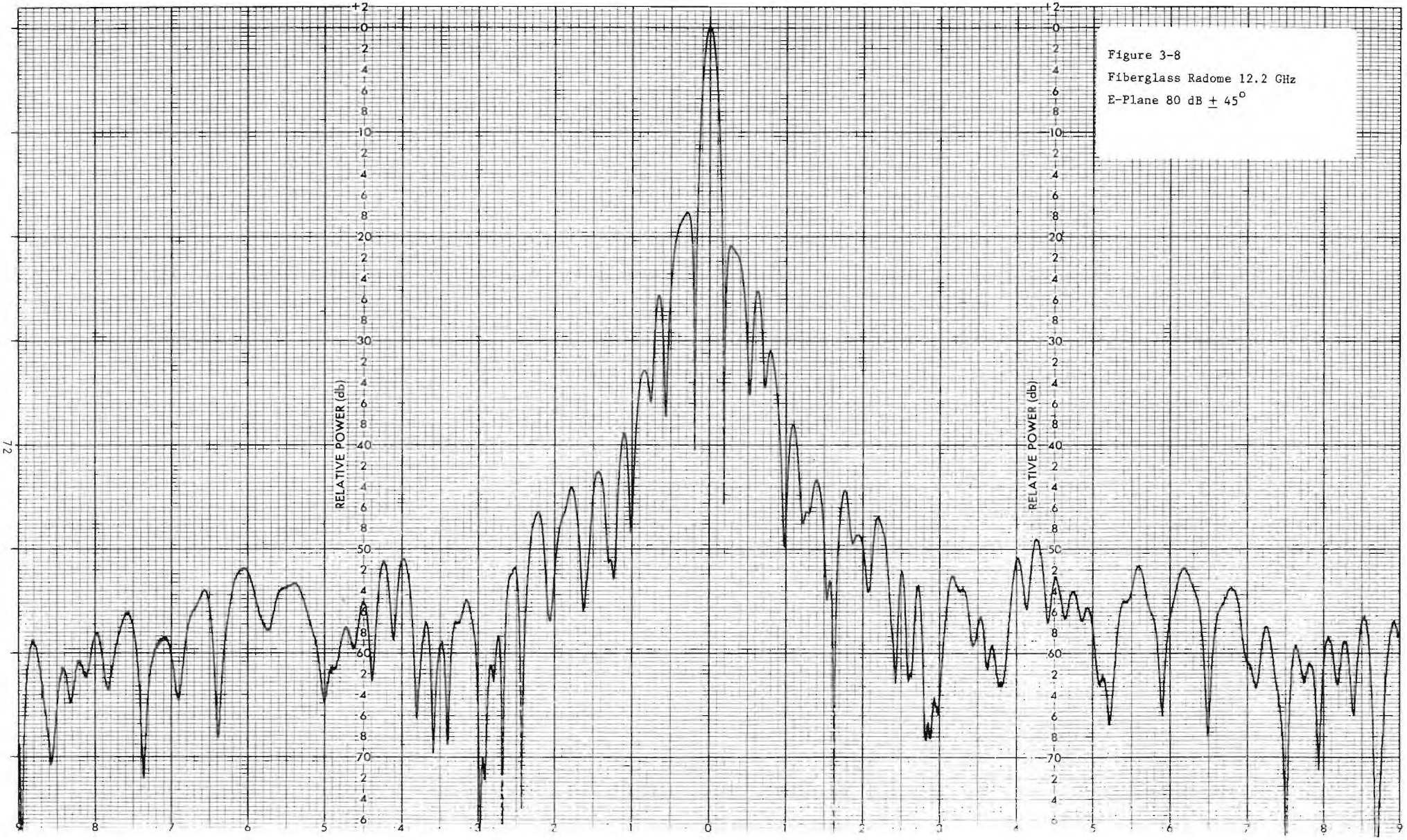

Figure 3-8
Fiberglass Radome 12.2 GHz
E-Plane 80 dB $\pm$ 45°

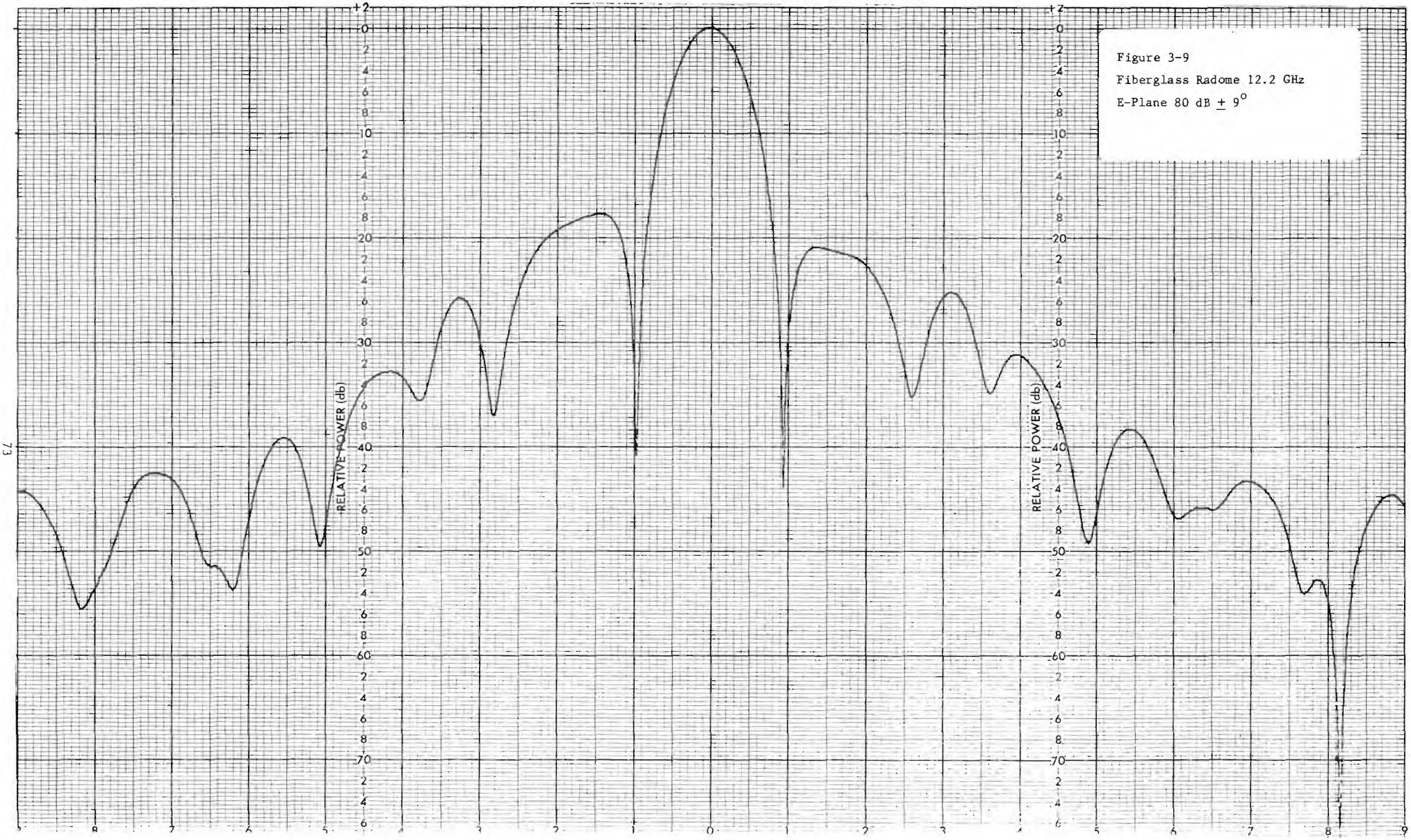

Figure 3-9
Fiberglass Radome 12.2 GHz
E-Plane 80 dB $\pm$ 9°

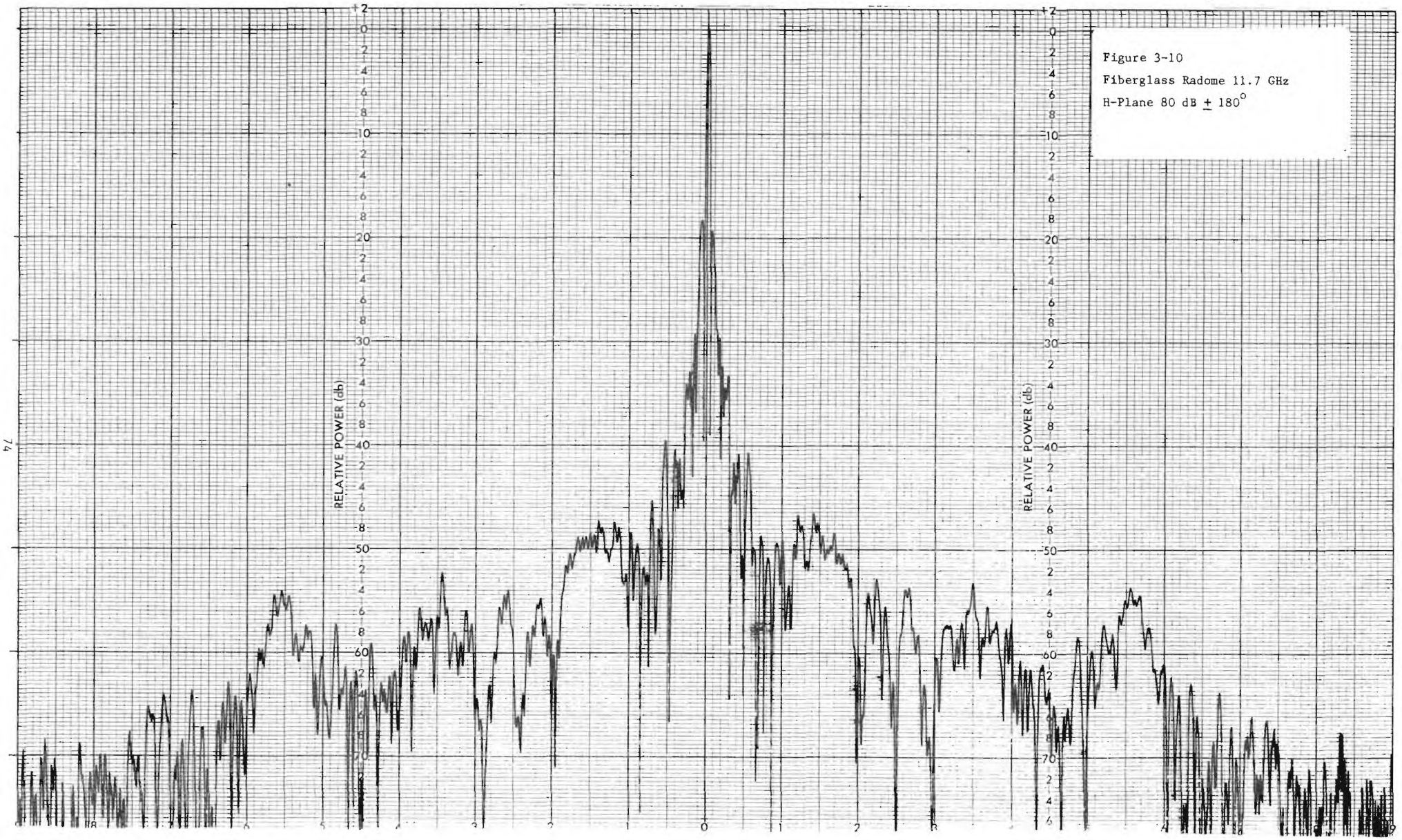

Figure 3-10
Fiberglass Radome 11.7 GHz
H-Plane 80 dB ± 180°

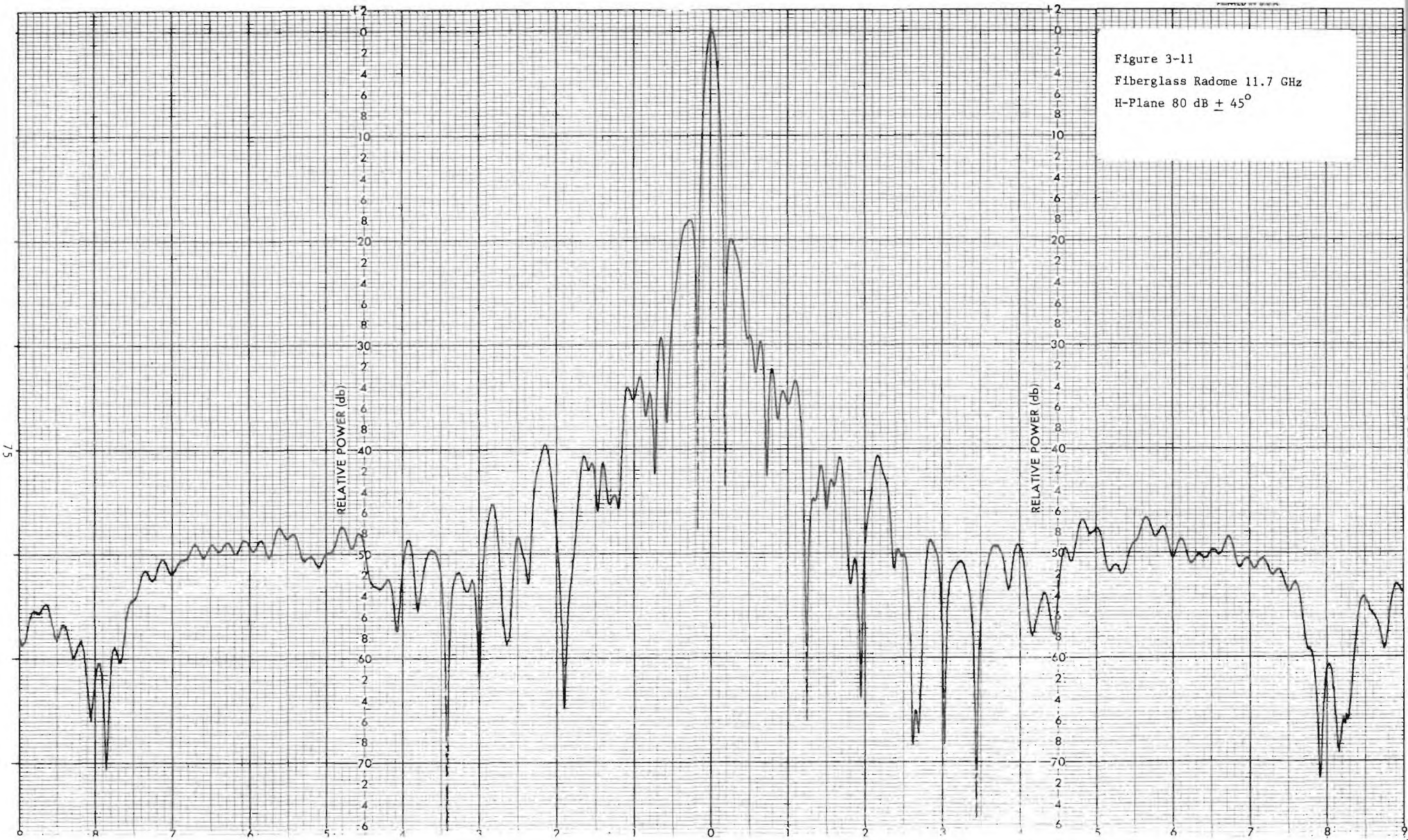

Figure 3-11
Fiberglass Radome 11.7 GHz
H-Plane 80 dB $\pm$ 45°

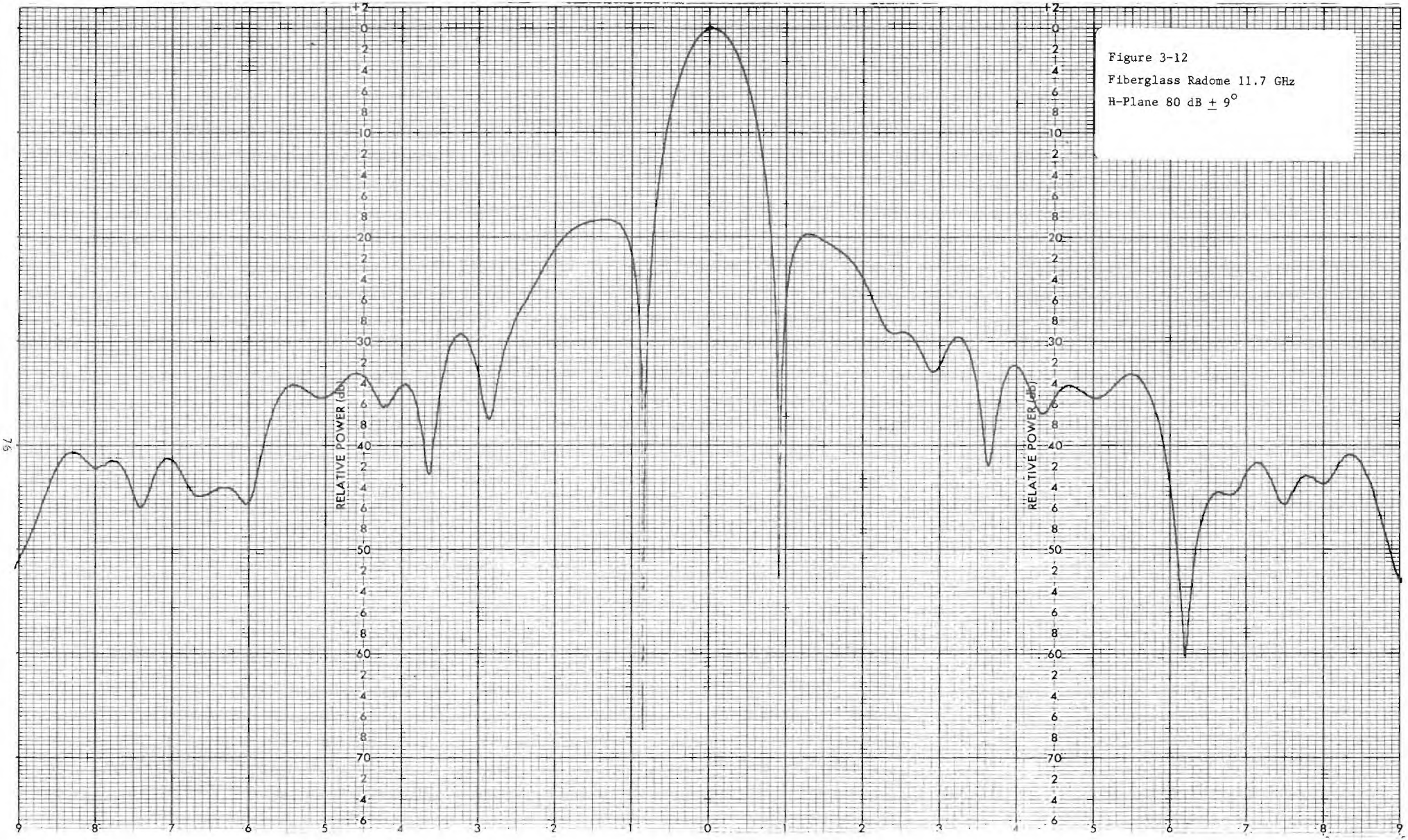

Figure 3-12
Fiberglass Radome 11.7 GHz
H-Plane 80 dB $\pm$ 9°

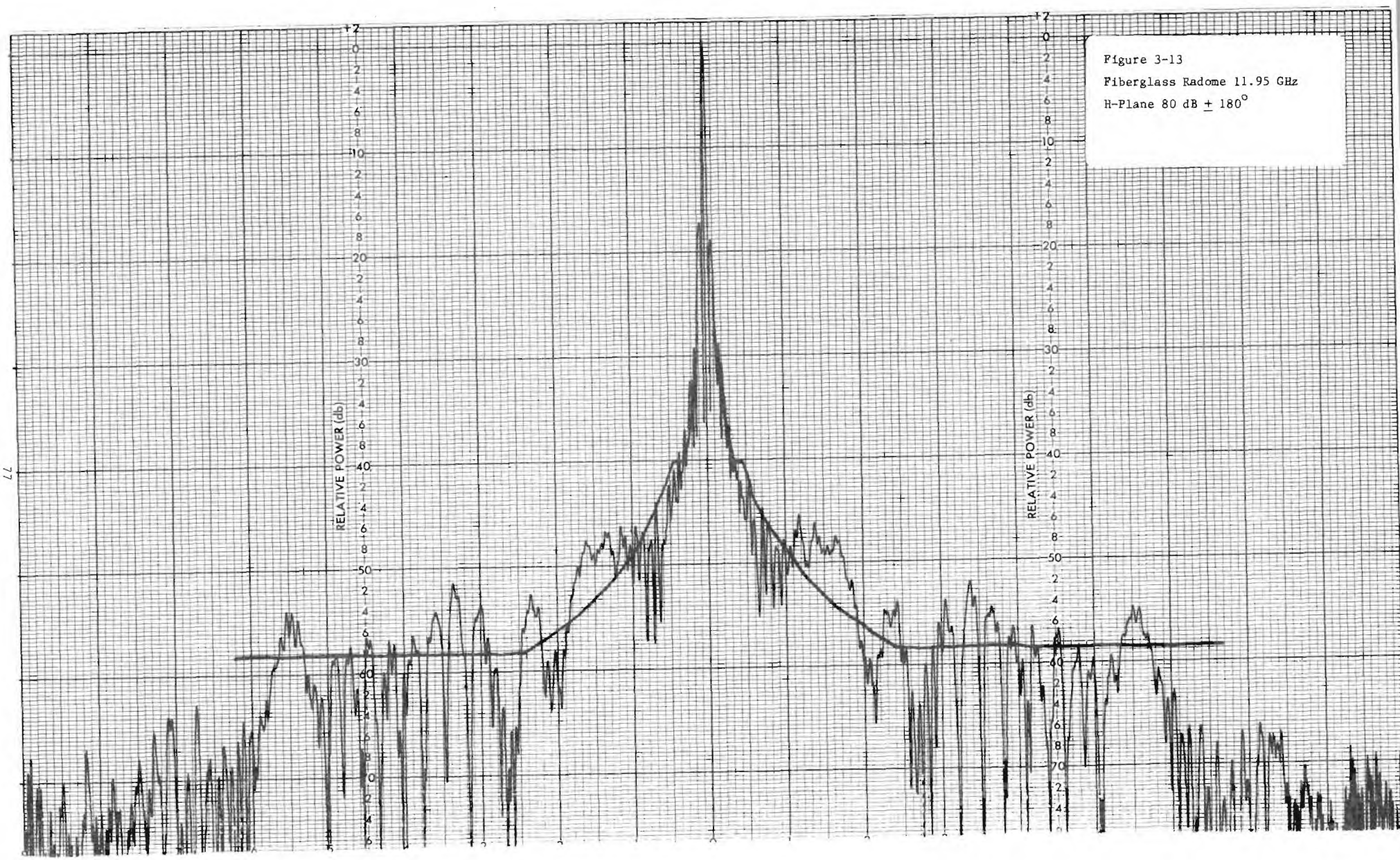

Figure 3-13
Fiberglass Radome 11.95 GHz
H-Plane 80 dB $\pm$ 180°

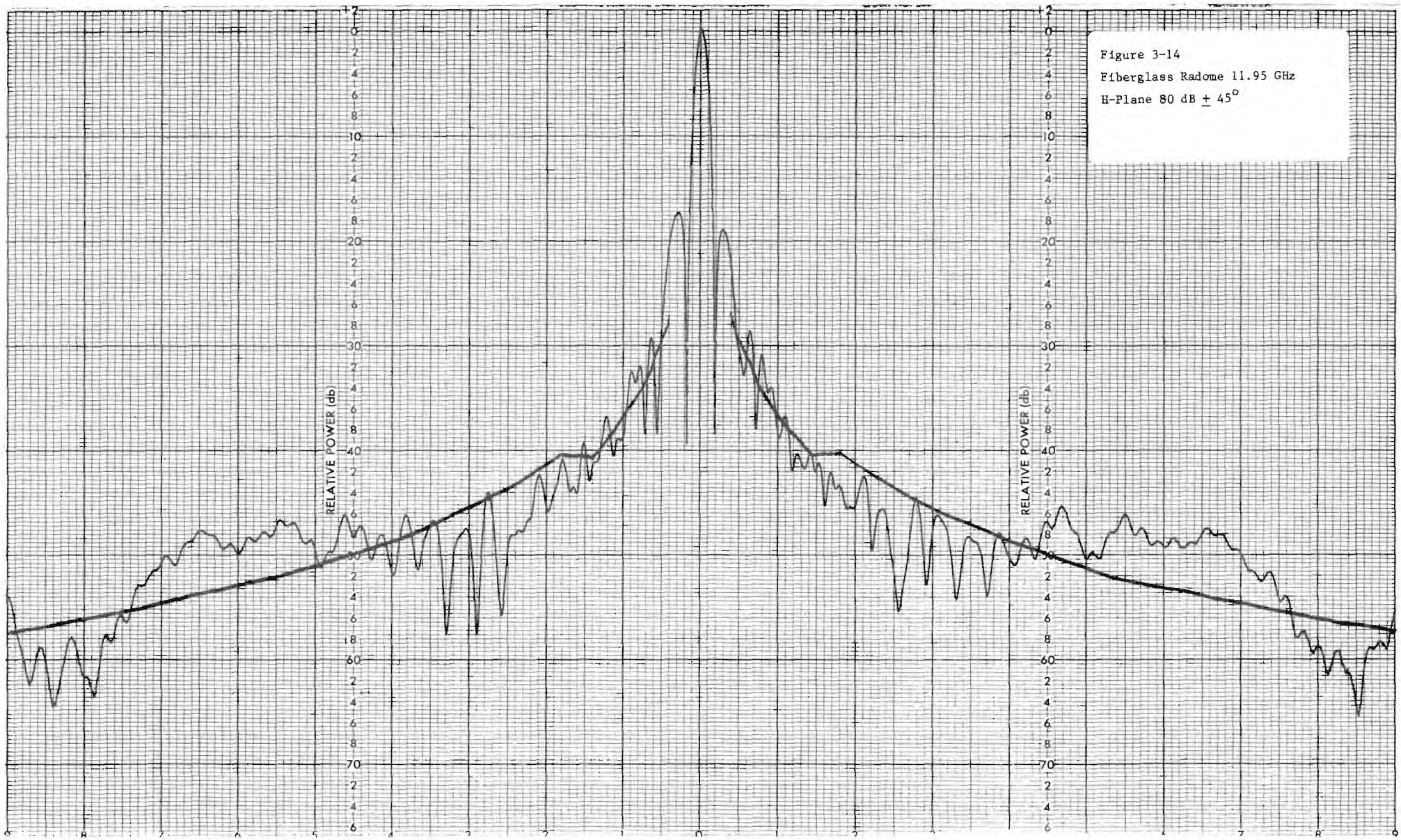

Figure 3-14
Fiberglass Radome 11.95 GHz
H-Plane 80 dB $\pm$ 45°

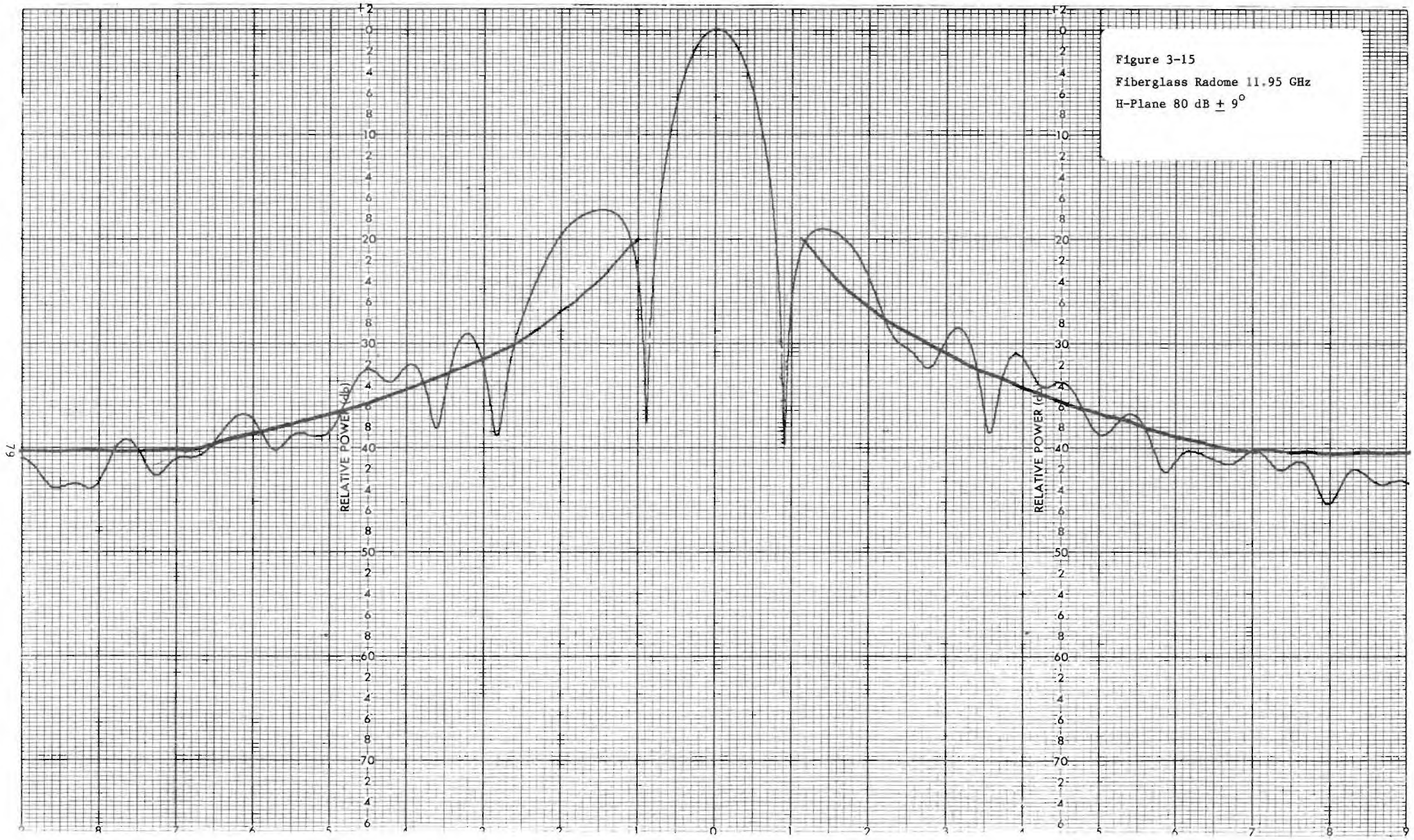

Figure 3-15
Fiberglass Radome 11.95 GHz
H-Plane 80 dB $\pm$ 9°

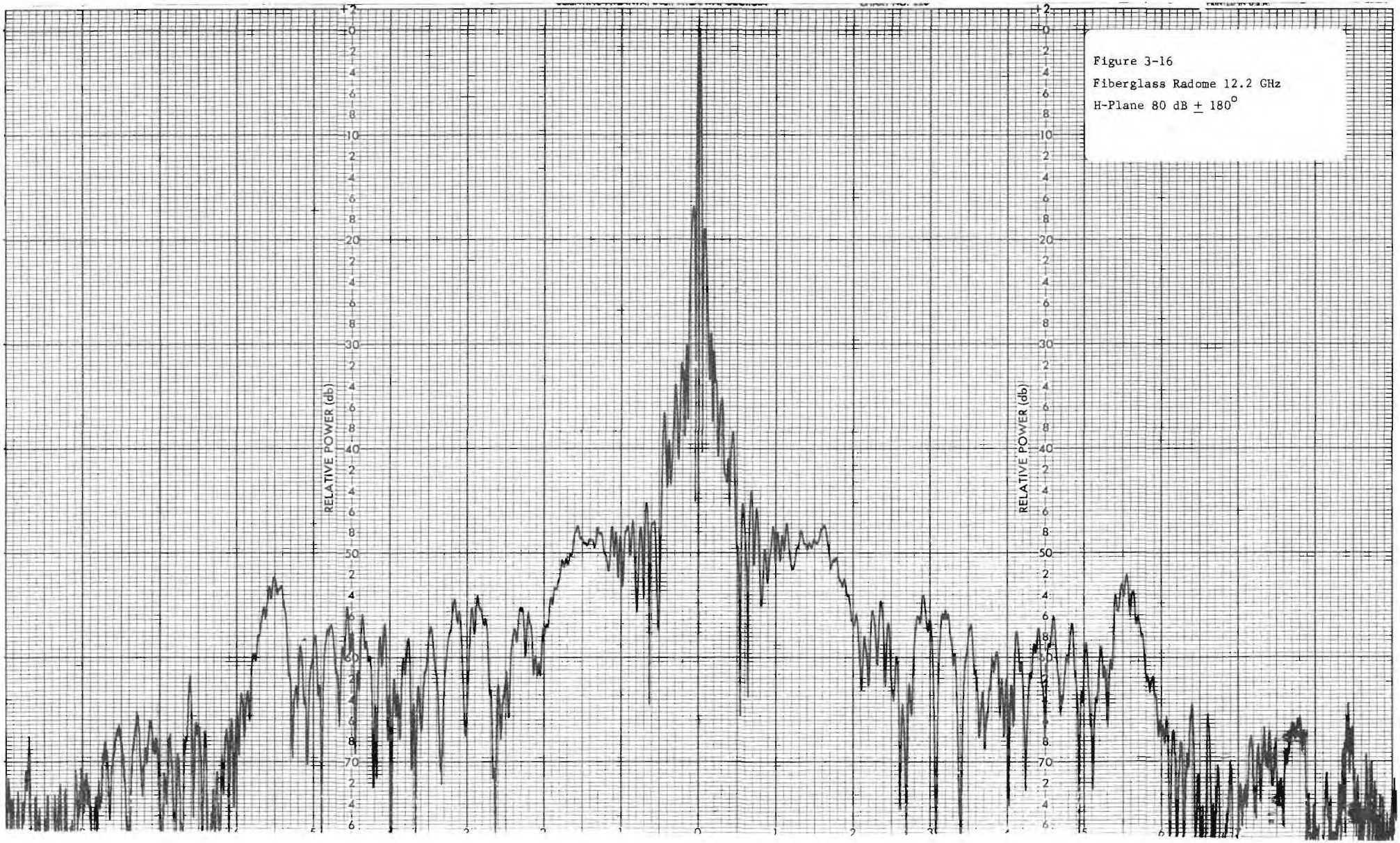

Figure 3-16
Fiberglass Radome 12.2 GHz
H-Plane 80 dB $\pm$ 180°

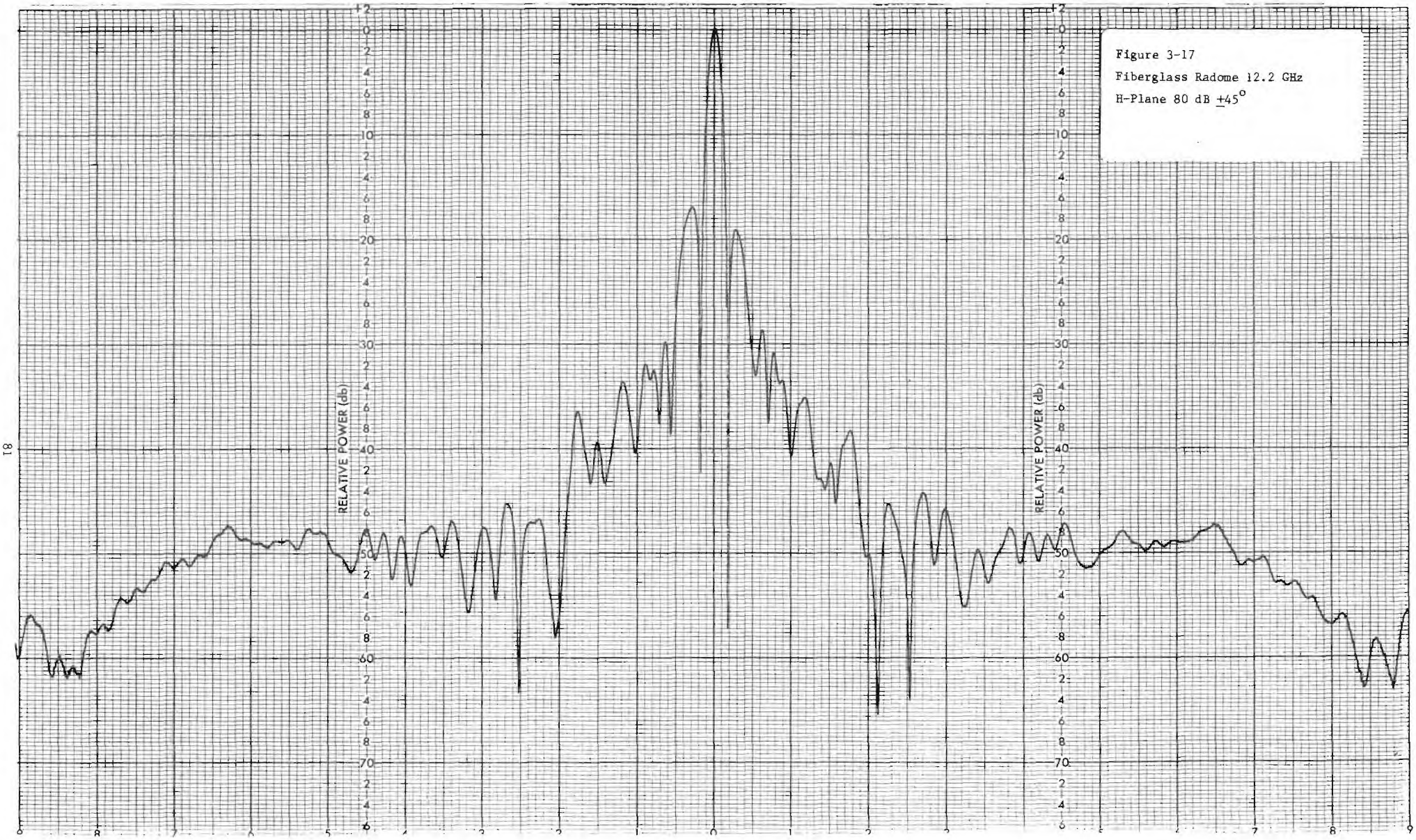

Figure 3-17
Fiberglass Radome 12.2 GHz
H-Plane 80 dB $\pm 45^{\circ}$

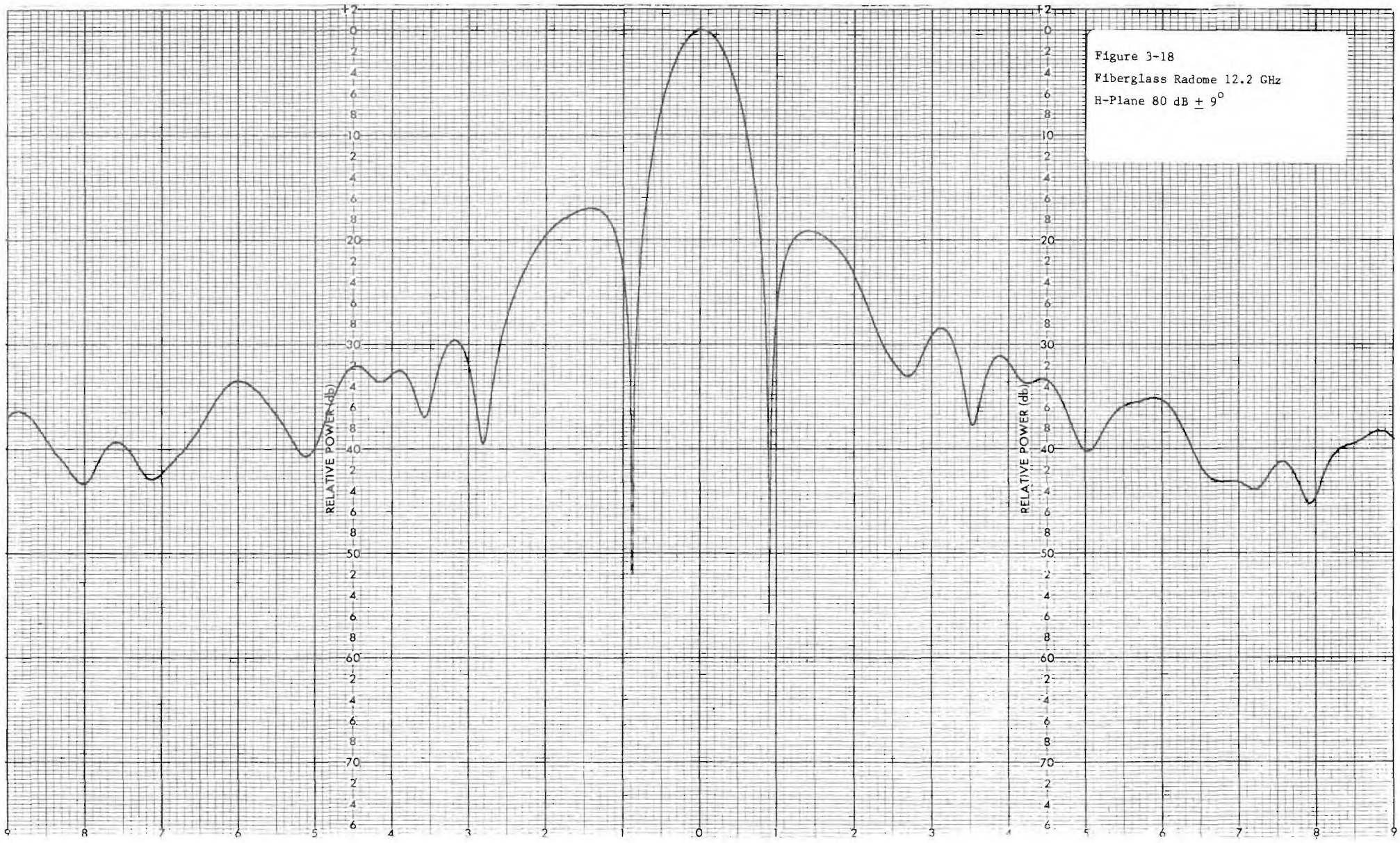

Figure 3-18
Fiberglass Radome 12.2 GHz
H-Plane 80 dB $\pm$ 9°

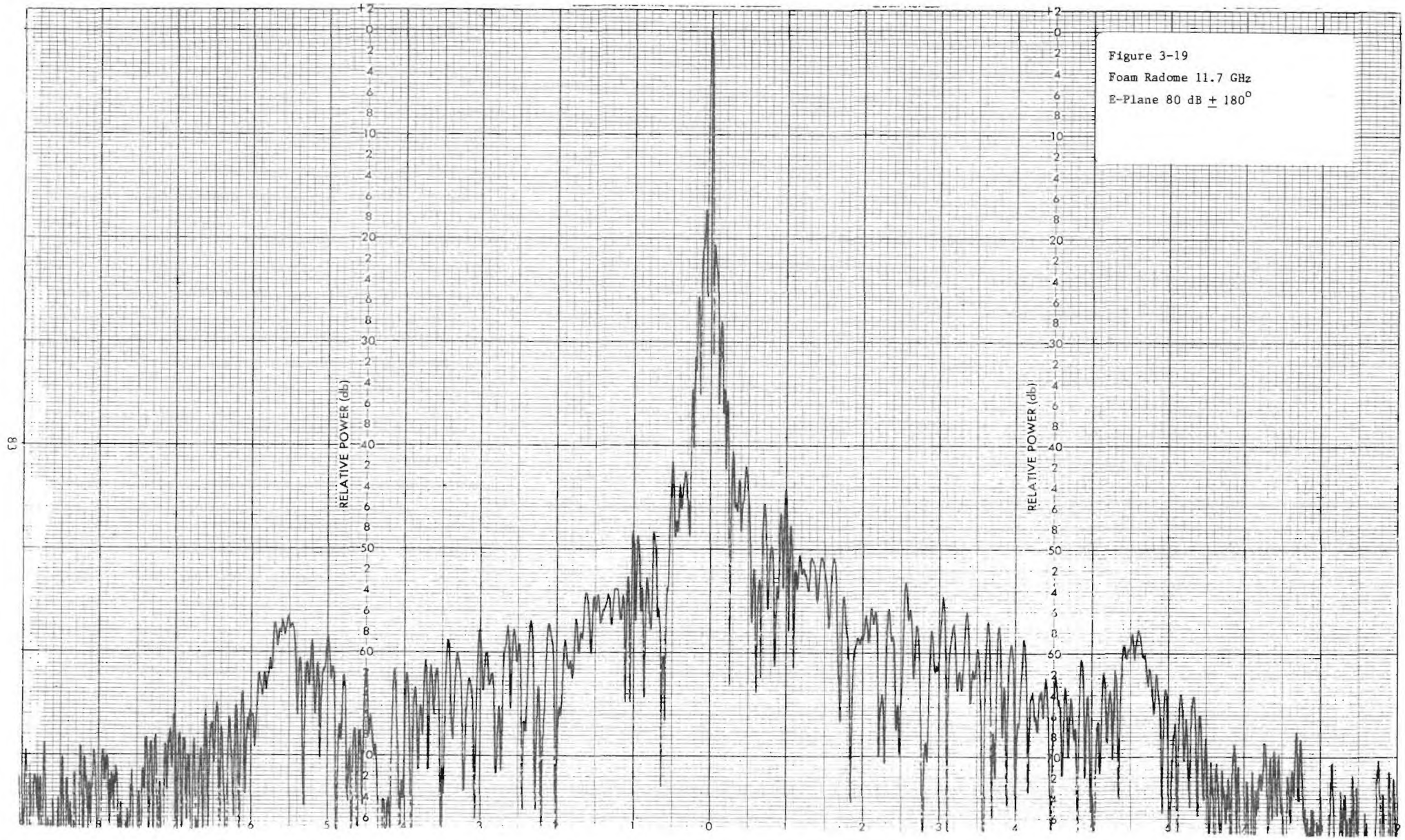

Figure 3-19
Foam Radome 11.7 GHz
E-Plane 80 dB $\pm$ 180°

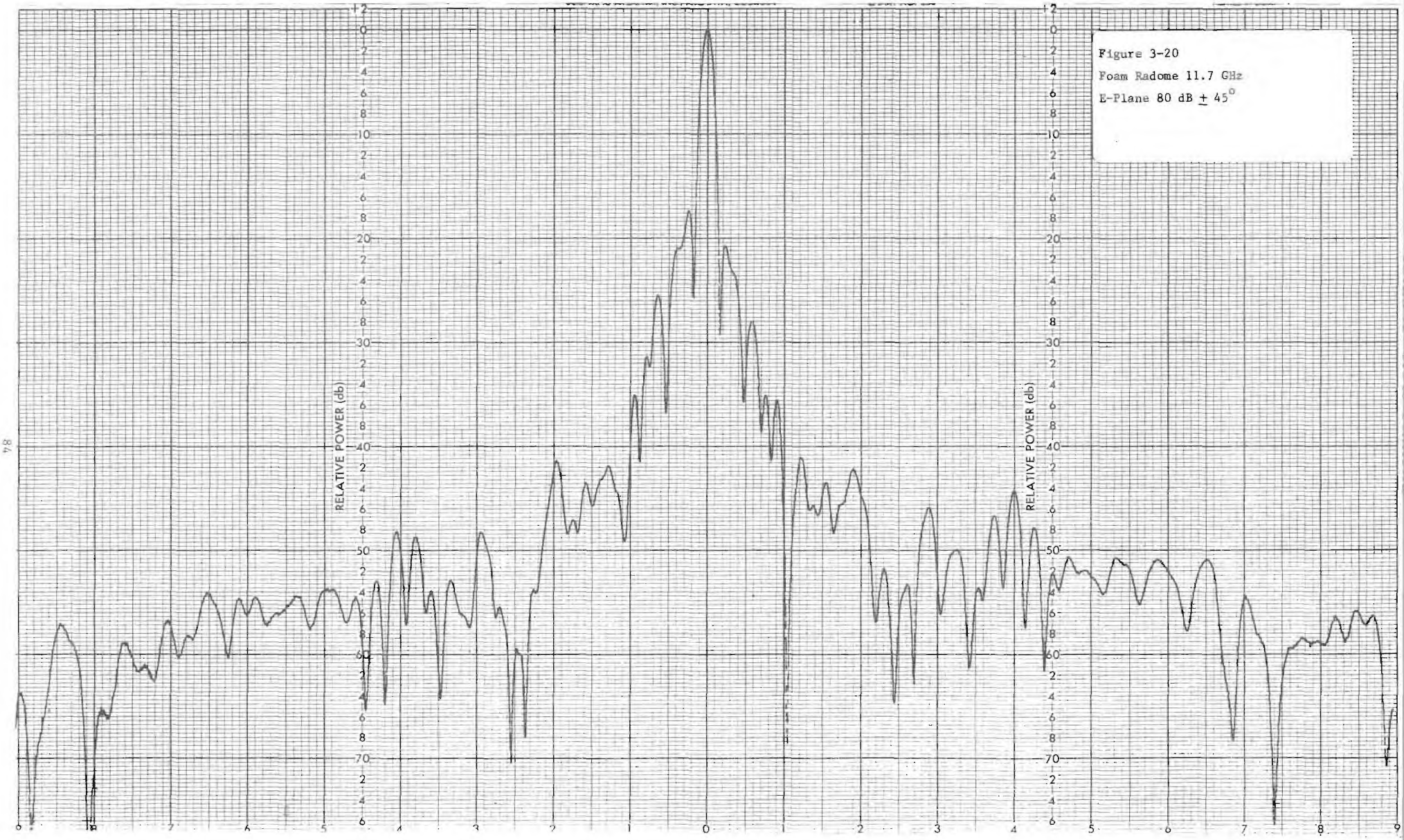

Figure 3-20
Foam Radome 11.7 GHz
E-Plane 80 dB $\pm$ 45°

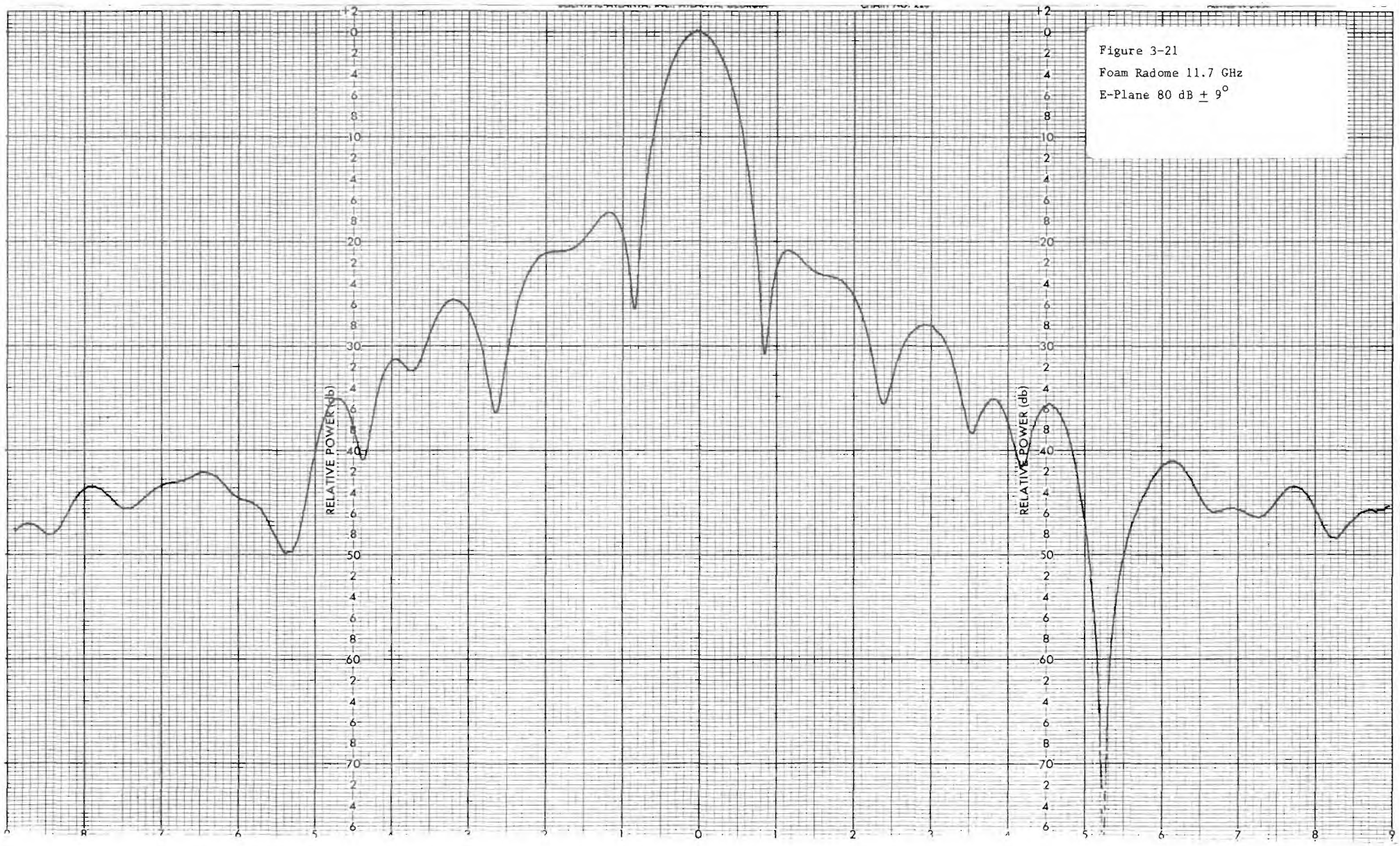

Figure 3-21
Foam Radome 11.7 GHz
E-Plane 80 dB $\pm$ 9°

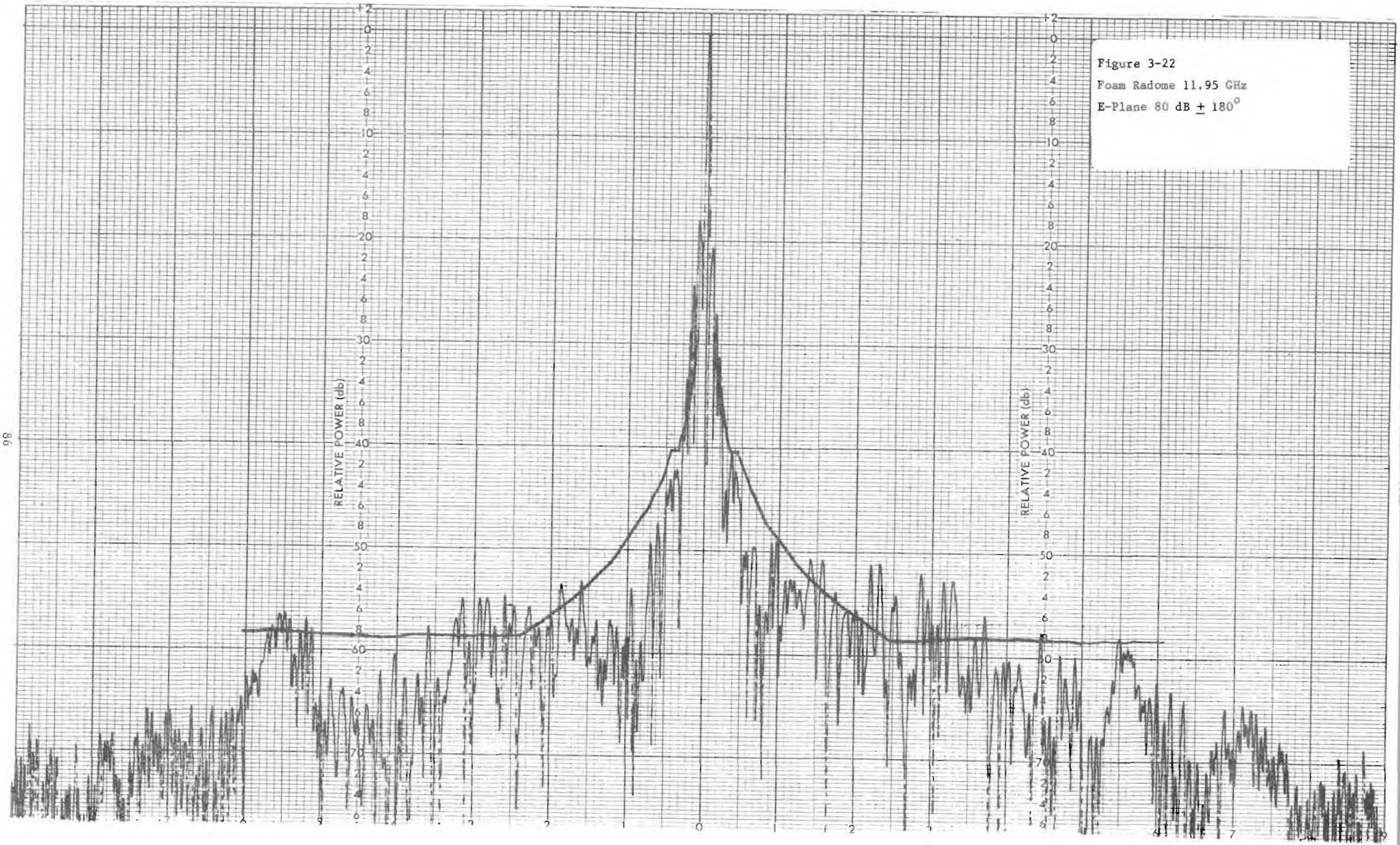

Figure 3-22
Foam Radome 11.95 GHz
E-Plane 80 dB $\pm$ 180°

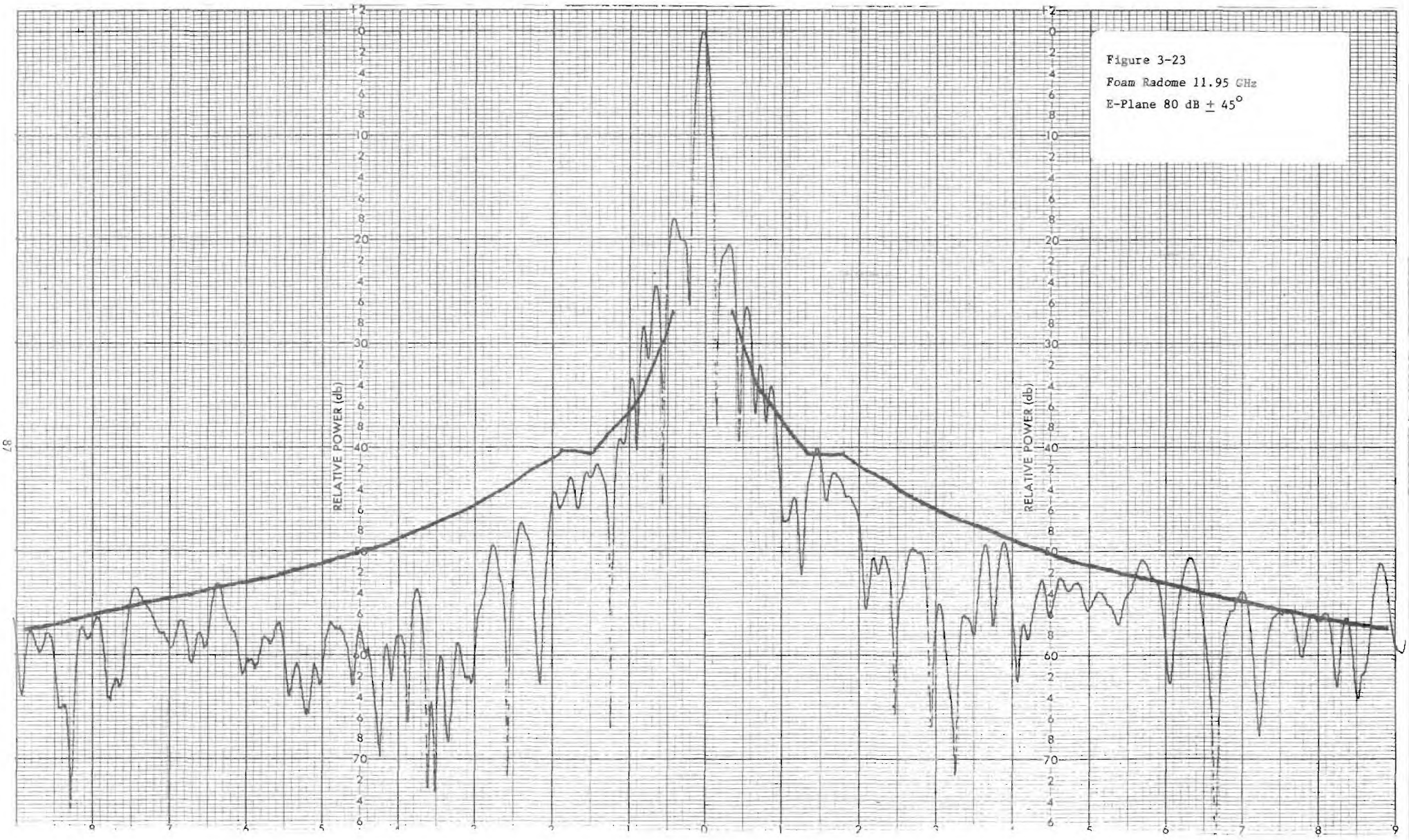

Figure 3-23
Foam Radome 11.95 GHz
E-Plane 80 dB $\pm$ 45°

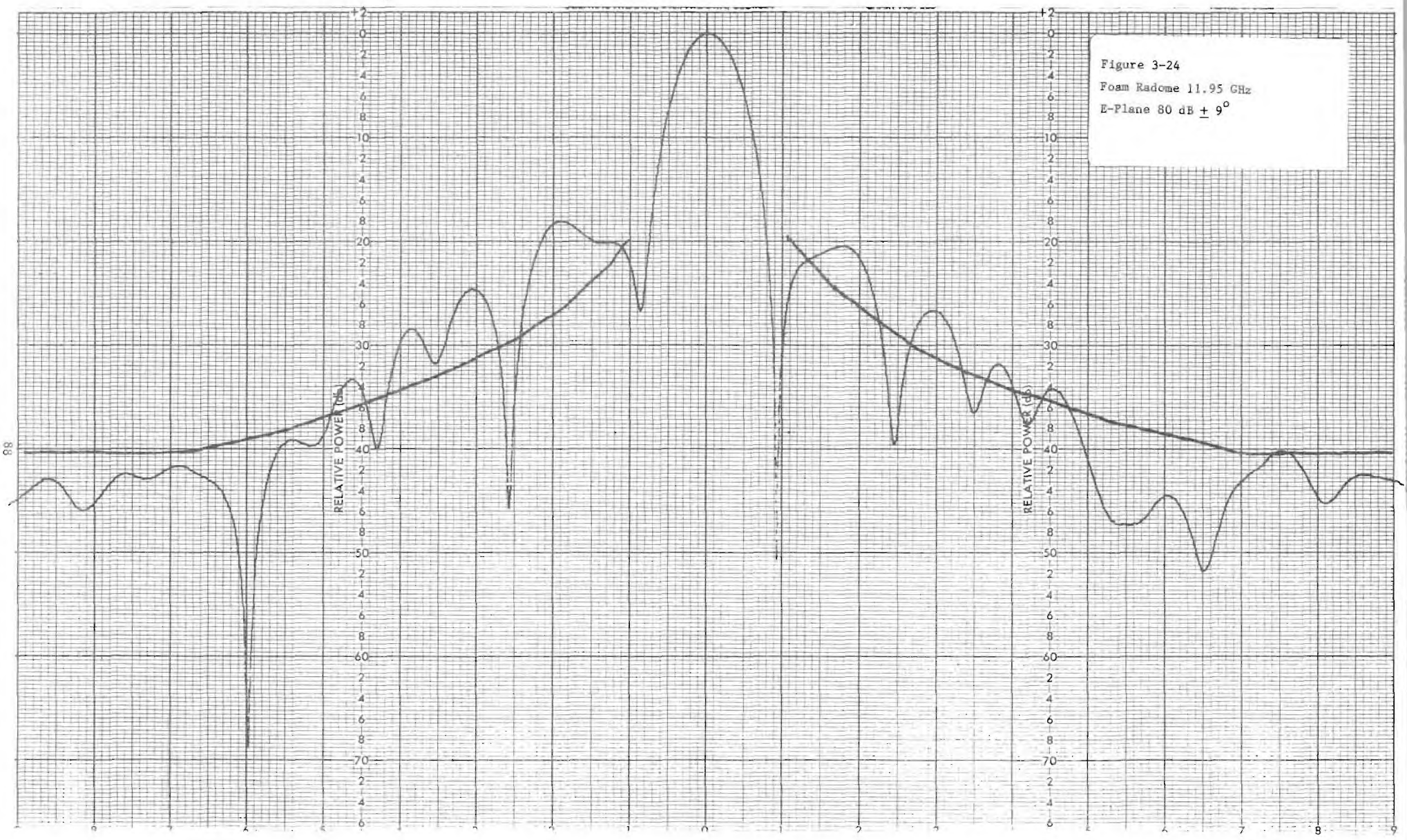

Figure 3-24
Foam Radome 11.95 GHz
E-Plane 80 dB $\pm$ 9°

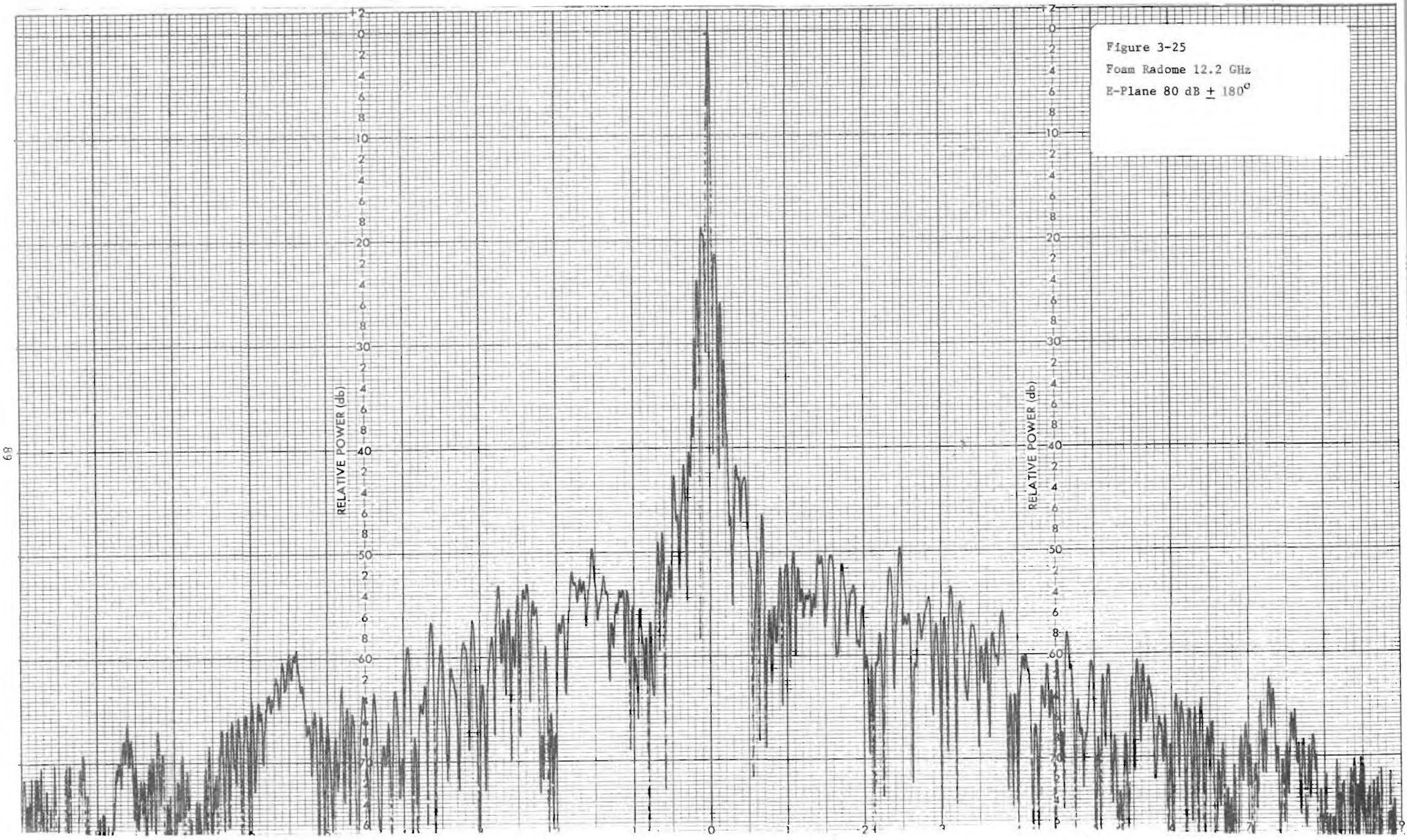

Figure 3-25
Foam Radome 12.2 GHz
E-Plane 80 dB $\pm$ 180°

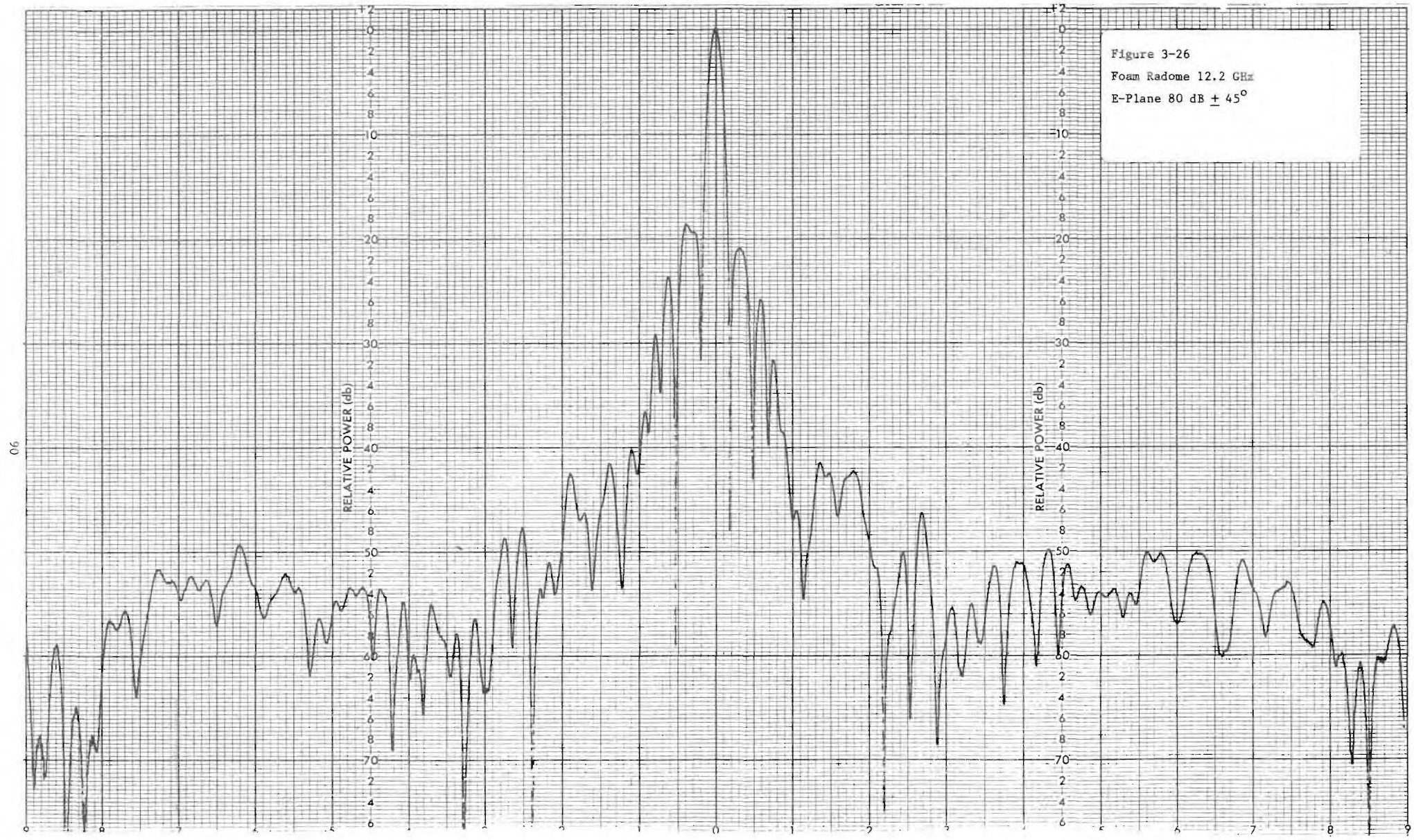

Figure 3-26
Foam Radome 12.2 GHz
E-Plane 80 dB $\pm$ 45°

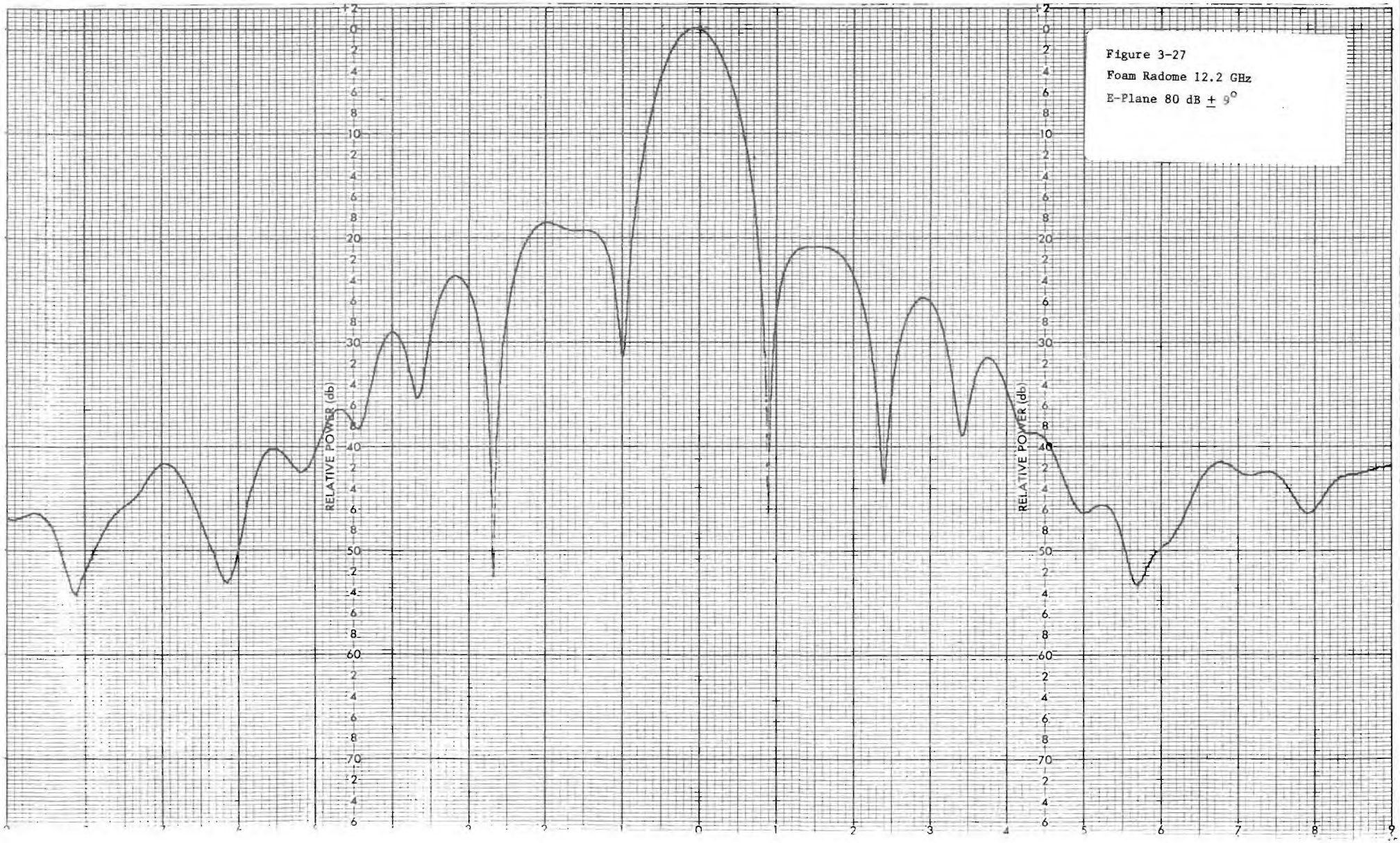

Figure 3-27
Foam Radome 12.2 GHz
E-Plane 80 dB ± 9°

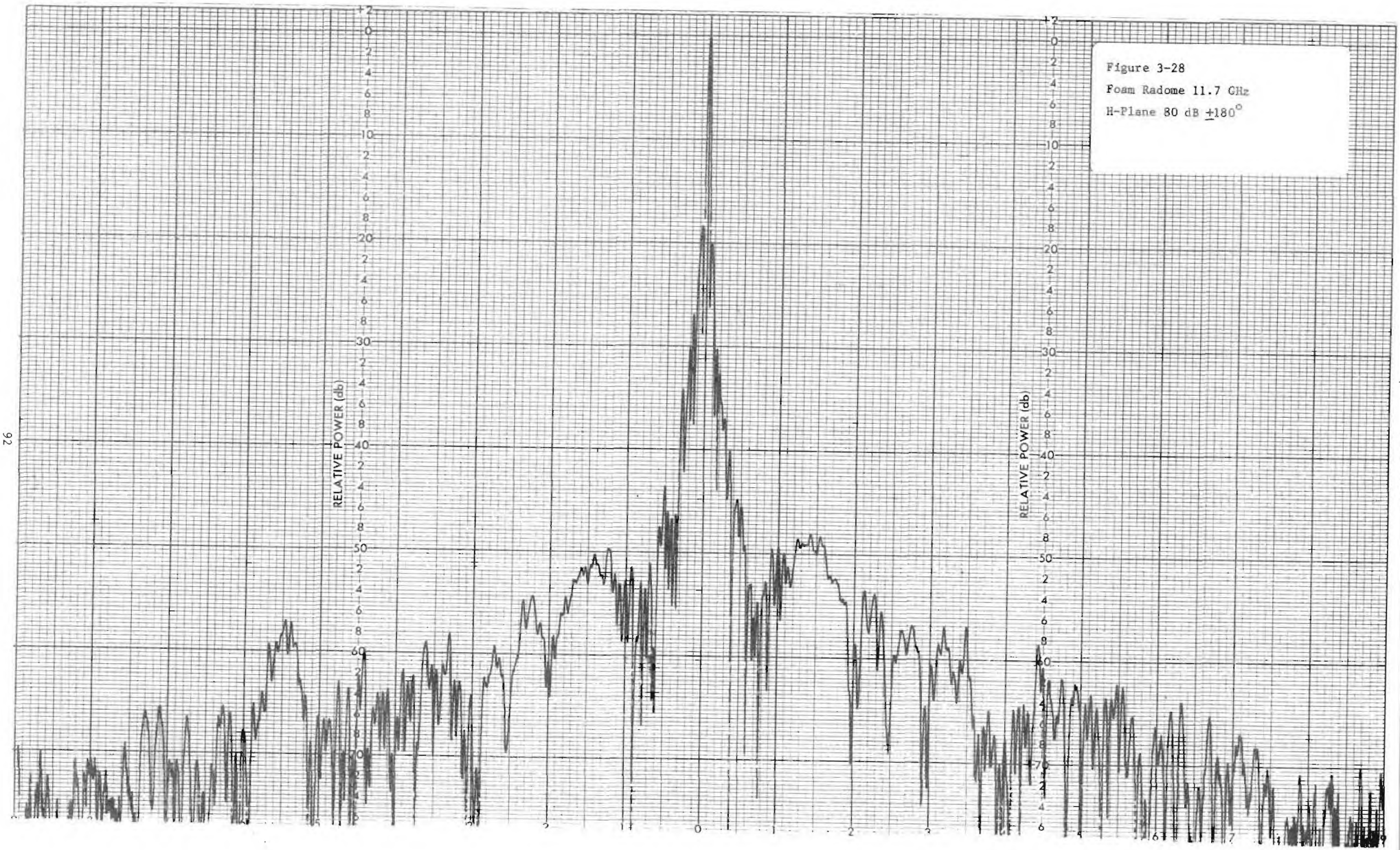

Figure 3-28
Foam Radome 11.7 GHz
H-Plane 80 dB $\pm 180^{\circ}$

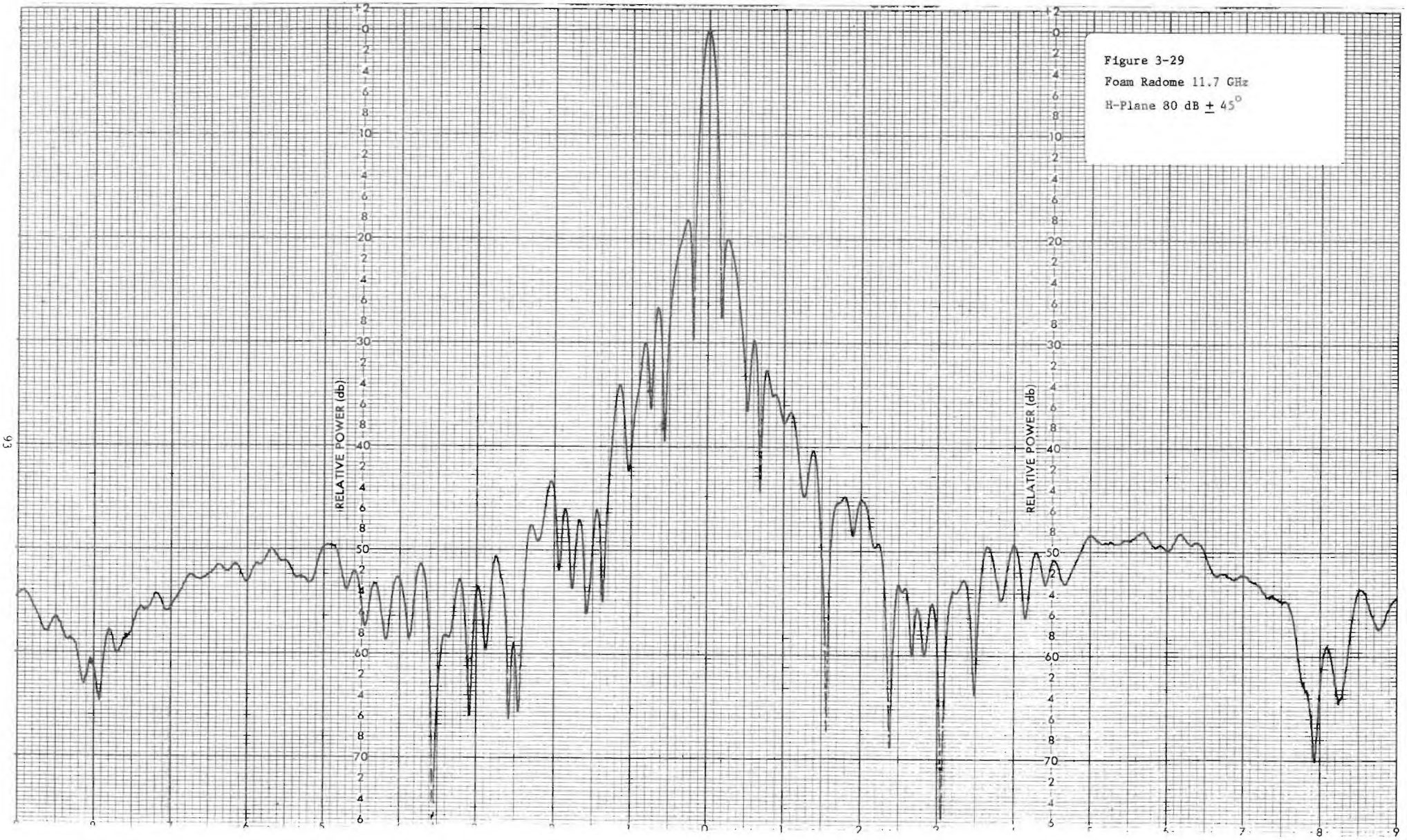

Figure 3-29
Foam Radome 11.7 GHz
H-Plane 80 dB $\pm$ 45°

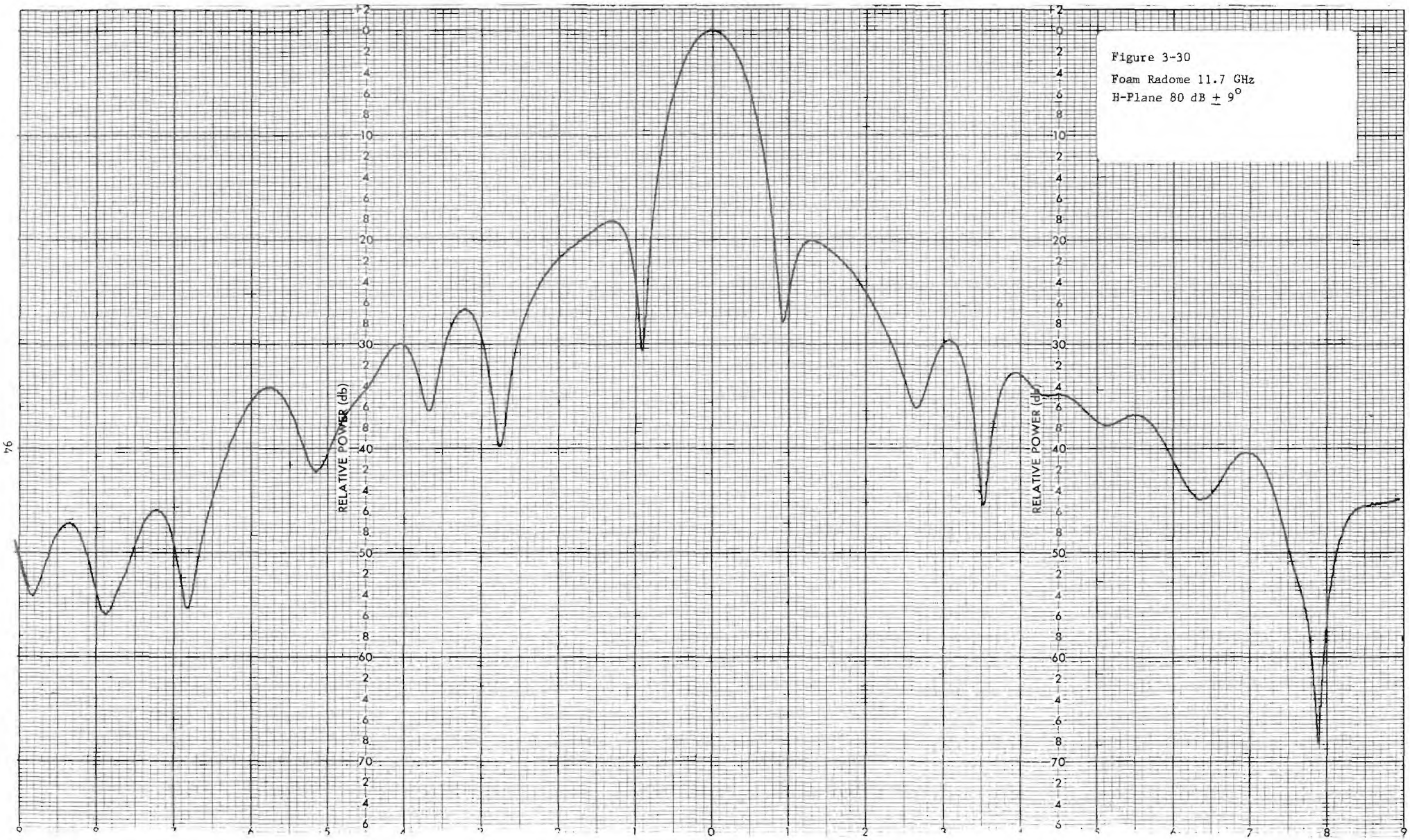

Figure 3-30
Foam Radome 11.7 GHz
H-Plane 80 dB $\pm$ 9°

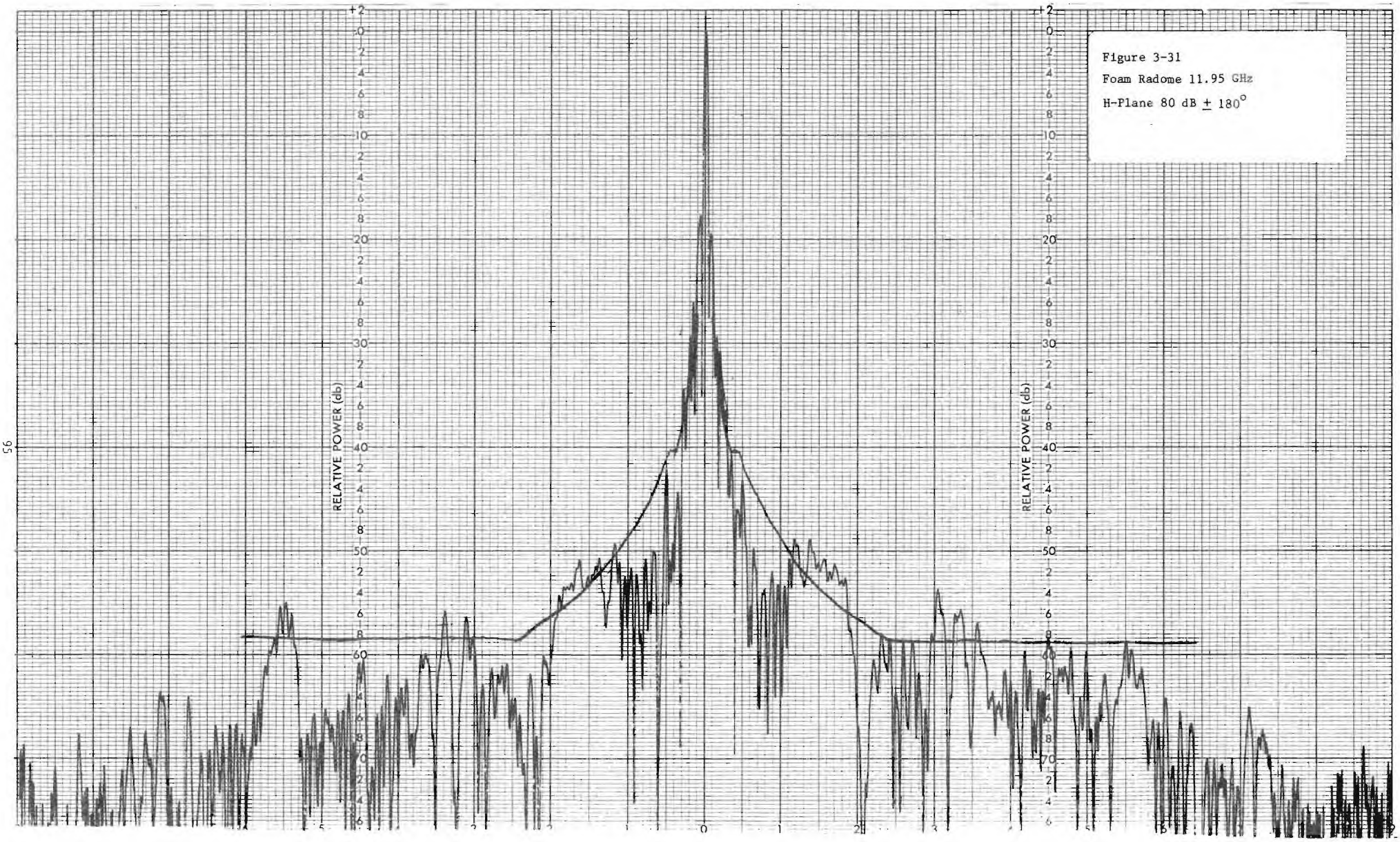

Figure 3-31
Foam Radome 11.95 GHz
H-Plane 80 dB ± 180°

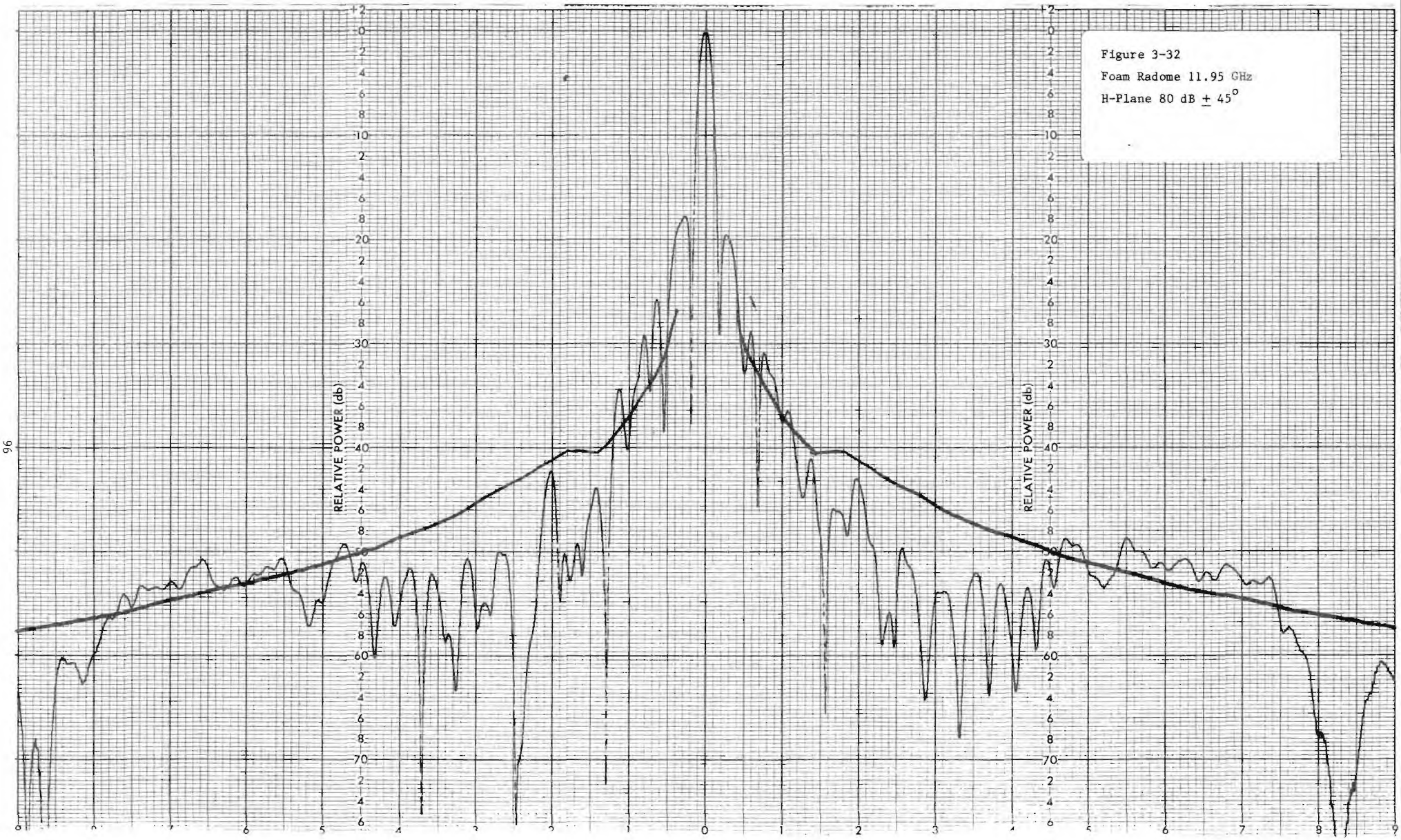

Figure 3-32
Foam Radome 11.95 GHz
H-Plane 80 dB $\pm$ 45°

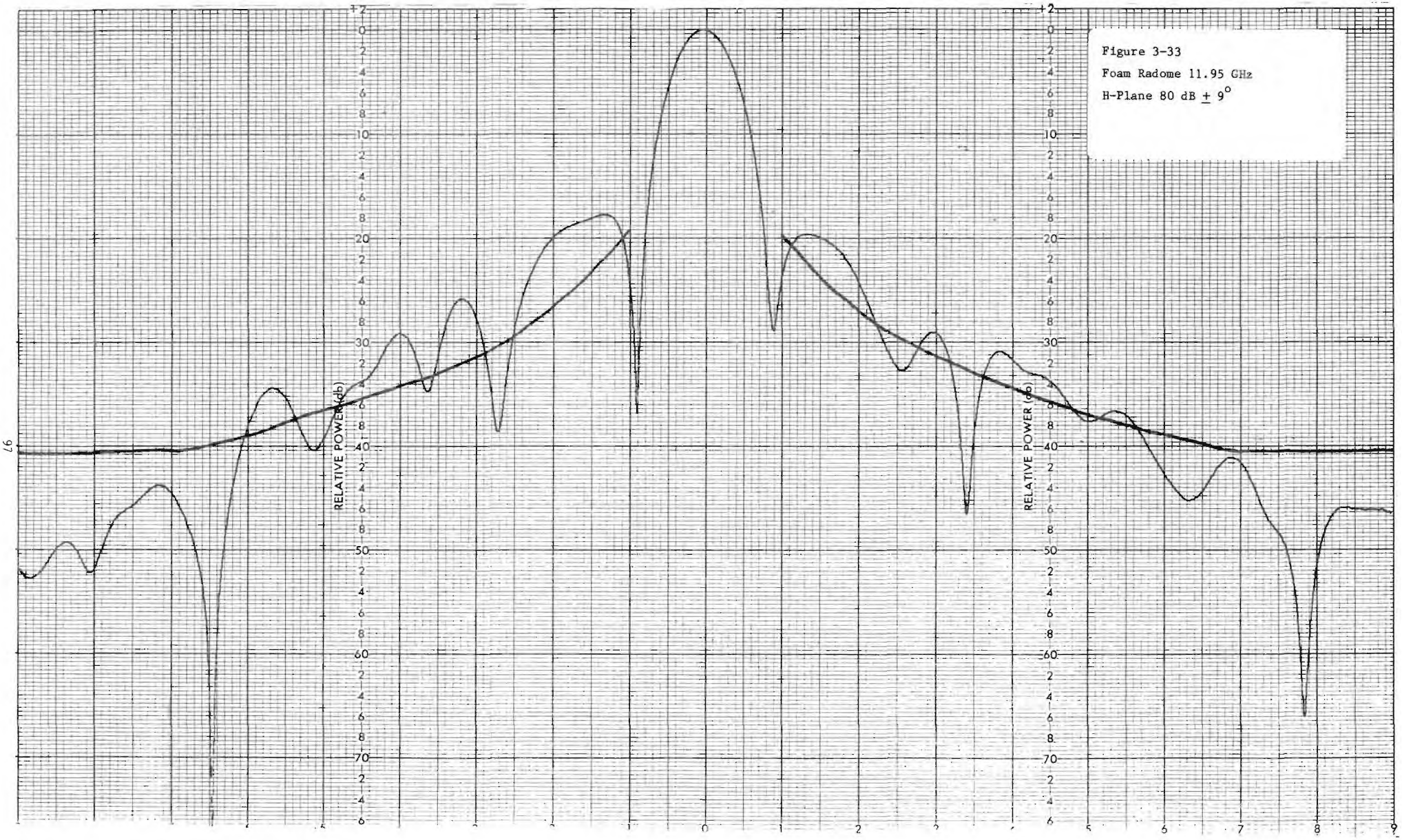

Figure 3-33
Foam Radome 11.95 GHz
H-Plane 80 dB $\pm$ 9°

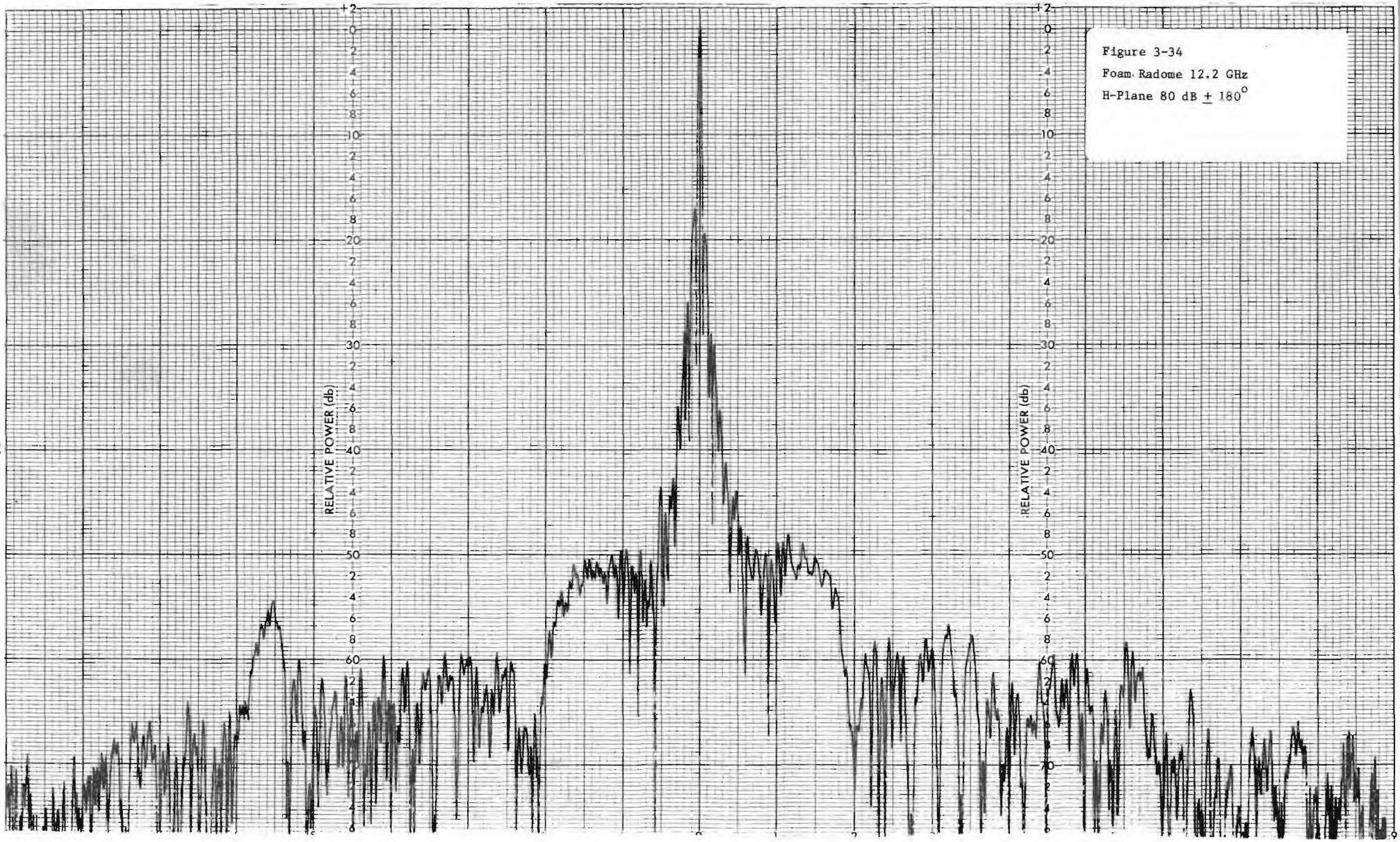

Figure 3-34
Foam Radome 12.2 GHz
H-Plane 80 dB $\pm$ 180°

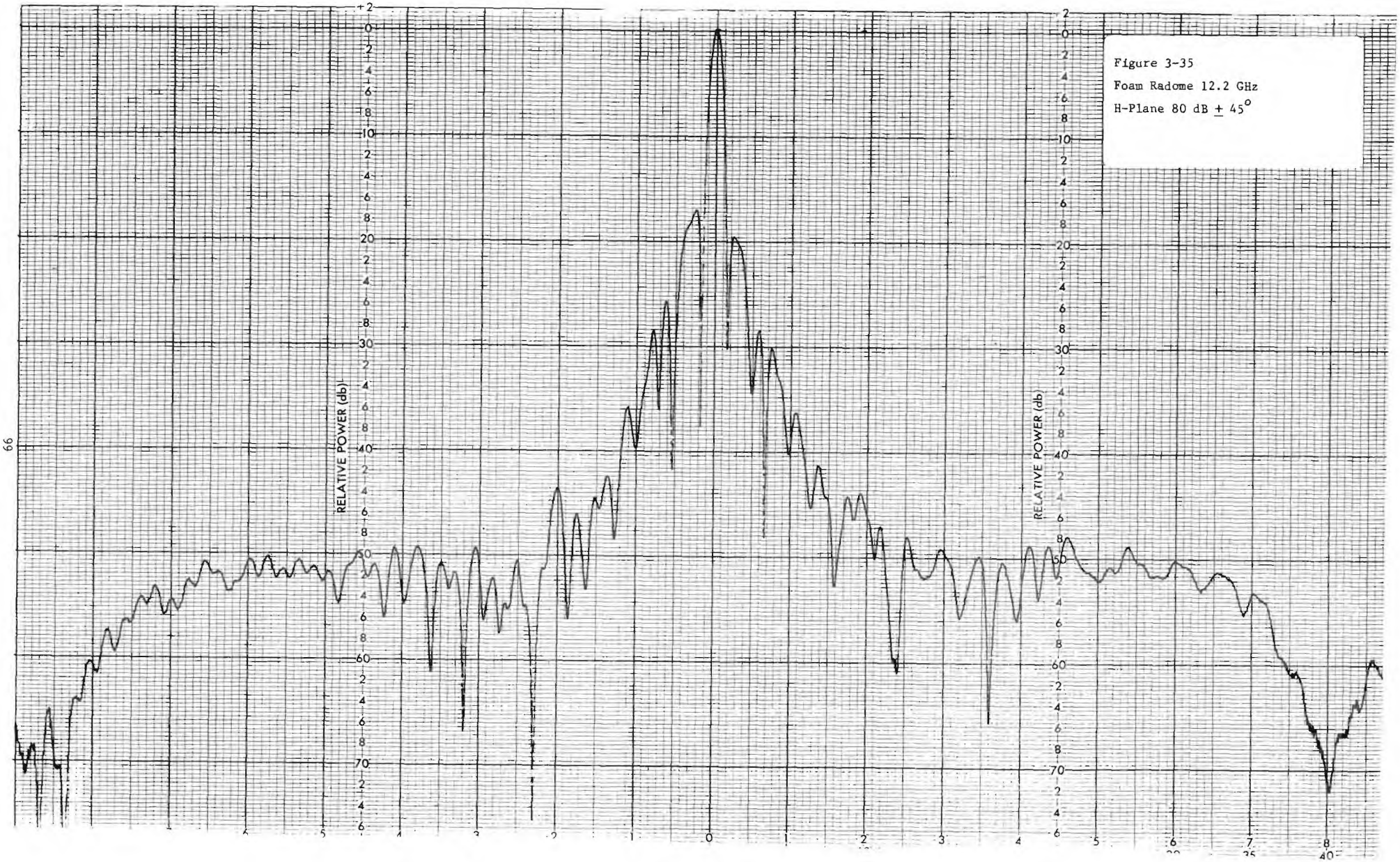

Figure 3-35
Foam Radome 12.2 GHz
H-Plane 80 dB ± 45°

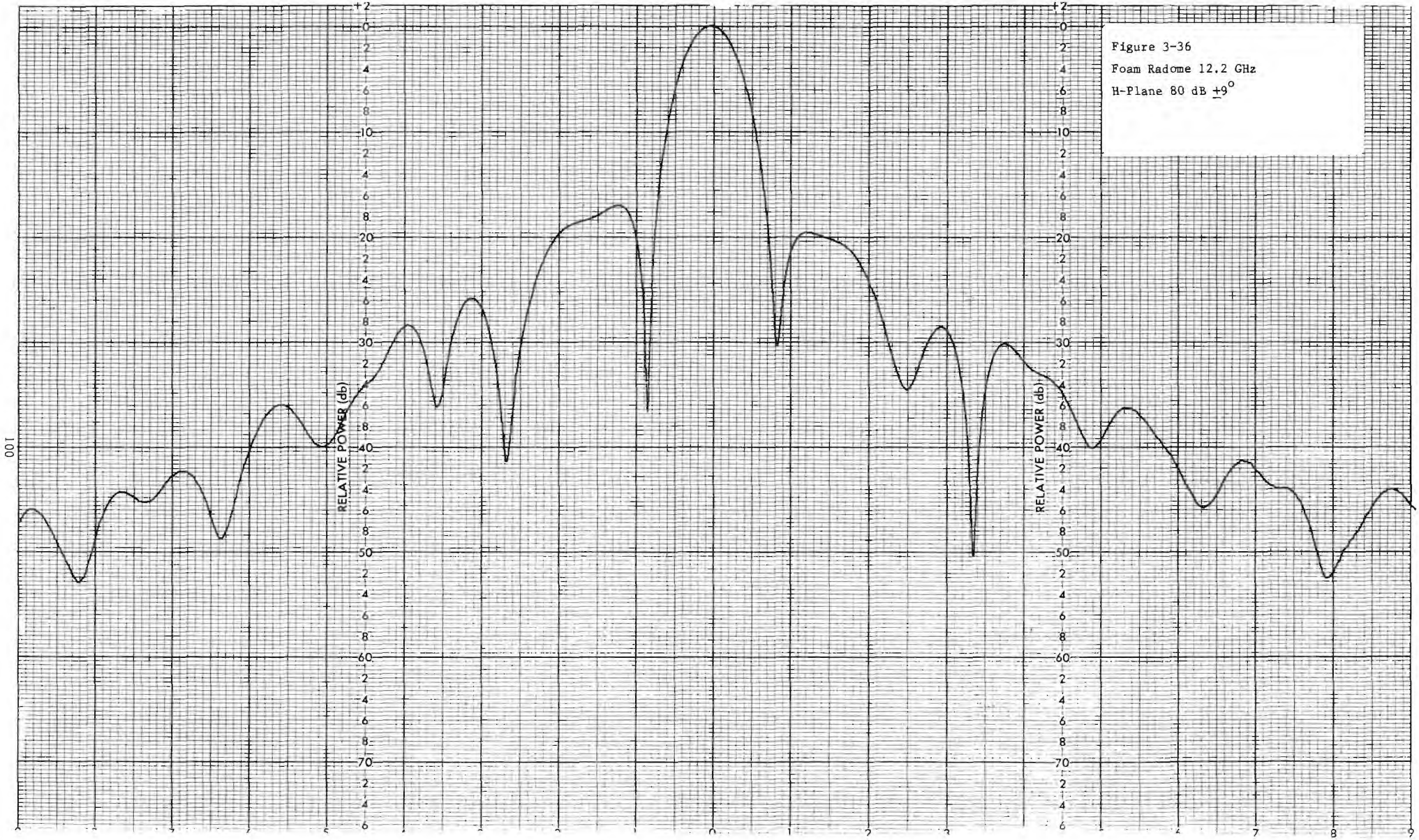

Figure 3-36
Foam Radome 12.2 GHz
H-Plane 80 dB $\pm 9^{\circ}$

TABLE 3-2 GAIN AND NOISE TEMPERATURE RESULTS

OXYGEN ABS	=	.015 DB/KM
WATER ABS	=	.007 DB/KM
FREQUENCY	=	11.950 GHZ
GAIN	=	48.140 DB

NOISE TEMPERATURE CONTRIBUTION:

ELEV	SUN	ATMOSPHERE	GROUND	TOTAL
10.0	.0848	33.8640	4.6455	38.5943
20.0	.1670	17.8708	4.4966	22.5344
30.0	.2441	12.4731	4.2431	16.9603
40.0	.3138	9.8301	3.9870	14.1310
50.0	.3740	8.3731	3.7007	12.4479
60.0	.4228	7.4909	3.4559	11.3696
70.0	.4588	6.8450	3.7416	11.0454
80.0	.4808	6.4449	3.9976	10.9234

TABLE 3-3 Reflector Surface RMS Measurements

BAR	LENGTH	RADIUS	PROFILE ERROR	IRREG. ERROR	TOTAL ERROR
1	51.506	51.009	-.002	.030	.030
2	39.944	39.911	.005	.022	.023
3	25.122	24.844	-.003	.021	.021
4	13.451	11.865	.-002	.007	.008
TOTAL			**.003**	**.024**	**.025**

Focal Length 45.666

NOTES:
1) All Dimensions are in Inches
2) Error is RMS Normal to Surface

FIGURE 3-37 PLOT OF MEASURED RMS DATA

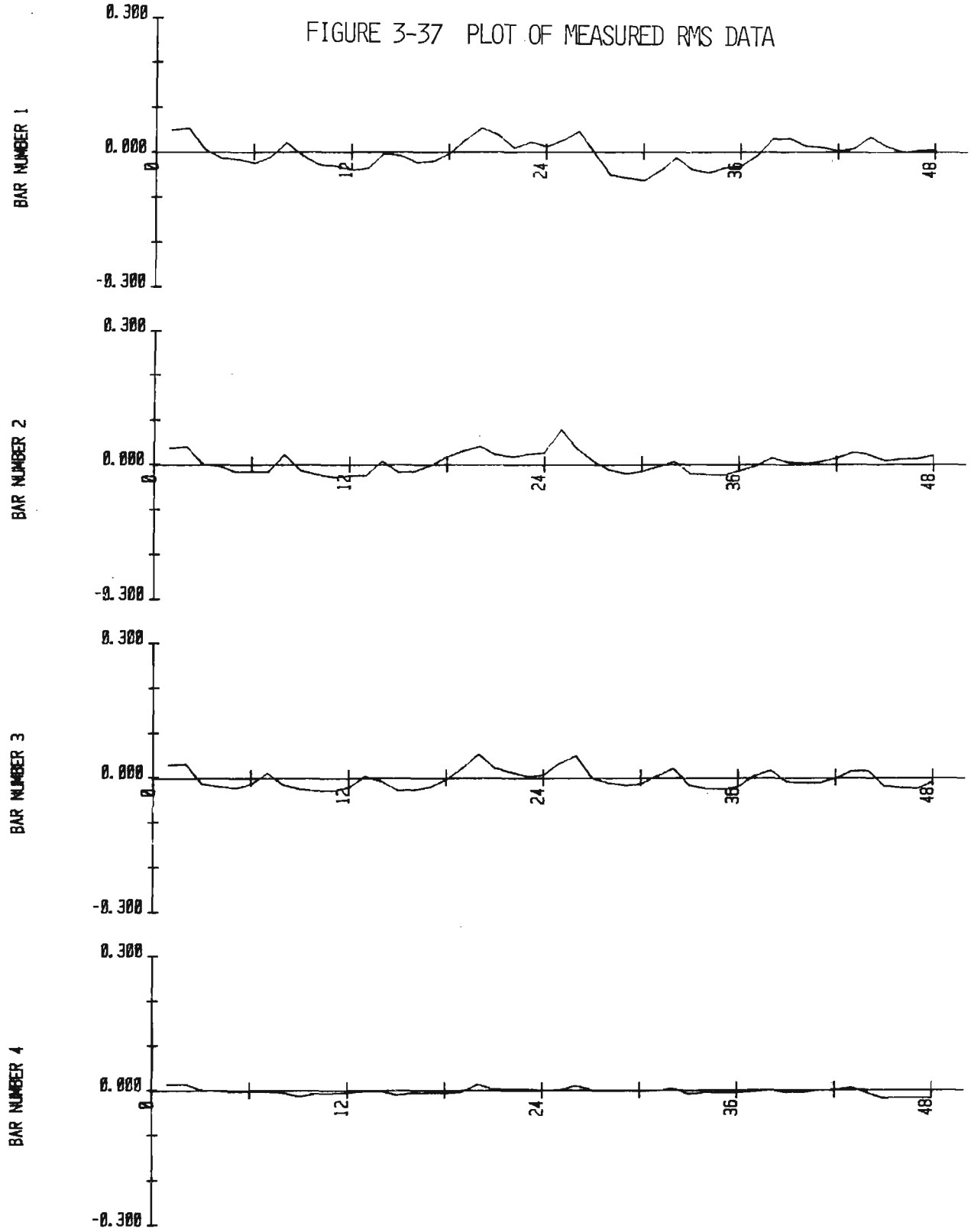

3.3 EVALUATION OF THE PRODUCTION UNIT TEST RESULTS

The foam-supported subreflector exhibits better sidelobe performance than the fiberglass configuration since scattering from the fiberglass interface causes high sidelobes in some regions. The support design could be improved by optimizing the radome characteristics of the support (i.e., maintain constant phase and minimize reflections). An improvement of several dB in the sidelobes and several tenths of a dB in gain could be realized by improving the radome.

The high sidelobes in the near-in region are caused by a combination of central blockage and surface error. The level of the first sidelobe is primarily determined by the illumination over the aperture and the central blockage. These two factors interact since a highly tapered aperture has less effective area than a uniform aperture which increases the significance of the central blockage. In the case of uniform illumination the blockage efficiency for a main reflector of radius R and a subreflector of radius r is [6]

$$E_B = [1 - (\frac{r}{R})^2]^2.$$

If the actual aperture illumination is considered, the blockage efficiency is

$$E_B = [1 - \frac{\int_0^r f(x)\, x\, dx}{\int_0^R f(x)\, x\, dx}]^2$$

where f(x) is the aperture power distribution. For example, if $f(x) = (1 - ax^2)^2$, then the blockage efficiency is [7]

$$E_B = [1 - \frac{(\frac{r}{R})^2}{1 - \frac{a}{2}}]^2.$$

For the case of -18dB edge taper, the blockage efficiency using the defined illumination function and a subreflector radius of 13.5 inches is 94.7%. The exact efficiency parameters for the production antenna tested are listed in Table 3-4.

TABLE 3-4 Antenna Efficiency Budget

ITEM	EFFICIENCY
Illumination	0.706
Blockage	0.920
Subreflector Spillover	0.954
Main Dish Spillover	0.992
Cross-Polarization	0.999
Phase	0.970
Mismatch	0.983
Feed Loss (Including Radome)	0.966
Surface Tolerance	0.937
TOTAL	**0.530**

Maximum Theoretical Gain (dB)	50.91
Net Gain (dB)	48.15

The subreflector spillover efficiency is calculated from the portion of feed energy which illuminates the subreflector. Energy from the feed which radiates beyond the angle subtended by the subreflector is lost. The main reflector spillover is calculated using a similar approach with reference to the energy scattered from the subreflector. Ideally, all the energy reflected by the subreflector would be intercepted by the main reflector. This ideal condition is approximated as the subreflector diameter becomes large in terms of wavelengths. However, in the present design the subreflector is on the order of only ten wavelengths. Energy is therefore reflected at wider angles than the angle to the edge of the main reflector. The distribution of energy scattered from the subreflector is referred to as a "scattered pattern." Figure 3-38 illustrates the subreflector scattered pattern for the H-plane. Figure 3-39 shows the E-plane scattered pattern. Energy radiated beyond approximately 61.7 degrees is lost. The amount of energy lost is also related to the edge taper. The lower the edge illumination, the less energy is lost. In the present design the spillover efficiency is high (99.2%) even though the subreflector diameter is small because the edge illumination is low.

The feed blockage is not included in the scattered pattern as shown. However, a measured scattered pattern would show a trough in the center caused by feed blockage. [9] Just as the scattered pattern does not cut off sharply at the edge of the main reflector, the feed blockage is not a sharply defined region. The trough may be broader than the physical blockage caused by the feed. Therefore, the illumination may behave as though a larger portion of the central aperture is unused than predicted by a direct calculation of the geometrical shadow diameter. The effect of the additional effective blockage is a change in the first sidelobe level.

The antenna design without blockage produces a first sidelobe level of -25 dB. The first sidelobe level with a blockage diameter of 13.5 inches is actually -21 dB (i.e., the central blockage contributes approximately 4 dB to the first sidelobe level). If the effective blockage diameter is increased to 16.5 inches to account for the observed trough in the reflector illumination, the additional contribution to the first sidelobe level is approximately 1.5 dB for a total of -19.5 dB.

The near-in sidelobes are strongly influenced by the mechanical surface error. A purely random surface error of .025 inch (RMS) can produce an increase in the sidelobe level of 2 or 3 dB in this region. A non-random error can produce an increase of 3 to 6 dB in the sidelobes in this region. Errors in reflector surfaces with systematic deformations are considered statistically correlated. "Application of the random error theory for the case of large correlation intervals results in a predicted scattering pattern which is directive and largely contained in the region of the main lobe and first few sidelobes." [10] In the design of the main reflector it is therefore desirable to reduce not only the RMS magnitude of surface error, but also the periodic accumulation of error.

The antenna noise temperature is affected by both the near-in and the wide angle sidelobes. At low elevation angles the near-in sidelobes are critical. At high elevation angles the wide-angle radiation is important (in particular the main reflector spillover). Assuming a feed loss of 0.15 dB, a waveguide loss

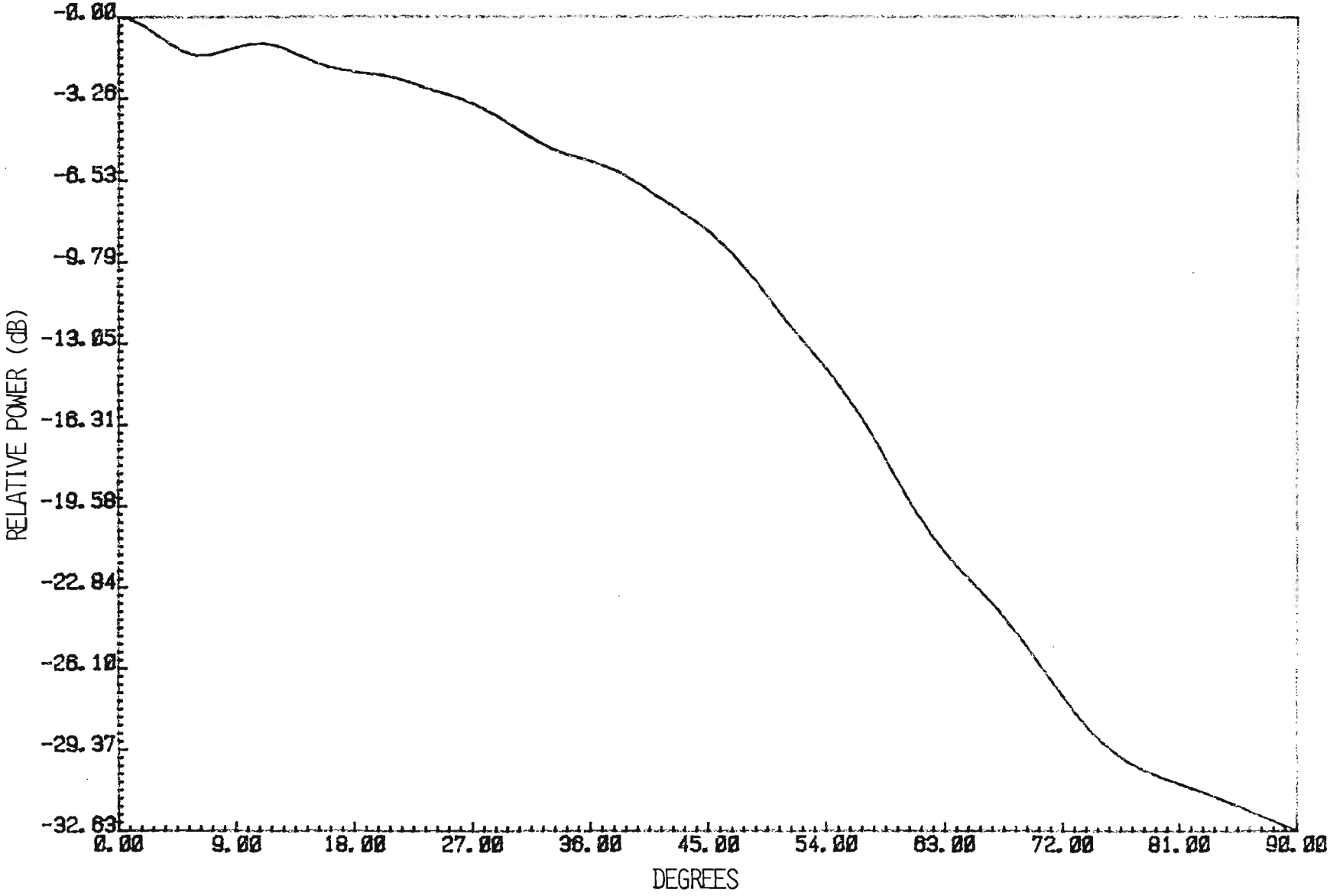

FIGURE 3-38. SUBREFLECTOR SCATTERED PATTERN (H-PLANE)

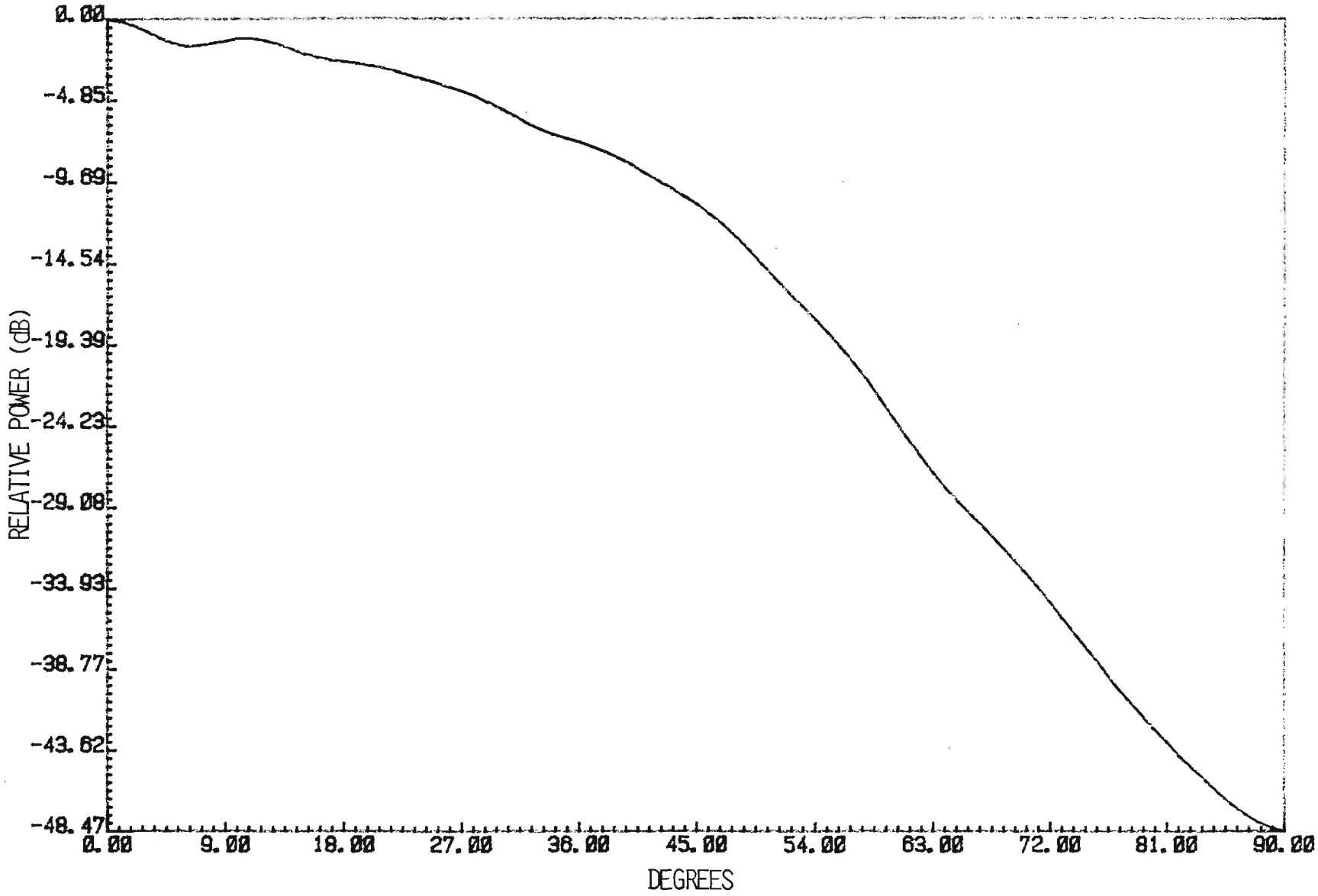

FIGURE 3-39. SUBREFLECTOR SCATTERED PATTERN (E-PLANE)

between the feed and the LNA of 0.05 dB, an LNA with 50 dB gain and noise figure of 3.5 dB, a receiver gain of 9 dB and noise figure of 9 dB, and a cable loss of 6 dB between the LNA and receiver, the G/T ratio at 20 degrees elevation is calculated for the antenna efficiency given in Table 3-5 and the noise temperature from Table 3-2. The result is calculated below.

$$T_s = \frac{T_a + T_f}{L_f} + T_L + \frac{T_2 + T_R L_2}{G_L}$$

$$= \frac{22.53 + 13.67}{1.05} + 359.23 + \frac{864.51 + (2013.55) \times (.25)}{100{,}000}$$

$$= 393.72°K \; or \; 25.95 \; dB°$$

where T_s is the system noise temperature, T_a is the antenna noise temperature, and T_f is the noise temperature from the combined feed loss of 0.15 dB (L_f) and 0.05 dB (L_1). L_1 is the loss between the feed and the LNA. L_2 is the loss between the LNA and the receiver.

$$G_s = G_a - L_f - L_1$$

$$= 48.2 - 0.2 - 0.05$$

$$= 47.95 \; dB$$

$$\frac{G}{T} = G_s - T_s = 22.0 \; \frac{dB}{°K}$$

The G/T is exactly the required value shown in Table 1-1. Therefore, the desired value of G/T is obtained even though the antenna gain is low since the sidelobes are low enough to reduce the antenna noise temperature . It is important to note that the net figure of merit for an antenna system is the ratio of G/T, not just the gain value. The overall system performance is then satisfied by this antenna design with regard to gain and noise temperature.

Figure 3-40 illustrates the final antenna configuration. Although the design focal length is 46.138 inches, the measured focal length of the antenna tested is approximately 45.6 inches. Figure 3-41 shows the final feed design. The feed design could be improved by lengthening the feed to include a phase matching section near the step junction. The additional section would also aid to reduce the unwanted TE_{12} mode. Figure 3-42 defines the final subreflector configuration. The subreflector is shown with a vertex matching plate and a diffraction skirt. In general, a vertex plate is undesirable if it can be avoided because of the effect on gain and contribution to the first sidelobe level. In this case, the size of the vertex plate is minimized to prevent significant performance degradation. If the design is pursued for optimization, it is possible to adjust the distance between the feed and subreflector so that a vertex plate is not required. Also, the shape of the subreflector could be optimized for the actual measured focal length.

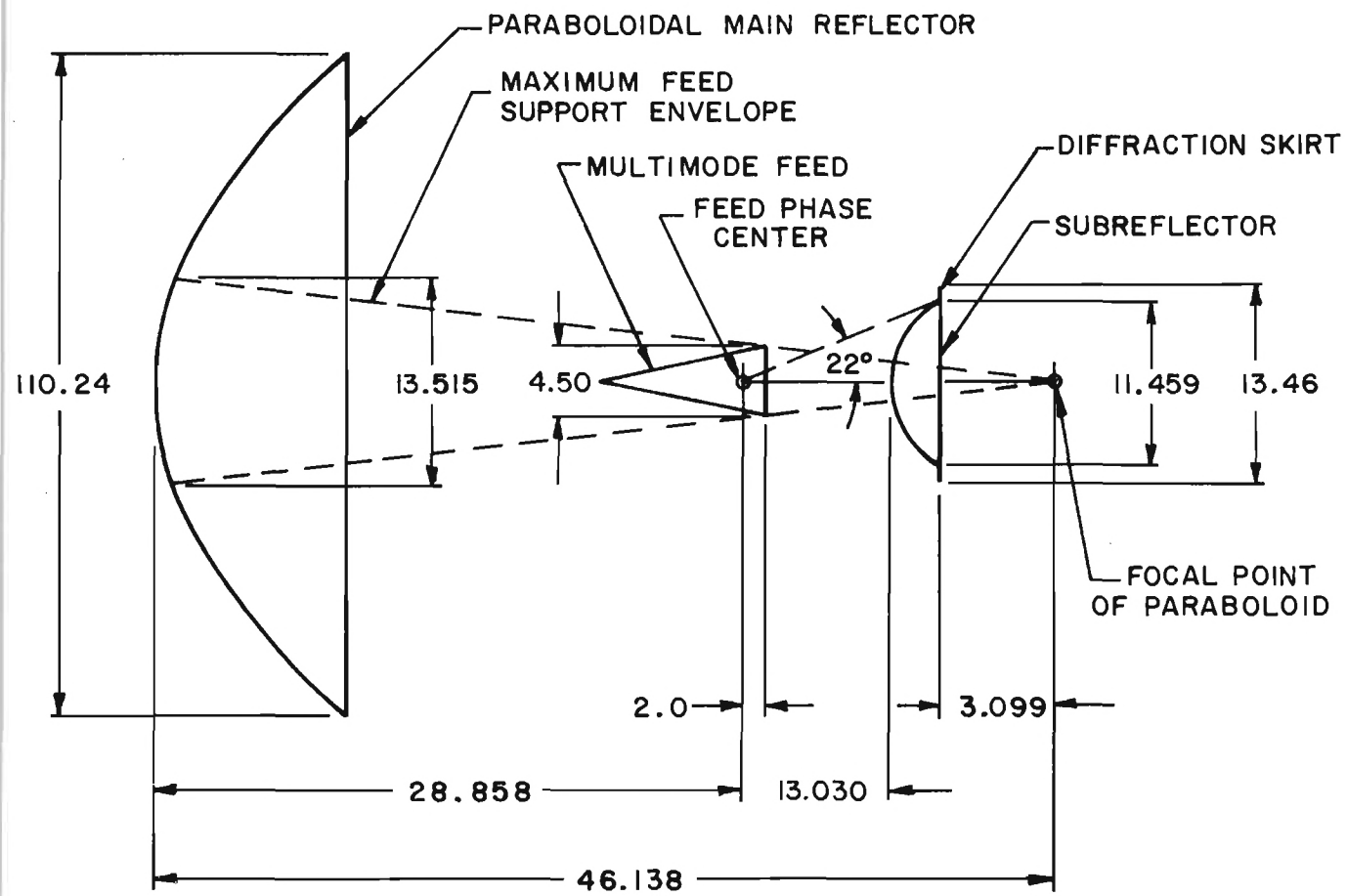

NOTE - DIMENSIONS ARE IN INCHES UNLESS OTHERWISE SPECIFIED.

FIGURE 3-40

CASSEGRAIN ANTENNA CONFIGURATION

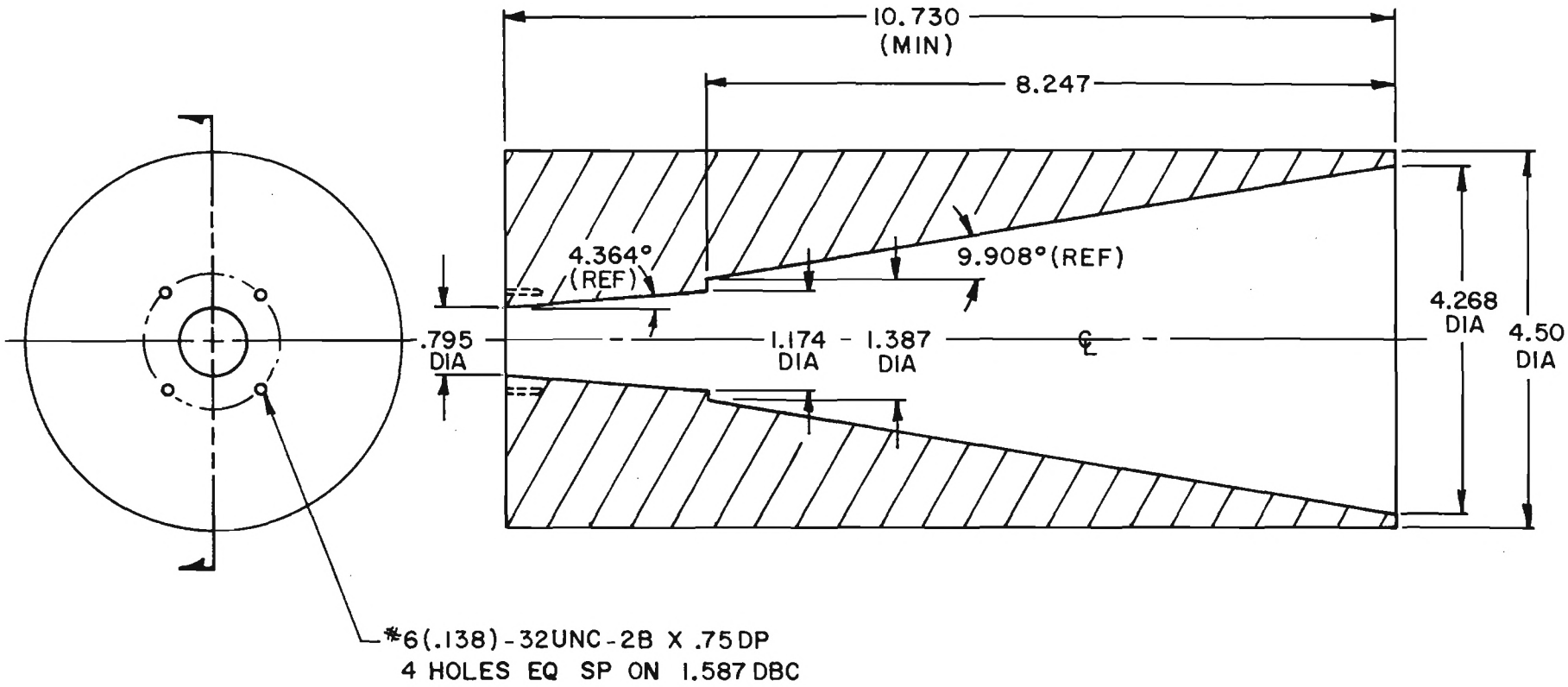

NOTE - DIMENSIONS ARE IN INCHES UNLESS
OTHERWISE SPECIFIED

FIGURE 3-41

KU-BAND MULTIMODE CONICAL FEED HORN

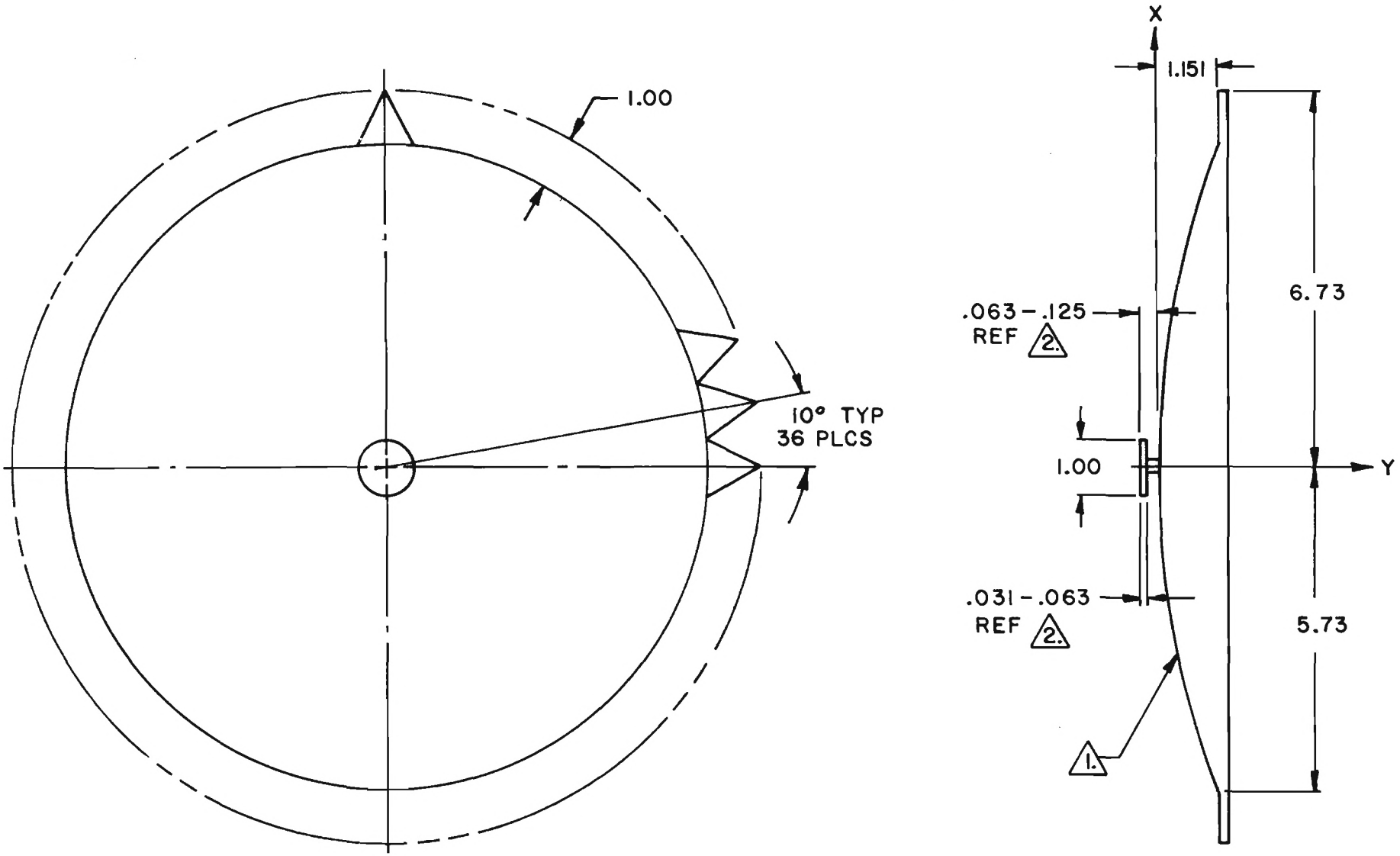

1. SURFACE GIVEN BY $AX^2 = CY^2 + EY$, WHERE $A = 18.060 \times 10^{-3}$; $C = 51.878 \times 10^{-3}$; $E = 455.534 \times 10^{-3}$
2. EXACT DIMENSION TO BE DETERMINED USING FINAL VERSION OF SUBREFLECTOR "IN SITU"

FIGURE 3-42

SUBREFLECTOR WITH MATCHING PLATE AND DIFFRACTION SKIRT

4.0 CONCLUSIONS

The first conclusion is that the feed design meets the requirements of performance in the given reflector with the exception of the near-in sidelobes (0° - 9°) which are caused by reflector surface error. Also, the gain is 0.5 dB below the desired value. However, the low gain is offset by the low noise temperature achieved by overall reduced sidelobe levels. The net figure of merit (G/T) of 22 dB/$^{\circ}$K is achieved by this design. Also, a portion of the gain loss is attributed to the high reflector surface error. Figure 4-1 illustrates the effect of random surface error on the near-in sidelobes. The case shown is for a circular aperture with no blockage and -18 dB edge illumination. Even with a small amount of surface error the sidelobes are affected significantly. In addition, if the correlation of surface error over distances larger than a wavelength is considered, the sidelobe levels are even higher than shown. In fact, the surface error is correlated over large distances as seen from the measured reflector RMS data.

The second conclusion is that although the feed design meets the general requirements, improvements are possible. The multimode feed design can be improved to reduce the phase dispersion between modes and to further attenuate the TE_{12} mode. The subreflector support design could be improved to enhance the transmission characteristic of the radome. A "sandwich" type radome could be considered which improves both structural and transmission properties. A simple design approach similar to the foam cylinder used in the prototype version but which is shaped to minimize phase error and internal reflections is shown in Figure 4-2. More "exotic" designs could also be pursued, such as tuned surface or circuit analog radomes.

Another possibility for improvement is to change the subreflector shape to correspond with the measured focal length of the reflector. Also, it would be possible to consider shaping of the subreflector to improve the illumination efficiency. Usually, both reflector surfaces require special shaping to maintain phase uniformity. [11] However, shaped subreflectors have been adapted to paraboloidal main reflectors to achieve optimization of aperture illumination while minimizing gain loss resulting from phase errors. [12] All the improvements mentioned would reduce the sidelobe levels and increase the antenna gain.

Other improvements or modifications in the feed design might be possible if a tradeoff study is conducted relating to sidelobe levels. Keeping in mind that the net figure of merit is the G/T ratio, certain angular regions of the sidelobe envelope are more critical than other angles. Also, if it is permitted that the sidelobe levels are specified only in the plane of the orbital arc, then other design options could be considered which have higher sidelobes in some planes but are nulled or reduced in the preferred plane. In particular, this tradeoff study should consider the recent FCC guidelines for sidelobe envelope requirements.

Once the optimum specifications have been determined, an optimum design approach should be selected. If the goal is to provide a low-cost, marginal-performance system, one approach may be dictated. If a superior-performing system for a moderate price is desired, a different approach is required. The performance requirements contained in the recent FCC directive are stringent

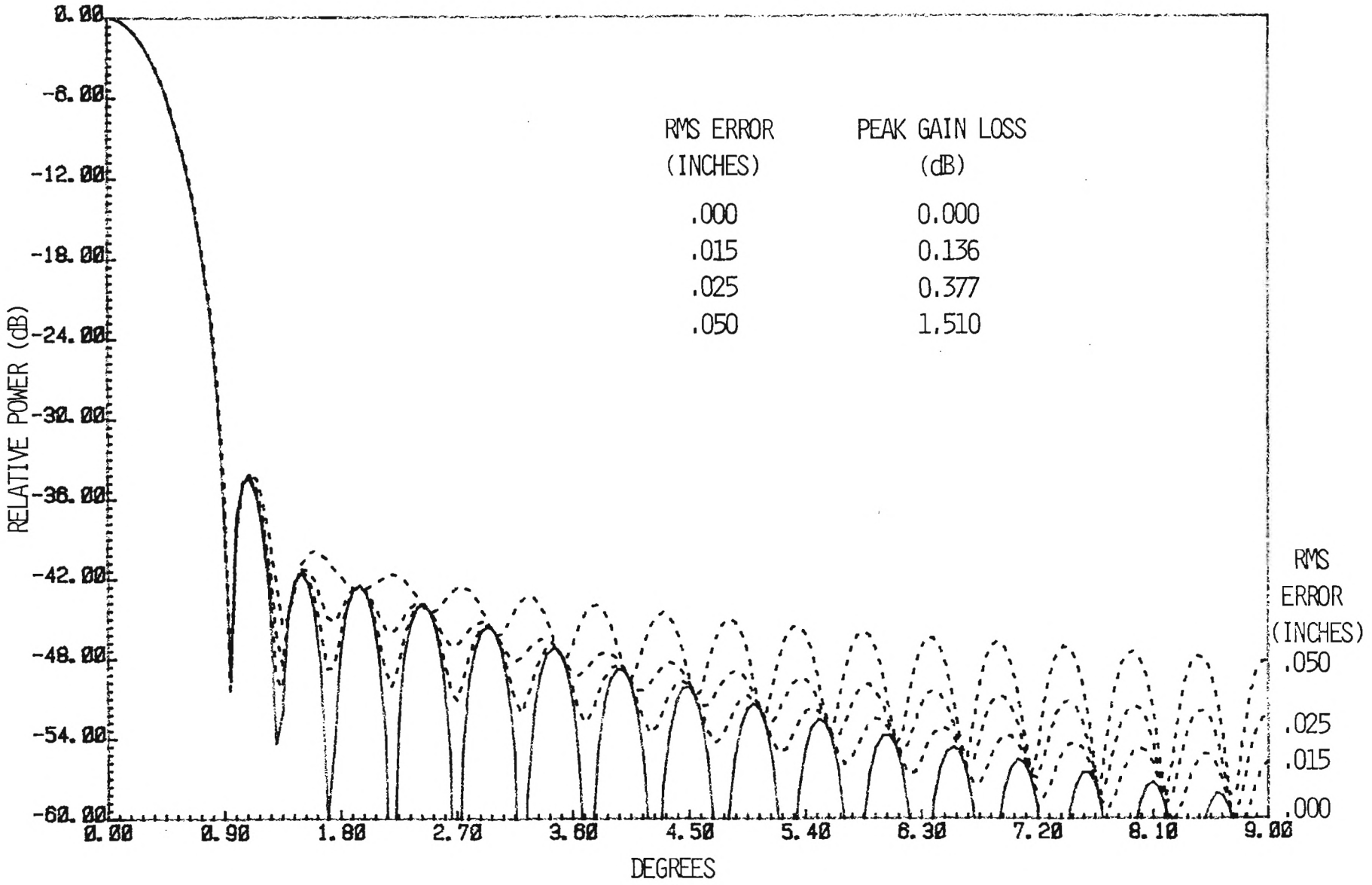

FIGURE 4-1. EFFECT OF SURFACE ERROR ON SIDELOBE LEVELS

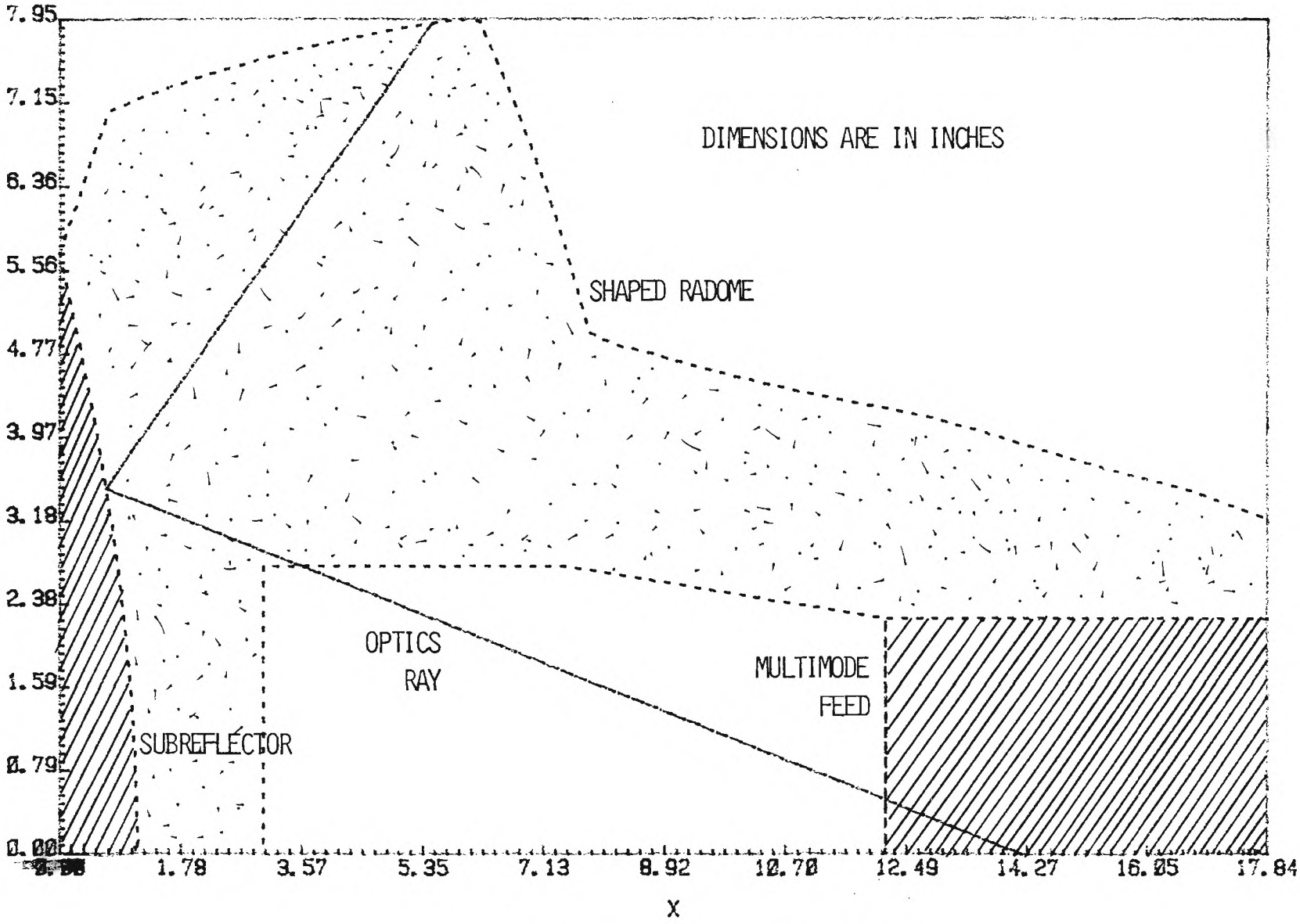

FIGURE 4-2 SHAPED RADOME GEOMETRY

and not to be taken lightly. If the intention is to comply fully with those requirements and to optimize the performance in every other way, a design tailored to meet those exact specifications is necessary. A simple adaptation of the present reflector is not possible. Stated another way, the general performance specified for this project as outlined in Table 1-1 was achieved only marginally as anticipated. The near-in sidelobe levels were even higher than predicted because of the reflector surface. The new FCC regulations are even stricter than those envisioned at the initiation of this project. Therefore, a unique design is necessary to meet these unique requirements.

One approach is to test the initial feed design in a guaranteed reflector (i.e., a highly accurate reflector surface) to isolate the feed performance from the effects of surface error. The results of this test would then indicate the allowed margin for surface error. Also, if the initial constraint to use the existing reflector is removed, other design approaches may be offered, such as an offset-fed reflector, an offset dual-shaped reflector, or even a multibeam spherical reflector if communication with adjacent satellites is desired. In addition, once a reflector is designed to operate at Ku-band, it is relatively simple to operate at a lower frequency such as C-band. A dual-band feed is even possible such that the antenna can operate simultaneously in both frequency bends. However, the reverse situation is less likely to succeed. A reflector surface designed for C-band operation is usually not satisfactory at Ku-band. The reflector surface as it is presently designed is an example.

The antenna configuration as presently set forth in its entirety performs closely to the initial specifications. Since the antenna is a receive-only terminal it is not mandatory to meet the stringent FCC specifications which are beyond the design goals forseen at the beginning of this project. The antenna may be used within these limitations. If these limitations are to be exceeded (i.e., if full compliance with the new FCC directive is required), then another design approach is necessary following a detailed tradeoff study as outlined previously. Table 4-1 summarizes the conclusions reached as a result of this development study.

TABLE 4-1 Summary of Conclusions

1. The feed design meets the performance requirements except for near-in sidelobe levels which are attributed to undue reflector surface error.

2. The overall feed design, though acceptable, could be further optimized for improved performance.

3. A tradeoff study should be conducted in consideration of the recent FCC directive concerning sidelobe envelope requirements.

4. An optimum design approach should be selected following the tradeoff study.

5. A unique design should be developed to meet the desired specifications.

6. Achievement of a quality reflector surface (low RMS error and reduction of systematic error) should be a primary mechanical consideration.

REFERENCES

1. C. C. Cutler, "Parabolic Antenna Design for Microwaves," Proc. IRE, Vol. 35, pp. 1284-1294, Nov. 1947.

2. M. S. Narasimhan, "Corrugated Conical Horns with Arbitrary Corrugation Depth," Radio Electron. Eng., Vol. 43, pp. 188-192, March 1973.

3. P. D. Potter, "A New Horn Antenna with Suppressed Sidelobes and Equal Beamwidths," Microwave Journal, Vol. VI, pp. 71-78, June 1963.

4. A. C. Ludwig, "Radiation Pattern Synthesis for Circular Aperture Horn Antennas," IEEE Trans. Antennas and Propagation, Vol. AP-14, pp. 434-440, July 1966.

5. M. S. Narasimhan, "Modes in a Conical Horn: New Approach," Proc. IEE, Vol. 118, pp. 287-292, Feb. 1971.

6. C. L. Gray, "Estimating the Effect of Feed Support Member Blocking on Antenna Gain and Sidelobe Level," Microwave Journal, pp. 88-91, March 1964.

7. J. Ruze, "Feed Support Blockage Loss in Parabolic Antennas," Microwave Journal, pp. 76-80, December, 1968.

8. W. V. T. Rusch, "Scattering from a Hyperboloidal Reflector in a Cassegrainian Feed System," IEEE Trans. Antennas and Propagation, pp. 414-421, July, 1963.

9. G. W. Collins, "Shaping of Subreflectors in Cassegrainian Antennas for Maximum Aperture Efficiency, "IEEE Trans. Antennas and Propagation, Vol. Ap-21, pp. 309-313, May 1973.

10. R. W. Kreutel, "Wide-Angle Sidelobe Envelopes of a Cassegrain Antenna," Consat Technical Review, Vol. 6, no. 1, pp. 71-88, Spring 1976.

11. S. K. Buchmeyer, "An Electrically Small Cassegrain Antenna with Optically Shaped Reflectors," IEEE Trans. Antennas and Propagation, pp. 346-351, May 1977.

12. S. V. Parekh, "On the Solution of Best Fit Paraboloid as Applied to Shaped Dual Reflector Antennas," IEEE Trans. Antennas and Propagation, Vol. AP-28, July 1980.